

CHARACTERISATION OF HEMP-LIME AS A COMPOSITE BUILDING MATERIAL

by

Edward Alexander Joseph HIRST

A thesis submitted for the degree of
Doctor of Philosophy

University of Bath

Faculty of Engineering and Design
Department of Architecture and Civil Engineering

June 2013

COPYRIGHT

Attention is drawn to the fact that copyright of this thesis rests with its author. A copy of this thesis has been supplied on condition that anyone who consults it is understood to recognise that its copyright rests with the author and they must not copy it or use material from it except as permitted by law or with the consent of the author.

This thesis may be made available for consultation within the University Library and may be photocopied or lent to other libraries for the purposes of consultation.

Author's signature:

A handwritten signature in blue ink, appearing to read "End list". The signature is written in a cursive, flowing style with a few loops and a small dot above the 'i' in "list".

ACKNOWLEDGEMENTS

The work on this thesis was carried out in the Department of Architecture and Civil Engineering and the Department of Chemical Engineering at the University of Bath between September 2007 and June 2013. Firstly, the author would like to thank the BRE Trust for the funding and sponsorship to conduct this research.

The greatest level of gratitude and thanks goes to my supervisors Professor Pete Walker, Dr. Kevin Paine and Dr. Tim Yates for their (almost) never-ending patience, support, guidance and expertise. The author would like to thank Professor Pete Walker in particular who has provided invaluable insight and skills which have helped evolve the thesis into its final form.

The laboratory staff at the University of Bath, Sophie, Will, Graham, Neil and Brian, also receive my thanks for their assistance and friendship. Particular mention goes to Sophie for her dedicated assistance during the most lengthy and mundane tests undertaken in this investigation.

University life would not have been nearly as fun or fulfilling without the friendship of Dr. Andrew Thomson, Dr. Chris Mundell and Dr. Mark Evernden.

Finally my gratitude and thanks go towards my family for their support and fortitude during this challenging and lengthy process.

DECLARATION

The author wishes to declare that, except for commonly understood and accepted ideas, or where specific reference is made to the work of others, the content of this thesis are his own work and includes nothing that is the outcome of work done in collaboration. This dissertation has not been submitted previously, in part or in whole, to any university or institution for any degree, diploma, or other qualification.

ABSTRACT

Hemp-lime is a comparatively novel renewable insulation material in the construction industry. Its use was first documented in the 1980's, however, recent increased interest and the release of popular publications has resulted in an increased need for scientific investigation into the material.

The research conducted in this investigation firstly focussed on furthering the empirical characterisation of hemp-lime and its constituents with particular attention paid to minimising fabrication variables and increasing the accuracy of final specimen bulk densities. Secondly attempts were made to quantify the degree of carbon sequestration that occurs as a result of the carbonation of the lime binder. A total of 196 specimens were fabricated for the main programme of work.

It has been demonstrated that the novel fabrication methodology developed and tested in this investigation allows for reliable and consistent fabrication of specimens with almost identical final bulk densities. An average intrinsic empirical variability of 0.8% was determined for hemp-lime composites.

It has been shown that the values of CO₂ sequestration varied between 151-192kg/m³ for the current formulated binders and composite bulk densities being used or considered in the UK construction industry. This resulted in a minimum 100% increase above the lowest estimated sequestration value from previous investigations.

Preliminary carbonation constant values for hemp-lime have been determined, however, further testing is required to establish definite values based on a wider sample of testing.

DISSEMINATION

Elements of this study have been published in the following peer reviewed journals:

HIRST, E. A. J., WALKER, P., PAINE, K. A., YATES, T. 2010. Characterisation of Low Density Hemp-Lime Composite Building Materials under Compression Loading. *In: Second International Conference on Sustainable Construction Materials and Technologies*, 2010-06-28 - 2010-06-30, Acona.

HIRST, E. A. J., WALKER, P., PAINE, K. A., YATES, T. 2012. Characteristics of low density hemp-lime building materials. *Proceedings of Institution of Civil Engineers, Construction Materials*, 165 (1), pp. 15-23. DOI: 10.1680/coma.1000021.

Copies of these publications can be found in Appendix V.

The author was also awarded 3rd place in the poster presentation competition during the 2009 Institute of Structural Engineers Young Researchers Conference.

CONTENTS

ACKNOWLEDGEMENTS.....	5
DECLARATION.....	7
ABSTRACT	9
DISSEMINATION.....	11
CONTENTS.....	13
LIST OF FIGURES	18
LIST OF TABLES	22
GLOSSARY	26
CHAPTER 1 - INTRODUCTION	27
1.1 INTRODUCTION	27
1.2 RENEWABLE MATERIALS IN CONSTRUCTION	27
1.3 HEMP-LIME.....	29
1.3.1 <i>Hemp-shiv</i>	29
1.3.2 <i>Binder</i>	33
1.3.3 <i>Water</i>	37

1.4	HISTORICAL AND CURRENT USE OF HEMP-LIME.....	37
1.4.1	<i>Construction techniques</i>	41
1.4.2	<i>Material advantages</i>	46
1.5	AIM AND OBJECTIVES	48
1.6	THE STRUCTURE OF THIS THESIS.....	49
CHAPTER 2 -	LITERATURE REVIEW.....	51
2.1	INTRODUCTION.....	51
2.2	HISTORICAL AND CURRENT PUBLICATIONS	52
2.3	SHIV	53
2.3.1	<i>Origin and processing</i>	54
2.3.2	<i>Granulometry</i>	56
2.3.3	<i>Bulk and particle density</i>	58
2.3.4	<i>Compressive strength</i>	60
2.3.5	<i>Porosity and water absorption</i>	61
2.3.6	<i>Thermal conductivity</i>	65
2.4	BINDER.....	66
2.4.1	<i>Pre-formulated binders</i>	66
2.4.2	<i>Carbonation and hydration of limes and cements</i>	68
2.5	HEMP-LIME.....	72
2.5.1	<i>Fabrication and curing methodologies</i>	72
2.5.2	<i>Mechanical properties</i>	77
2.5.3	<i>Environmental characteristics</i>	78
2.6	MEASUREMENT OF CARBONATION	86
2.6.1	<i>Chemical staining</i>	86
2.6.2	<i>Thermogravimetric analysis</i>	88
2.7	90
2.8	SUMMARY OF FINDINGS.....	90
CHAPTER 3 -	EXPERIMENTAL PROGRAMME.....	92
3.1	INTRODUCTION.....	92
3.2	SELECTION OF MATERIALS	93
3.2.1	<i>Binders</i>	93
3.2.2	<i>Bio-aggregates</i>	94
3.3	SAFETY DURING HANDLING AND PREPARATION OF MATERIALS	96
3.4	CHARACTERISATION OF BINDERS	97
3.4.1	<i>Bulk density</i>	97
3.4.2	<i>Setting times and consistanvce of binders</i>	98
3.4.3	<i>Flexural and compressive strength</i>	100

3.4.4	<i>Moisture absorption</i>	103
3.4.5	<i>Particle grading</i>	104
3.5	MAIN PROGRAMME OF WORK FOR COMPOSITE TESTING	105
3.5.1	<i>Composite specimen design</i>	106
3.5.2	<i>Specimen fabrication matrix</i>	112
3.5.3	<i>Specimen fabrication</i>	114
3.5.4	<i>Testing methodology</i>	118
3.6	PROGRAMME OF WORK FOR CHEMICAL TESTING	125
3.6.1	<i>Phenolphthalein indicator</i>	125
3.6.2	<i>Thermogravimetric analysis</i>	126
CHAPTER 4 -	PROPERTIES OF CONSTITUENT MATERIALS	132
4.1	INTRODUCTION	132
4.2	HEMP SHIV	133
4.2.1	<i>Moisture content</i>	133
4.2.2	<i>Hemp shiv grading</i>	134
4.2.3	<i>Hemp shiv water absorption characteristics</i>	138
4.3	BINDER CHARACTERISATION	142
4.3.1	<i>Initial setting times</i>	143
4.3.2	<i>Bulk density</i>	143
4.3.3	<i>Flexural and compressive strength</i>	145
4.3.4	<i>Binder carbonation</i>	150
4.4	SUMMARY OF FINDINGS	155
CHAPTER 5 -	CHEMICAL CHARACTERISTICS OF HEMP-LIME	156
5.1	INTRODUCTION	156
5.2	PHENOLPHTHALEIN INDICATOR STAINING OF COMPOSITE SPECIMENS	157
5.2.1	<i>Testing and analysis methodology</i>	157
5.2.2	<i>Carbonation results</i>	162
5.2.3	<i>Summary of findings</i>	171
5.3	THERMOGRAVIMETRIC ANALYSIS OF HEMP-LIME	171
5.3.1	<i>Treatment of thermogravimetric analysis results</i>	171
5.3.2	<i>TG analysis of bio-aggregates</i>	176
5.3.3	<i>Carbon content of hemp shiv</i>	177
5.3.4	<i>TG analysis of fresh binder</i>	178
5.3.5	<i>TG analysis of hydration products</i>	180
5.3.6	<i>Thermogravimetric analysis of hemp-lime composite specimens</i>	183
5.4	SUMMARY OF FINDINGS	189
CHAPTER 6 -	MECHANICAL CHARACTERISTICS OF HEMP-LIME	191

6.1	INTRODUCTION.....	191
6.2	CONSISTENCY IN COMPOSITE SPECIMEN FABRICATION.....	192
6.3	MECHANICAL CHARACTERISATION	198
6.3.1	<i>Treatment of results</i>	198
6.3.2	<i>Results and discussion</i>	199
6.3.3	<i>Specimen failure</i>	207
CHAPTER 7 -	CONCLUSIONS.....	210
7.1	INTRODUCTION.....	210
7.1.1	<i>Specimen fabrication</i>	211
7.1.2	<i>Material characterisation</i>	212
7.1.3	<i>Carbonation</i>	212
7.1.4	<i>Carbon dioxide sequestration</i>	212
7.2	RECOMMENDATIONS FOR FURTHER WORK	214
REFERENCES.....		217
APPENDIX I – CALCULATION OF WET MASS OF MATERIAL DURING FABRICATION		
	226
APPENDIX II – COMPOSITE SPECIMEN COMPRESSION TESTING PHOTOGRAPHS..		228
APPENDIX III – COMPOSITE SPECIMEN CARBONATION TESTING PHOTOGRAPHS		238
APPENDIX IV – MORTAR SPECIMEN CARBONATION TESTING PHOTOGRAPHS.....		246
APPENDIX V – PEER REVIEWED PUBLICATIONS.....		251

LIST OF FIGURES

Figure 1.1 – Total number of hectares per European member state that contributes with industrial hemp production [European Commission, 2009].	30
Figure 1.2 – Dried stalk of the hemp plant showing the woody core and unwrapped fibres [Wikipedia, 2009].	32
Figure 1.3 – Typical hemp shiv particles processed from the woody core of the industrial hemp plant [Hemp Technology website, 2008].	33
Figure 1.4 – The lime cycle [www.naturalhydrauliclime.com]	35
Figure 1.5 – Maison de la Turquie. Timber frame with hemp-lime infill [Ceyte, 2008].	38
Figure 1.6 – The Renewable house at the BRE [www.nnfcc.co.uk].....	39
Figure 1.7 – Hemp-lime house in Asheville, North Carolina [www.hemp.com, 2011].	40
Figure 1.8 - Adnams distribution centre [www.fabricarchitecture.com, 2008].	40
Figure 1.9 – Finished hemp-lime wall surrounding a timber primary structure [Evrard, 2008].....	42
Figure 1.10 – Efficient removable shuttering currently used in the UK hemp-lime construction industry [Lime Technology website].....	43
Figure 1.11 – Spraying of hemp-lime [Lime Technology website].	44

Figure 1.12 – Hemp-lime block wall.....	45
Figure 1.13 – Prefabricated panel filled with hemp-lime drying before being rendered [www.recycledarchitecture.blogspot.no].....	46
Figure 2.1 – Particle grading curves of shiv from different origins/countries, [Gourlay, 2008]	57
Figure 2.2 – Shiv specimen [Cerezo, 2005].....	60
Figure 2.3 – Monotonic (blue) and cyclic (pink) compressive tests on hemp aggregate specimens [Cerezo, 2005].	61
Figure 2.4 – Sorption and de-sorption isotherms of shiv at 20°C [Garnier, 2000]. ..	63
Figure 2.5 – Water absorption of shiv in vacuum oven at 78°C, [Gourlay, 2008].	64
Figure 2.6 – Mass gain of immersed hemp shiv aggregate [Cerezo, 2005].	65
Figure 2.7 – Thermal conductivity of hemp shiv as a function of bulk density [Cerezo, 2005].	66
Figure 2.8 – 180 day old THB-52.5R mortar specimen	87
Figure 3.1 – Shiv (left) and Oil Seed Rape straw (right).....	96
Figure 3.2 – Vicat apparatus for determining standard consistence and setting times (www.controls-group.com).	98
Figure 3.3 – Automatic mortar mixer [www.controls-group.com].	99
Figure 3.4 – Steel mould used for casting mortars [www.controls-group.com].	102
Figure 3.5 – Typical mortar flexure and compressive test.	103
Figure 3.6 – Electromechanical sieve shaker, [www.controls-group.com].	105
Figure 3.7 – Mix proportions by percentage mass of the three mixes studied	108
Figure 3.8 – Pan mixer, weighed constituent materials and mixed material.	114
Figure 3.9 – Casting procedure for fresh hemp-lime material	116
Figure 3.10 – Capped and un-capped composite specimens.....	117
Figure 3.11 – De-moulded composite specimen.	117
Figure 3.12 – De-moulded composite specimens standing on mesh.	118
Figure 3.13 – Composite specimen end cutting using a band saw (left) and stone cutting saw (right).	119
Figure 3.14 – Equipment for capping (left) and use of tri-axial spirit level for the capping of the first end.....	120
Figure 3.15 – Capped composite specimen.	121
Figure 3.16 – Stress vs. Strain comparison of different strain measurement techniques.	123
Figure 3.17 – Typical compression test setup.....	124
Figure 3.18 – Respective phenolphthalein stains on 28 day and 180 day old THB- 52.5R hemp-lime and mortar specimen.	126

Figure 3.19 – Setram-92 high resolution TGA/DTA analyser with expanded view of crucibles.....	127
Figure 3.20 – Typical TG plot for a partially carbonated sample of hemp binder...	128
Figure 4.1 – All particle distribution curves for OPP and NPP samples.....	135
Figure 4.2 – Average particle distribution curves for OPP, NPP, HB and CB samples.	136
Figure 4.3 – Typical hemp fibre material from material grading process.....	137
Figure 4.4 – Water absorption curves for NPP hemp shiv.....	139
Figure 4.5 – Water absorption curve of first hour of immersion for NPP shiv.	140
Figure 4.6 – Bulk density development over time of standards sand mortar prisms.	145
Figure 4.7 – Flexural strength of all binders at all testing ages.	148
Figure 4.8 – Compressive strength of all binders at all testing ages.....	148
Figure 4.9 – Mortar carbonation depth analysis for a 91 day old NHL5 specimen.	150
Figure 4.10 – Mortar carbonation depth analysis for a 180 day old NHL5 specimen.	151
Figure 4.11 – Average carbonation depth of all mortars at all testing ages.	153
Figure 4.12 – Carbonation vs. Compressive strength over age for pre-formulated binders.	154
Figure 5.1 – Phenolphthalein stain on a 28 day SH-275 hemp-lime specimen within 5 seconds of spraying.....	158
Figure 5.2 – Phenolphthalein stain on a 28 day SH-275 hemp-lime specimen one minute after spraying.....	159
Figure 5.3 – Phenolphthalein staining on a 28 day FR-275 (above) and SH-275 specimen (below).....	161
Figure 5.4 – Colour change seen in phenolphthalein according to pH level [Lawrence, 2006].	162
Figure 5.5 – Carbonation depth development against sqrt. of carbonation age for THB52.5R composite specimens.	165
Figure 5.6 – Carbonation depth development of FR-275 specimens.	167
Figure 5.7 – Effect of density of hemp-lime on K_c and t_{50} for binder THB52.5R. ...	170
Figure 5.8 – dTGA results for core sample of 14 day THB52.5R-275.	172
Figure 5.9 – Heat flow chart of 14 day THB52.5R-275.	173
Figure 5.10 – Typical methodology for the determination of the start and end temperatures of dehydroxylation and decarboxylation mass loss phases in edge samples of hemp-lime specimens.	174

Figure 5.11 – Typical methodology for the determination of the start and end temperatures of dehydroxylation and decarboxylation mass loss phases in core samples of hemp-lime specimens.	175
Figure 5.12 – TGA mass loss curve for hemp shiv and OSR particles.	177
Figure 5.13 – TGA analysis of fresh binder	179
Figure 5.14 – TGA mass loss curves for 0.4w/b ratio THB52.5R pastes.	181
Figure 5.15 – TGA mass loss curves for 0.5w/b ratio THB52.5R pastes.	182
Figure 5.16 – CO ₂ content development of the two curing regimes.	185
Figure 6.1 – Typical THB52.5R-275 specimen prior to testing.....	196
Figure 6.3 – THB52.5R-220 specimen failure tested in the same orientation as fabrication (left). THB52.5R-220 specimen failure tested in the reverse orientation as when fabricated (right).	208

LIST OF TABLES

Table 2.1 – Chemical composition of shiv from current literature.....	55
Table 2.2 – Shiv bulk density values from current literature.....	58
Table 2.3 – Shiv particle density.....	59
Table 2.4 – Binders used in current literature [Lawrence, unpublished; Hustache & Arnaud 2008].....	67
Table 2.5 – Mineral content of ordinary Portland cement.	70
Table 2.6 – Constituent ratios, fabrication and curing methodoogies from previous publications.....	73
Table 2.7 – Mechanical performance of hemp-lime from current literature [Lawrence, unpublished; Hustache & Arnaud,2008].	78
Table 2.8 – Carbon dioxide emissions of a typical cavity wall and a comparative hemp-lime wall [Bevan & Woolley, 2008].	79
Table 2.9 – 100 year potential environmental impact associated with the fabrication of 1m ³ shuttered hemp-lime wall on a timber frame [Boutin et al., 2005].....	81
Table 2.10 – Chemical composition of hemp shiv [Carcia-Jaldon, 1992].....	83
Table 2.11 – Chemical solutions used to indicate carbonation [Parrot, 1990].	87
Table 2.12 – TGA regimes followed by different researchers [Lawrence, 2006].	89

Table 2.13 – Thermal decomposition temperatures of hydrated compounds [Ellis, 2000; Ubbriaco & Tasselli, 1998].....	90
Table 3.1 – Mass of distilled water required to achieve standard consistency for VICAT testing.	99
Table 3.2 – Particle size distribution of CEN standard sand in accordance with BS EN 196-1:2005.....	101
Table 3.3 – Speed of mixer blade according to BS EN 196-1:2005.....	101
Table 3.4 – Wet and dry cylinder masses and densities.....	110
Table 3.5 – Composite specimen fabrication matrix.	113
Table 4.1 – Comparison of shiv storage conditions.....	133
Table 4.2 – Mean percentage of material passing each sieve.....	134
Table 4.3 – Vicat test results for initial setting times.....	143
Table 4.4 – Bulk density development of all standard sand mortar specimens from 14 to 360 days.	144
Table 4.5 – Flexural and compressive strength results for all mortar specimens at all testing ages.....	147
Table 4.6 – Average carbonation depth, range of results and average carbonation rate for all mortar specimens.....	152
Table 4.7 – Interval carbonation rates of all binders.....	152
Table 5.1 – Average carbonation depths, rates and interval carbonation rates for all composite specimens at all curing ages. * indicates readings taken from large specimens.	164
Table 5.2 – Mean carbonation constants and time for full carbonation to take place in all binder types and densities. * indicates readings taken from large specimens.	169
Table 5.3 – CO ₂ sequestration values for specimen densities and constituent ratios used within this investigation.....	178
Table 5.4 – Embodied mineralogical content of fresh binders.....	179
Table 5.5 – Ca(OH) ₂ and CaCO ₃ developmet of THB52.5R binder pastes over time	183
Table 5.6 – Edge and core CO ₂ sequestration development over time for all binders.	184
Table 5.7 – Average CO ₂ content and sequestration values for all binders at all ages.	186
Table 5.8 – Total CO ₂ sequestration values, including hemp shiv, for all binders and bulk densities of large specimens.	187
Table 5.9 – Calcium hydroxide content comparison of 353 day cured binders against fresh binders.....	189

Table 6.1 – Mean bulk densities of specimens at all testing ages. Symbols † and * indicate results obtained from one and two specimens respectively.	193
Table 6.2 – Mean dry bulk densities of specimens at all testing ages. Symbols † and * indicate results obtained from one and two specimens respectively.	194
Table 6.3 – Mean bulk density of small specimens used for phenolphthalein testing compared to large specimens used for strength testing.....	197
Table 6.4 – Mechanical characteristics of all specimens at all ages. Symbols † and * indicate results obtained from one and two specimens respectively.	200

GLOSSARY

CaCO_3	Calcium Carbonate
CaO	Calcium oxide
Ca(OH)_2	Calcium hydroxide
CI	Cementation Index
CO_2	Carbon dioxide
C_2S	Bicalcium silicate - Belite
C_3S	Tricalcium silicate - Alite
C-S-H	Calcium silicate hydrate
H_2O	Water
PC	Portland cement

CHAPTER 1 - INTRODUCTION

1.1 Introduction

This chapter introduces the subject of hemp-lime construction by outlining its historical background, its current use and potential future developments. Initially a broad overview of renewable construction materials use in the UK is presented, followed by the outline of the benefits and potential limitations of hemp-lime. This leads on to the main subject of this thesis in which the aims and objectives are outlined.

1.2 Renewable materials in construction

Earth's mineral resources are finite. Mining fossil fuels scars the landscape, irrecoverably harms biodiversity, is energy intensive, inefficient and does not provide a sustainable solution to climate change and job security. Since the

beginning of the Industrial Revolution (taken as the year 1750), the burning of fossil fuels has contributed to a 40% increase in the atmospheric concentration of carbon dioxide [Blasting, 2013]; it is expected to grow rapidly with globalization and population growth. The increasing buildup of carbon dioxide in the atmosphere is worrying and significant pressure is on the construction industry to reduce its carbon emissions [Stern, 2006]. The UK has committed to reducing carbon emissions by 80% by 2050 [HM Government, 2008]. Renewable materials can be produced indefinitely with strong environmental benefits. Materials such as hemp, jute, flax, sisal, bamboo, coco/palm fibres, natural mineral wools, straw and timber fibres are increasingly being used as structural and/or thermal insulation in low-energy, passive buildings where sustainability, carbon emissions and social responsibility are principle decision motivators in the design process.

Lighting, heating and cooling buildings generates approximately 40% of Britain's CO₂ emissions while the production of building materials accounts for a further 10% [Constructing Excellence, 2008]. In total 400 million tonnes of materials get delivered to site each year. Of these 60 million tonnes go straight to landfill due to over ordering, damage resulting from poor storage or because of inappropriate ordering [Barker, 2008].

Governmental policy is driving the need to use low energy intensive and natural building materials within construction. Guidelines such as the Code for Sustainable Homes (CSH) and groups such as the UK Green Building Council aim to influence the industry to reduce net CO₂ emissions by 80% (compared to 1990 figures) [HM Government, 2008] by 2050 whilst ensuring 90% carbon savings for all new housing by 2016. Industrial fibre production also ties in with sustainable farming policies [DEFRA, 2013]. Although carbon savings are to be achieved primarily by reducing energy consumed during building use, reductions can also be achieved through the adoption of renewable construction materials within the fabric of buildings as all plants store carbon during its growth. Furthermore, when used as insulation materials, renewable materials such as hemp-lime and straw bales have the ability to regulate the internal thermal and relative humidity microclimate to within healthy boundaries using comparatively minimal heating energy

[Evrard & De Herde, 2006; Arnaud, 2009; Elfordy et al., 2008; Cerezo, 2005; Evrard, 2003; Arnud & Cerezo, 2001]. Concurrently the carbon footprint of the building is drastically reduced and social perception can be changed to more widely accept this logical change in construction trends.

Renewable and natural building materials clearly have a place in the modern UK construction industry, however, for them to become more main stream empirical and analytical research into these materials and technologies must form the foundations for future development.

It is generally accepted that the construction industry and buildings have to become more energy efficient and sustainable. To encourage this, government policy initiatives such as The Code for Sustainable Homes [CSH, 2013], Landfill Tax [HMRC, 2013], Aggregates Levy [HMRC, 2013a] and The Sustainable and Secure Buildings Act [SSBA, 2004] have been introduced to encourage greater adoption of low carbon and low waste building solutions. Concurrently, certification schemes such as BREEAM and LEED Have been set up with the aim of grading buildings and the construction projects based on their environmental credentials; an attractive proposition to designers and contractors as the better the grading, the more desirable the building may be to prospective buyers.

1.3 Hemp-lime

Hemp-lime (also known as Hempcrete or hemp & lime) is a sustainable, ecological and renewable composite material currently used in a growing variety of construction applications. Hemp-lime is composed of three main constituents: hemp shiv, a lime-based binder and water.

1.3.1 Hemp-shiv

Hemp has been grown for millennia in Asia and the Middle East for its fibre with hemp fibre imprints found in pottery shards in China and Taiwan over 10,000 years ago [Abel, 1980]. It was also later used to make clothes, shoes, ropes and an early form of paper [Stafford, 1992]. Commercial production of

hemp in the West commenced in the eighteenth century but due to higher demand for rope from the navy hemp has grown in eastern England since the sixteenth century [Bradshaw et.al., 1981].

Like the marijuana plant, industrial hemp belongs to the species *Cannabis sativa L.* However, unlike marijuana, it only contains small quantities of the psychoactive drug delta-9 tetrahydrocannabinol (THC) [AAFC, 2013]. Throughout its history the plant's versatility has meant its seeds, fibres, flowers and oils have been used in a wide variety of applications including agriculture, maritime, automotive industries, cosmetics, furniture, paper, textile and food stuffs [Khestl 2010].

The recent increase in demand from the automotive and construction industries for differing parts of the industrial hemp plant have resulted in an increase in cultivated area across Europe with France, Germany and the UK contributing to approximately 78% of the total number of hectares harvested (Figure 1.1).

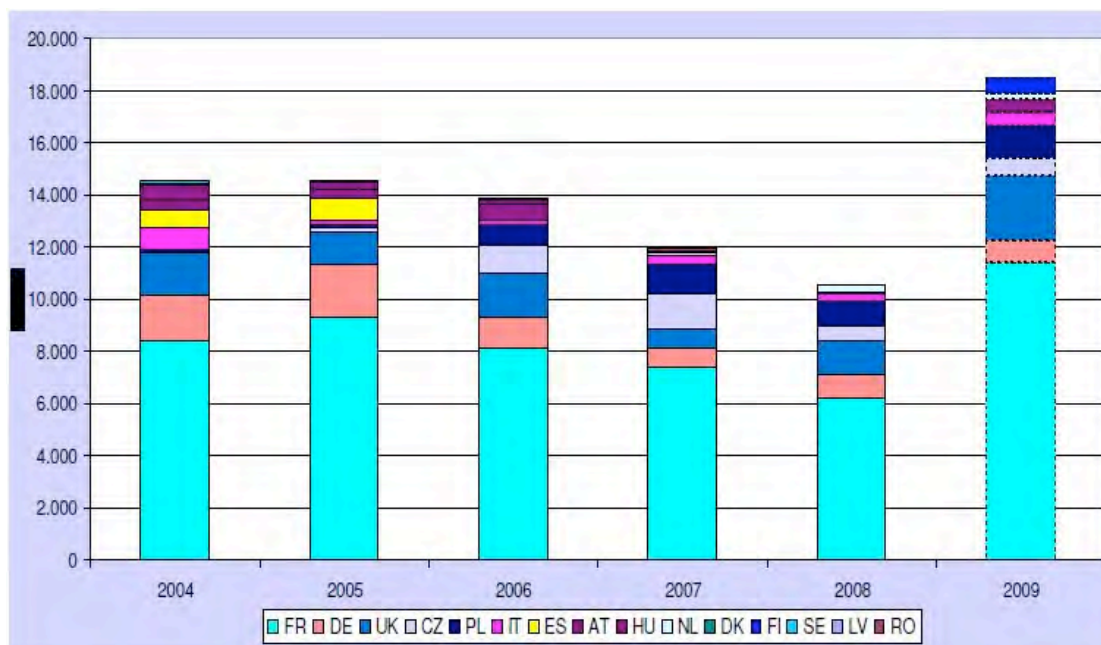


Figure 1.1 – Total number of hectares per European member state that contributes with industrial hemp production [European Commission, 2009].

Industrial hemp (hemp) is one of the fastest growing biomasses in the world [Dewey & Merrill, 1916] after certain types of bamboo and once established in the soil, growth rates of 15-25mm per day may be observed. Planted in April and harvested in August, hemp can be used as a break crop to cereal and is nutritionally beneficial to the soil [HempTechnology website, 2010]. Hemp has a deep rooting system and curtails the presence of nematodes and fungi [Piotrowski & Carus, 2011]. After cultivation, the soil is left in optimum conditions due to the complete weed suppression; previous studies report 10–20 percent higher wheat yields after the cultivation of hemp [Bócsa & Karus, 1998]. Furthermore, due to its vigorous growth, hemp is known to be a pioneer plant that can be used for land reclamation; suitable to remediate land polluted by heavy metals (phytoremediation), [Kozłowski et al. 2004].

Hemp's growth rate, shading capacity and disease resistance means that the crop can be grown without the use of herbicides, pesticides or fungicides. Hemp therefore easily complies with requirements of organic farming and is suitable for cultivation near surface water. In practice, no pesticides are applied in the UK, Germany and the Netherlands. Only in France, approx. every eight years an application against the hemp flea beetle (*Psylliodes attenuatus*) is common. Moreover, hemp has been shown to be resistant to most herbicides which precludes its use in the first place [Piotrowski & Carus, 2011].

Current UK yields range between 5.5 to 8 tonnes per hectare (t/ha), which are in line with other European yields quoted at between 3.5t/ha to 7.5t/ha [HempTechnology website, 2011]. On average the plant will attain 2.5 – 4m in height when harvested, where it will be cut and generally left lying in the field, a process called retting, for the moisture content to reduce from 90–95% to approximately 12% before baling and storage for processing.

The hemp crop contains three fractions; hemp fibre, shiv and dust/fines. In the UK these fractions are mechanically separated (by hammering) and converted into baled hemp fibre, bagged shiv and fuel logs respectively. Continental hemp producers use retting as a means of naturally allowing the fibres to separate from the stem. No chemicals are used in the processing of

hemp crops. The main markets for hemp fibre are currently within the automotive, paper and the textile industries. The shiv is primarily used as high quality horse bedding but has recently experienced an increasing demand within the construction industry and the solid fuel logs are sold to be used in wood or coal burning stoves.

Making up 40-60% of the plant by mass [Evrard, 2003] hemp-lime uses the woody core of the plant stalk known as shiv (also known as hurds) as shown in Figure 1.2. The core is then processed (by hammering) into shiv particles (Figure 1.3) before being bagged and distributed.



Figure 1.2 – Dried stalk of the hemp plant showing the woody core and unwrapped fibres [Wikipedia, 2009].



Figure 1.3 – Typical hemp shiv particles processed from the woody core of the industrial hemp plant [Hemp Technology website, 2008].

1.3.2 Binder

Binders create a connective matrix between the shiv particles whilst also providing fire and fungal protection. Once hardened in the composite material, the binder matrix also provides the primary load path through which compressive stresses can be transmitted.

Lime has been used as a binder in construction for thousands of years, examples of which have been found in Palestine and Turkey dating back from 12000 BC [Von Landsburg, 1992]. Lime is commonly produced from carbonate rocks which constitutes 4% of the earth's crust and is made up from particles of shells or corals deposited on the sea bed over millennia. Over this time, and along with the high pressures within the sea bed, the sedimentary rock is formed and can later be quarried once plate tectonics have moved the sea bed up onto land [Allin, 2005].

Generally, there are three categories of lime binders used for hemp-lime construction:

Air Lime: Air lime is a non-hydraulic lime (it does not set or harden under water) produced from relatively pure quarried material that sets initially by drying and subsequently and more significantly through the process of carbonation. Compressive strengths at 28 days vary typically from 0.5 – 2N/mm², depending on lime:aggregate proportions and fine aggregate characteristics. Air lime is produced from burning crushed limestone, chemically known as calcium carbonate (CaCO₃). When heated (calcined) CO₂ is driven off to produce quicklime (also known as lump-lime or burnt lime), chemically known as calcium oxide (CaO). The product is then hydrated (slaked) by adding a predetermined amount of water, causing a vigorous exothermic reaction resulting in a fine, dry, hydrated lime powder, chemically known as calcium hydroxide (Ca(OH)₂) which is then packed or bulk stored and used widely including within the construction, agricultural, steel and water industries. Once mixed and applied in construction, either as a mortar, plaster, render or in conjunction with hemp shiv, the process of carbonation begins whereby atmospheric CO₂ is absorbed into the binder matrix causing a setting reaction to take place. The reaction converts the calcium hydroxide back into its original mineral calcium carbonate completing what is known as the 'Lime cycle' (Figure 1.4). This absorption of CO₂ offsets, to some extent, the CO₂ given off during the production of air lime binders.

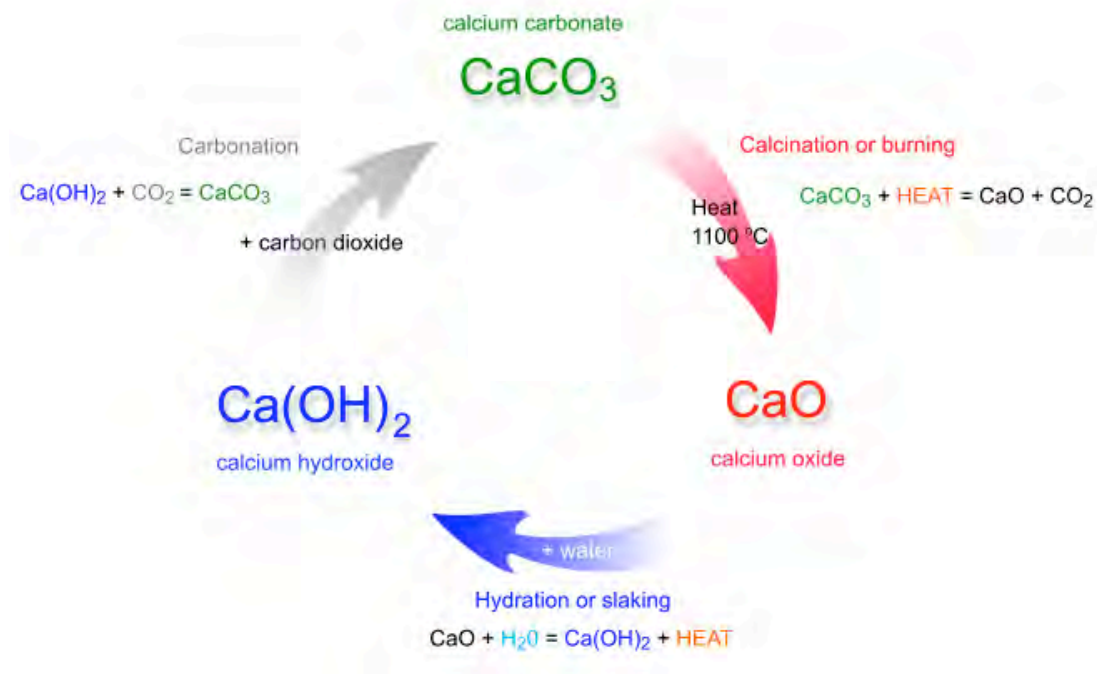


Figure 1.4 – The lime cycle [www.naturalhydrauliclime.com]

Natural Hydraulic Limes (NHL): Hydraulic limes have the ability to set and harden under water, as a result of containing clay impurities within the quarried material. To be classified as an NHL no performance enhancing additives have been artificially added. NHLs are produced in the same manner as Air Limes, however NHLs set using a combination of a hydraulic set (hydration) and carbonation. NHLs are categorized into three groups by BS EN 459-1:2010: NHL2 (feebly hydraulic), NHL3.5 (moderately hydraulic) and NHL5 (eminently hydraulic). The number indicates the minimum 28 day compressive strength of the binder when prepared in rich mix with standard sand. The final type of lime produced depends on the mineralogical makeup of the raw material and the temperature at which it was manufactured.

Formulated binders: Historically hemp-lime was made by mixing hemp shiv, water and either air lime, cement, natural hydraulic lime binders or a mix of the aforementioned. These options had limitations: air limes, setting through the process of carbonation, can take a significant amount of time to harden. The properties of natural hydraulic limes can be inconsistent as the mineralogical make-up is dependant on the origin of the raw material.

Cements only set via hydraulic reactions and are therefore highly dependant on the availability of free water; when mixed with hemp shiv and water, the hemp shivs absorption characteristics absorb large parts of the available free water thereby inhibiting the setting of the cement and causing a phenomenon called flouring. Flouring has been previously mentioned by researchers in France and is identified when cylinders display a hard outer shell along with a powdery core lacking in interparticular cohesion. Figure 1.5 shows a specimen displaying typical flouring symptoms. Currently the precise mechanism and/or reasoning for flouring is not fully understood.



Figure 1.5 – Specimen displaying flouring during preliminary investigations.

Modern construction demands consistency and with this in mind formulated lime binders were developed specifically for hemp aggregates. Formulated lime binders are a dry blend of air lime, cement, pozzolanic material and other minor but important additives. As a result, the majority of current hemp-lime construction projects use formulated binders. These binders contain varying quantities of hydraulic cements, pozzolans, and other additives to improve properties including dispersion and permeability. There are four main pre-formulated binders in the hemp-lime industry, manufactured by two different companies. A collaborative development

between Lhoist, a major lime producer, Hanson and Lime Technology distribute Tradical® hemp binders in the UK. Similar binders are produced by Lhoist in Germany, France and Spain. The characteristics of these similar binders vary as a result of the variation in properties of raw materials. All Tradical® hemp binders use hydrated CL90 high calcium air lime based, manufactured by Lhoist to BS EN 459-1. The fourth commonly used pre-formulated binder, Batichanvre, is produced by St. Astier in France however due to patent protection it is not possible to obtain the exact constituent proportions for these binders along with the exact type of additives.

1.3.3 Water

Clean water is essential to produce a workable mixture and for activating the reactive hydraulic elements within the formulated binder. The ratio of water can be adjusted to suit different climates, final desired bulk densities, building and/or application techniques. Much of the initial mix water is absorbed by the hemp shiv aggregates and is not available for the binder hydraulic elements. The subsequent drying of the composite material governs its suitability for use.

1.4 Historical and current use of hemp-lime

There are numerous Oak framed buildings in the Champagne region of France that were originally in-filled with wattle and daub [Allin, 2005]. The use of hemp-lime resulted from the need to mimic the behaviour of these original materials during restoration, where previous repairs carried out during the 1950's and 1960's on timber framed buildings with cement had caused disastrous results. Hemp-lime's inherent flexibility and vapour permeability were found to be complementary with the original building materials. Hemp-lime was also considered to be more consistent than the original infill materials, a favourable characteristic within the construction industry.

The first example of the use of hemp-lime was in 1986 in France with the renovation of the Maison de la Turquie in Nogent-sur-Seine by the innovator Charles Rasetti [Ceyte, 2008] (Figure 1.6). During the 1980's and 1990's the use of hemp-lime then grew within the construction industry, primarily in France, where the practise is now widespread with many thousands of buildings now completed.



Figure 1.6 – Maison de la Turquie. Timber frame with hemp-lime infill [Ceyte, 2008].

The first UK hemp houses were constructed in 2000 in Haverhill for the Suffolk Housing Society as part of a social housing development [Yates, 2002]. A total of 18 houses were constructed; 16 using traditional construction methods and materials and two using hemp-lime which would be scientifically monitored by the Building Research Establishment (BRE). The development at Haverhill was to some degree an experimental project

from the outset and intended to allow a comparison to be made between 'hemp' houses and those of traditional construction [Yates, 2002]. Results were favourable with the hemp houses requiring less energy to maintain the same internal temperature as the traditionally built houses.

Completed in 2009, The Renewable House (Figure 1.7) is one of the most technologically advanced dwellings made from hemp-based materials. The first US building constructed of hemp-lime materials was completed in August 2010 in Asheville, North Carolina (Figure 1.8).



Figure 1.7 – The Renewable house at the BRE [www.nnfcc.co.uk].



Figure 1.8 – Hemp-lime house in Asheville, North Carolina
[www.hemp.com, 2011].

Modern UK commercial projects include the new Lime Technology headquarters in Oxfordshire, the Wales Institute for Sustainable Education (WISE) and the award winning Adnams brewery distribution centre (Figure 1.9) which used 90,000 hemp blocks which is the largest use of hemp-lime used to date. Other examples of hemp-lime construction can also be found in Sweden [Bruijn, 2012].



Figure 1.9 - Adnams distribution centre [www.fabricarchitecture.com,

2008].

1.4.1 Construction techniques

The primary function of hemp-lime in the modern UK construction industry is to create an exterior insulating vapour permeable fabric that provides protection against the cold, heat, noise and humidity of the outside world, whilst also passively regulating the interior microclimate of a building to within acceptable and healthy boundaries of temperature and relative humidity. Figure 1.10 illustrates the different locations hemp-lime can be used in a building along with examples of different exterior finishes which can be incorporated showing both timber weathering boards or lime based renders.

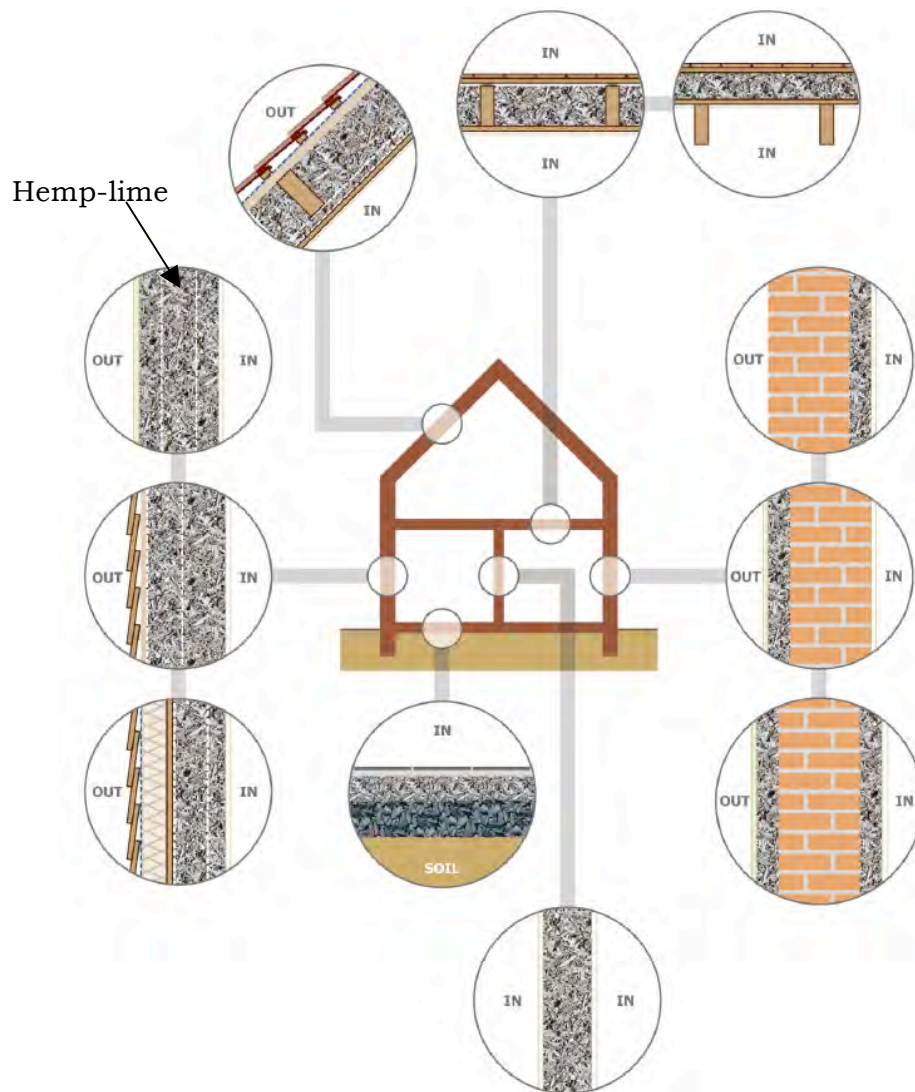


Figure 1.10 – Finished hemp-lime wall surrounding a timber primary structure [Evrard, 2008].

The main use of hemp-lime in the UK is within non-structural applications (mainly in walls), where the material is used in conjunction with a primary building structure, generally timber rather than steel (to avoid condensation issues and cold joints). Once in place and to the desired depth, usually between 250mm and 500mm, it is left to set and dry before compatible (usually lime based) renders and plasters are applied to both sides to finish. There are currently four different methods in use for the application of hemp-lime:

Casting - This application method refers to any process whereby the constituents are mixed in batches and then manually inserted into the wall cavity separated by shuttering and tamped by hand. Casting guidelines are described in “*Règles professionnelles d’exécution d’ouvrages en bétons et mortiers de chanvre*” [Chanvre, 2007]. Casting is the main method used in most countries as, with the use of efficient removable shuttering (Figure 1.11) or temporary waterproof shuttering, construction can proceed rapidly on small to medium sized projects. The use of permanent shuttering on either one or both faces is now becoming commonplace with the UK construction industry. Manual application of hemp-lime is also the most commonly used method of specimen fabrication in empirical investigations.

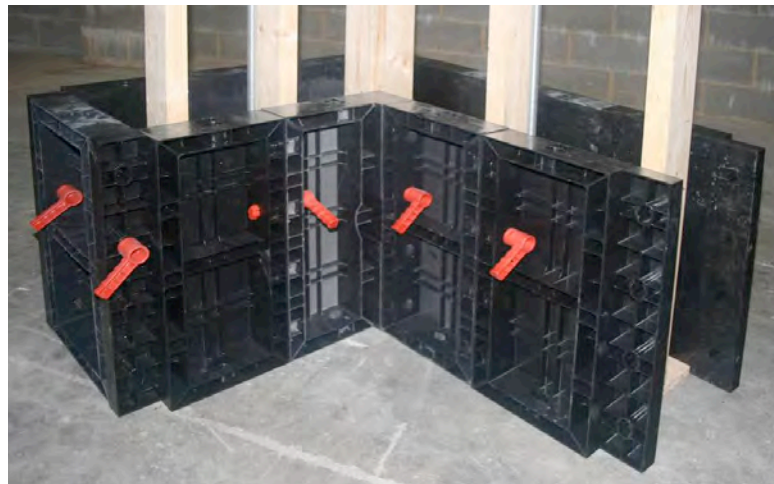


Figure 1.11 – Efficient removable shuttering currently used in the UK hemp-lime construction industry [Lime Technology website].

Spraying – Mechanical spraying is employed on larger projects as the use of specialist equipment and operatives is costly. The technique spraying the material towards the wall, floor or roof cavity where it is being applied (Figure 1.12) where one layer of waterproof plywood has been temporarily placed. The characteristics of spray applied hemp-lime have been documented in a number of publications [Elfordy et. al, 2008; CSTB, 2007]. Spraying is not as favoured as casting as there are high levels of waste (~10%) [Ian Pritchett pers. comm. March 2008].



Figure 1.12 – Spraying of hemp-lime [Lime Technology website].

- **Blocks** – Blocks are becoming more mainstream in the hemp-lime construction industry in France as the majority of contractors are familiar with laying blocks, effectively ‘de-skilling’ the building site. Such blocks are not strong enough to be used for structural elements; they must be supported by a brick, timber, or steel frame (Figure 1.13). Each block produces about one tenth of the CO₂ of a conventional concrete block [www.fabricarchitecturemag.com] and are bonded with, for example, an NHL mortar.



Figure 1.13 – Hemp-lime block wall.

Prefabrication – Many other construction materials (such as straw bales, panelised systems, timber frame modular structures) suit themselves to prefabrication. Advantages of off-site fabrication include greater consistency, higher accuracy, and improved building efficiency. Modcell® in the UK has patented a panelised construction system using a load bearing timber frame infilled with straw bales (Figure 1.14). Recent trials using hemp-lime as infill material and then rendered with lime have been carried out. To date no projects have been completed using Modcell® panels due to practical (hemp-lime must dry enough for renders to be applied) and cost implications (£150/m³ for hemp-lime compared to £18/m³ for straw bales).



Figure 1.14 – Prefabricated panel filled with hemp-lime drying before being rendered [www.recycledarchitecture.blogspot.no].

1.4.2 Material advantages

The use of hemp-lime in construction is increasing as the advantages of the materials are better understood and conveyed to the public. These advantages include:

- **Simplified construction profile** – in its minimal state, hemp-lime may consist of three layers; render, hemp-lime and plaster. Compared to other methods hemp-lime does not require the use of membranes, tapes, cavities, plasterboards.
- **Favourable hygrothermal properties** – due to the particular pore structure [Evrard, 2008] both the hemp shiv and the binder offer, this lightweight material is able to buffer external temperatures with a 12 hour time delay, i.e. when hot outside, the interior will be kept cool

and visa-versa; concurrently the material controls the internal RH environment to within healthy limits [Bevan & Woolley, 2008]. This attribute reduces real time energy costs to both private and commercial property owners [Yates, 2002]. There is also no cold bridging as the timber used in the primary structure has very similar thermal property values as hemp-lime; this also eradicates issues of condensation between the two different construction materials [Evrard, 2003].

- **Reduced carbon footprint** - Like all plants, hemp stores carbon during its growth as a result of photosynthesis. Following carbonation, hemp-lime has been marketed as being a 'better than zero carbon footprint' material, storing up to 135 kg of CO₂/m³ and is one of the most carbon friendly building materials currently available on the market [Bevan and Woolley, 2008; Boutin *et al.*, 2005, Lime Technology website, 2011]. The use of hemp-lime in building construction directly replaces high energy and/or petrochemical materials, such as concrete, fired clay bricks and foam insulation products.
- **Air tight but breathable and flexible** – UK building codes require air tightness values of 10 air changes per hour or less [CSH, 2013]. Hemp-lime construction provides a homogenous and monolithic insulative layer between the chosen exterior rain screen and the interior wall finish providing air tightness values well within building regulation requirements (subject to good window and door frame fitting) of 2 air changes per hour or less [Lhoist Tradical factsheet]. It also naturally permits the diffusion of air and water vapour through the wall, contributing to the low maintenance of the building fabric as it does not trap moisture.
- **Fire resistant and durable** – The highly alkaline lime content in the binder provides good protection against fungal and insect attack both for the hemp-lime and the timber structure it surrounds. For similar reasons, hemp-lime has demonstrated more than adequate fire

resistance characteristics in accordance with UK building regulations as the binder encases the shiv particles whilst at the same time the material encases the timber primary structure.

- **Reduced waste and recyclability** – Hemp-lime reduces construction waste as the material is mixed on-demand at the building site. It is also made using highly consistent constituent materials, minimising the risk of rejection as a result of faulty and/or damaged materials.

1.5 Aim and objectives

There is very limited understanding of hemp-lime performance characteristics compared to other modern construction materials, such as timber and concrete. Hemp-lime is marketed as a carbon negative building material and where 100% of the calcium hydroxide content in the lime based formulated binders is assumed to carbonate into calcium carbonate. However, there are no empirical data pertaining to the determination of how much carbon dioxide is absorbed by the binder and locked into the building fabric. These data are necessary to verify any assumptions which are made related to the carbon sequestration potential of hemp-lime. It has been found that the degree of carbonation in a 360 day old pure lime mortar can vary between 38.5-95.6% [Lawrence, 2006] depending on the type of aggregate, the porosity and the fabrication and curing methodology of the mortars. This introduces a large degree of uncertainty into how much hemp binders may actually be carbonating when used within the building fabric.

The aim of this thesis is to characterise the properties lightweight hemp-lime mixtures, relating microstructural and chemical properties with physical development of the material. This aim will be fulfilled by completing the following objectives:

- To review, improve, verify and document fabrication, curing and testing techniques for the empirical investigation of hemp-lime and its constituents.

- To further characterise the material as it currently stands in the UK construction industry paying particular attention to mix proportions, density and compressive strength.
- To document the progression of the carbonation front across the material cross-section under laboratory conditions both within the composite and the standard sand mortar prisms.
- To empirically determine the amount of CO₂ the binder within the composite could sequester over the whole life of a building.
- To provide a preliminary understanding of the hydration reaction within the binder and the amount of CO₂ this phase of the binder could contribute towards the total sequestration value of the composite material.

1.6 The structure of this thesis

This thesis is comprised of seven main chapters. The following chapter collates and reviews public and scientific publications which are relevant to hemp-lime construction and empirical studies. Particular emphasis is given to the study of mechanical behaviour, overall material characterisation and chemical testing techniques of mortars and cements for incorporation into the main programme of work.

Chapter 3 sets out the programme of experimental work for material characterisation and both the mechanical and chemical tests undertaken. It also includes the results of preliminary tests which were carried out to refine and focus the main body of investigation such as methods for predicting fabricated bulk densities, differing storage conditions and tests comparing various methods for calculating strain measurements of cylinders under compression testing. Chapters 4, 5 and 6 present the characterisation, chemical and mechanical results of these tests respectively along with discussion and comparison to previous investigations and other materials used within the same applications.

The industry implications of the results along with overall conclusions and recommendations for further work are presented in Chapter 7.

CHAPTER 2 - LITERATURE REVIEW

2.1 Introduction

This chapter aims to review popular literature and empirical investigations which have been published on hemp-lime and its constituents paying particular attention to those related to the core objectives of this investigation. In the first instance a general overview of the development of publications is presented. Subsequently literature related to hemp-lime constituents will be reviewed including origins, binder chemical reactions and testing methodologies. Literature related to hemp-lime as a composite will then be reviewed including its practical use and up-to-date laboratory testing. The outcome of this review will help determine, refine and outline testing methodologies to be used within the programme of work.

2.2 Historical and current publications

The precise details of the very beginning of the hemp-lime building system are not known [Allin, 2005] however, Hustache & Arnaud [2008] suggest the first practical use of hemp-lime was more than 25 years ago when shiv was mixed with lime binders for use as an infill material during the restoration of timber framed houses. Furthermore Ceyte [2008] proposed that Maison de la Turque was the first practicable application. The material's use was not the result of any scientific development but rather the consequence of a process supported or practised by artisan craftsmen: an example of a transfer from the building site to the laboratory. The first scientific investigations were carried out in the early 1990's and concentrated on simple characterisation of the materials and building processes [Garcia-Jaldon, 1992; Courgey, 1993; Van der Werf, 1994]. Subsequent investigations focused on preliminarily understanding the durability of the material and the hygrothermal characteristics hemp-lime [Cordier, 1999; Arnaud, 2000; Collet, 2004; Kioy, 2005]. Scientific investigations now largely focuses on numerical modelling of the acoustic and hygro-thermal characteristics of the material along with the structural contribution the material gives to a buildings primary structure [Cerezo, 2005; Goyer, 2007; Helmich, 2008; Evrard, 2009].

With empirical work on hemp-lime having been carried out in many countries from Sweden and Finland [Nikter, 2006; Brujin, 2008] to Canada and Switzerland [Deshenaux & Macheret, 2000; Butschi et al., 2003], there was need for synthesising the current knowledge into one document. Hustache & Arnaud [2008] have collated all current knowledge, the objective being *“to report on and analyses the current state of our knowledge of the scientific (physical, structural, hygrothermal etc.), economic, environmental and health aspects of this modern material”* and serves as a valuable reference tool.

A number of popular publications concentrate on furthering public awareness on the advantages of using hemp-lime compared to other more conventional building materials. Bevan & Woolley [2008], produced in collaboration with the Building Research Establishment and Lime Technology, currently provides the most comprehensive and holistic overview of the hemp-lime industry in the UK including legislative information, practical guides for self-builders, scientific data and architectural building element drawings. Allin [2005] provides a comparatively un-scientific publication, focussing on the history of the material, its current uses and how the material can be used for the exterior and interior design and aesthetics of the building. However, it does provide a detailed and well illustrated introduction to the practical use of hemp-lime and is a good source for beginners.

There are currently no national or international standards for the empirical fabrication or testing of hemp-lime and/or its constituents. Along with the popular publications published in the UK, a set of professional guidelines aimed at informing builders on the correct preparation and implementation of the material have been published by the “Construire en Chanvre” association in France [Chanvre, 2007].

2.3 Shiv

Over 30 countries produce industrial hemp including Australia, Austria, Canada, China, UK, France, Germany, Russia and Spain [www.azhemp.org, 2001; www.thehia.org, 2009]. France is Europe’s largest cultivator with approximately 10000 hectares annually in 2009 [European Commission AGRI 5, 2009]. The fibre is being increasingly used for the production of new materials such as composite fibres, insulating batts for the construction industry and pressure moulded parts for use in car manufacture [Boutin et al., 2005].

2.3.1 Origin and processing

It should be borne in mind that, because of its vegetal nature, there is an intrinsic variability in the characteristics of the hemp plant [Evrard, 2003]. Furthermore, Evrard states that the type of operation used for the transformation of the plant stem into shiv will have an influence on different factors such as the grain size of the particles, residual fibre rate, average length of the fibres, degree and composition of fines and the presence of other organic or mineral elements.

Bouyer [2008] identified the sources of variability that influence the quality and characteristics, including the porosity, of the raw material which include:

- Varietal selection and seed production.
- Date of sowing.
- The soil conditions.
- The weather.
- The topography.
- Fertiliser application.
- The maturity of the plant at harvest.
- The harvesting methodology.
- The processing methodology.

Table 2.1 presents the chemical composition values for shiv stated in various publications. Data presented by Allin does not state its sources or mention whether or not it is derived from peer reviewed sources.

Table 2.1 – Chemical composition of shiv from current literature.

Publication	Shiv origin	Biological make-up (%wt)					
		Cellulose	Hemi-cellulose	Lignin	Pectin	Extratives	Ash, Silica, Tannin & Other
Allin, 2005	France	37	16.5	21.8	5	8.9	10.8
Chanvre, 2007	France	45-60	15-20	15-30	-	-	-
Evrard, 2003 & 2008	France	50-60	15-20	20-30	-	-	4-5
C. Garcia-Jaldon, 1992	France	48	12	28	6	-	6
Kymäläinen & Sjöberg, 2008	Ireland	40-52	n/a	22-30	-	-	-

According to Evrard [2008] the resulting chemical composition indicates that shiv can thus be considered a type of wood; in addition their cellular pattern is close to Birch and Willow. The publications clearly show large differences in chemical composition, even from shiv harvested in the same country, with cellulose varying from 37-60% and lignin from 15-30 %. The reasons for these variations have not been made clear.

Gourlay [2008] compared cylindrical hemp-lime specimens whilst using shiv from ten different origins (different countries and/or national hemp producers) including France, Germany, UK and Belgium; attempts to distinguish how the morphological differences affected overall physical and mechanical properties were made. Although fundamentally useful, the

results were unreliable. The empirical constants included using the same binder (Tradical PF70), a constant compaction force during specimen fabrication and the same testing methodologies, however, only one specimen for each shiv type was tested and all the specimen bulk densities differed, varying between 247-386kg/m³. This does not allow direct comparison between the different shiv origins. Differences in specific surface areas and porosity were also identified by Gourlay [2008]. Specific surface areas ranged between 13.8m²/g and 29m²/g and porosity values between 2.2cm³/g and 3.4cm³/g were observed signifying both that differing processing methodologies (of the hemp plant into shiv) have an effect on the end product and that the porosity of the shiv as a function of the origin is extremely variable.

By only using shiv from one manufacturer and one growing season, these variations can be kept to a minimum in this investigation.

2.3.2 Granulometry

Evrard (2003) and Cerezo (2005) used the classical (vibration) sieving method (as commonly employed to determine the particle distribution curve of soil, sand and/or aggregates) to produce particle grading curves similar in shape but within different ranges; this may have resulted from different processing methods and/or from testing shiv from different manufacturers. Although straightforward, sieving shiv will only provide the investigator with the length of particles as a result of the particular motion the equipment imparts on the particles.

Presently, the majority of granulometry testing in France is now carried out using an optical system which has been developed by ENTPE (Ecole Nationale des Travaux Publics de l'Etat) [Ceyte, 2008; Hustache & Arnaud, 2008]. This method of analysis automatically calculates the length and breadth of each individual particle from a photographed group of shiv particles which has been spread out against a blank background. Apart from the depth of the particle, this method fully characterises the length and

width of the shiv; the data is then automatically graphed to empirically define the material.

The draft French standard for construction of hemp-lime walls [RP2C, 2006] specifies shiv should fall within the following parameters, *‘Particles in a parallelepiped form with widths between 1 and 5mm and lengths of 1 to 30mm. Granulometry (by sieve) with a maximum 5% by mass passing a 0.5mm sieve, around 90% by mass between 1mm and 4mm, and less than 3% by mass exceeding 4mm.’* However, no empirical evidence has been found by the author into why these particular guidelines specify the given ranges.

Gourlay [2008] has carried out the most comprehensive granulometric comparison between shiv from different origins and countries. A total of ten samples from France, UK, Germany and Belgium were manually sieved for a period of five minutes through a sieve tower reducing from 8mm to 0.5mm. Figure 2.1 presents the particle grading curves.

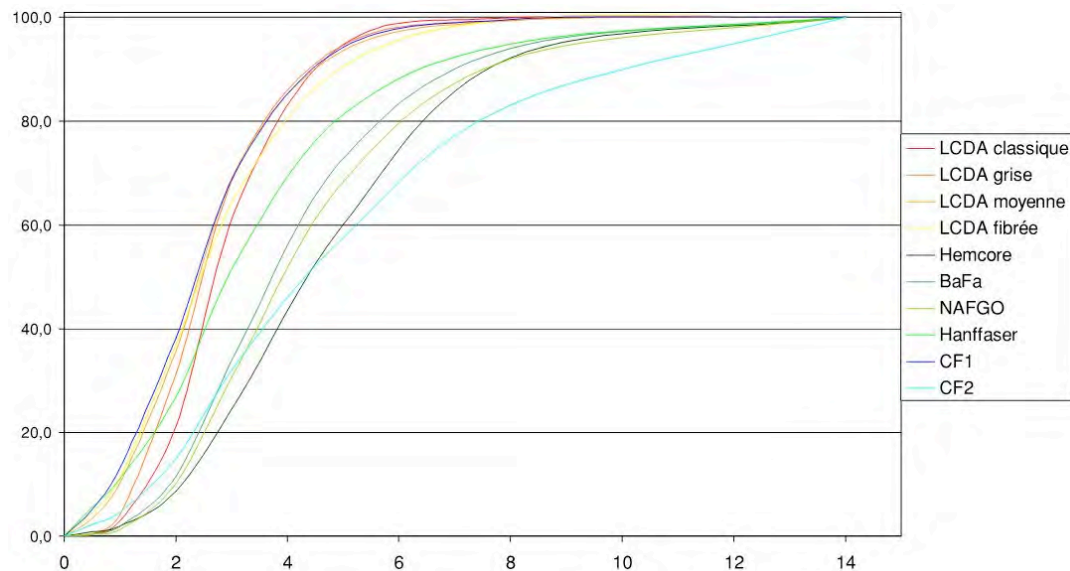


Figure 2.1 – Particle grading curves of shiv from different origins/countries, [Gourlay, 2008]

Above 8mm Gourlay found that bundles of hemp fibre would accumulate with trapped particles of shiv. None of the ten samples tested displayed particle grading curves that fell within the guidelines set out by the draft

standard. However the four samples originating from the same processing plant in the l'Aube region of France (LCDA) fell closest to the guidelines with an average of 85% of the mass of material falling between 1 and 4mm grading sieves.

Manufacturer literature from St Astier [Batichanvre, 2005] states that typical hemp to be used with their binders contains particles of shiv between 5 and 25mm in length however the literature does not state which is the manufacturer of hemp or which country it is produced.

2.3.3 Bulk and particle density

The values for bulk density (the mass of the particles, including voids, in a unit volume) of shiv under empirical investigation depend on a number of factors:

- Particle grading and orientation.
- Relative proportions of shiv, fibres and fines.
- The moisture content of the shiv.
- Whether or not any compaction is applied to the sample.
- The biological make-up (porosity, cellular density et.) of the shiv which is dependent on growing location and conditions.

Table 2.2 presents the bulk density of shiv from the available literature.

Table 2.2 – Shiv bulk density values from current literature.

Publication	Bulk density (kg/m³)
Evrard, 2003	110 – 150
Cerezo, 2005	~130
RP2C, 2006	~100
De Bruijn, 2008	98
Evrard, 2008	52 – 162
Nguyen, 2008	113
St Astier Literature	105 – 115
Chanvribat Literature	~100
Gourlay, 2008	62.2 – 110

The values stated by Evrard [2003] did not seem to be the result of any testing but Evrard did also confirm that the values of bulk density depends on the amount of compaction and the moisture content of the shiv. Evrard [2008] performed tests on shiv from two manufacturers by both ‘softly pouring’ shiv into a 1 litre receptacle before measuring the bulk density. The same sample was then ‘bumped’ 50 times before another reading was taken. Evrard found that the very light bulk densities came from one manufacturer with a less refined processing methodology resulting in shiv containing larger particles and a higher percentage of fibres; these generated ‘arches’ in the sample leaving empty (low density) zones underneath.

Gourlay [2008] determined differences in bulk density between the same set of shiv varieties as previously mentioned. Shiv was gently poured into five litre buckets and levelled with a ruler longer than the diameter of the bucket. The repeatability of this method was confirmed by carrying out a number of tests on different batches from the same origin; ‘good consistency was achieved’. The densities varied from 62.2 – 110kg/m³. Gourlay concluded that the origin of the shiv may have an effect on the mechanical characteristics of hemp-lime as a composite as constituents are mixed by percentage mass.

Table 2.3 presents shiv particles densities as stated in previous publications. It is assumed Cerezo [2005] states the value directly from Evrard [2003]. No other information related to these values or the methodologies employed is available as the testing methods were not detailed; consequently there is no explanation for the differences in values.

Table 2.3 – Shiv particle density

Publication	Particle density (kg/m³)
Evrard, 2003 & 2008	320
Cerezo, 2005	320
Nguyen, 2008	254

2.3.4 Compressive strength

The compressive strength of cylindrical shiv specimens has been determined by Cerezo [2005] by fabricating specimens, with dimensions ~160mm diameter by 320mm long, for testing in a compression rig. Figure 2.2 shows a typical specimen and Figure 2.3 displays the strength/strain relationship. The specimen fabrication procedure was not detailed in the publication.



Figure 2.2 – Shiv specimen [Cerezo, 2005].

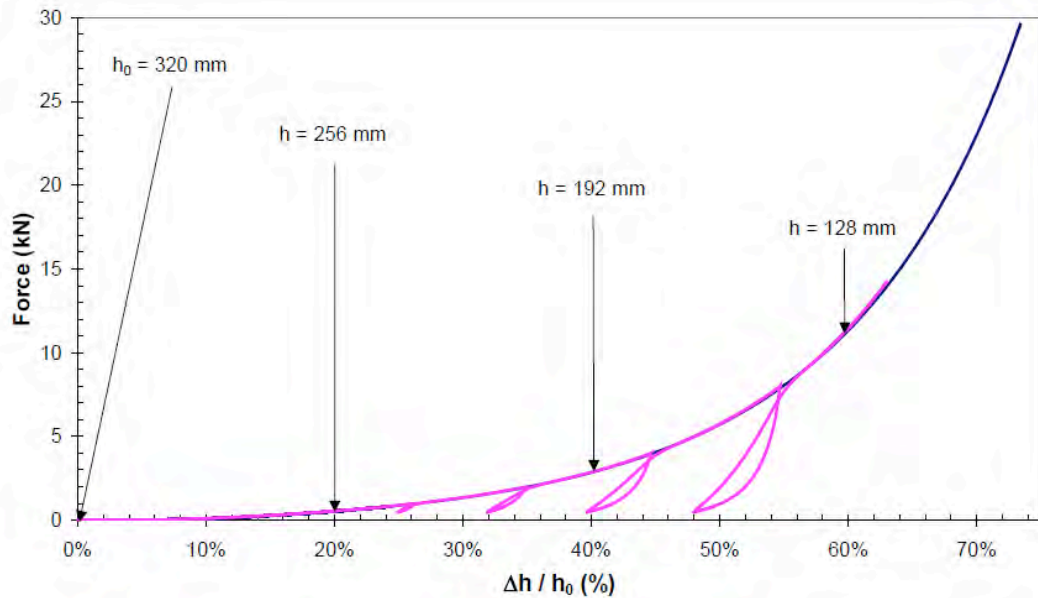


Figure 2.3 – Monotonic (blue) and cyclic (pink) compressive tests on hemp aggregate specimens [Cerezo, 2005].

The results indicate high levels of ductility, compressibility and densification causing the strength of the material to increase as the specimen reduces in size; the specimen does not fail at any point. The specimen decreased from a height of 320mm to under 85mm at the end of the test, without achieving rupture ($\Delta h/h_0=75\%$). The particles steadily crush as the density of the specimens increase from 130kg/m^3 to more than 330kg/m^3 . The crushing of the aggregate is confirmed by the density values; effectively, when $\Delta h/h_0$ is greater than 60%, the density of the specimens becomes greater than the particle density of the shiv. The elastic modulus of the cylinder increased from 0.24 N/mm^2 to 4.6 N/mm^2 at the end of the test. What these tests may indicate is that friction between adjacent shiv particles (inter-granular cohesion) could play an important role in the mechanical behaviour of hemp-lime as a composite [Cerezo, 2005].

2.3.5 Porosity and water absorption

The dewatering effects of the hemp shiv, as a result of its high porosity, is known to have significant impact on the hygric dynamics of hemp-lime when

it is mixed (Evrard 2003). It has now been well established that the microstructure is the source of certain fundamental properties of hemp-lime [Hustache & Aranud, 2008]. The pores inside a shiv particle are tubes that lie in the longitudinal direction; the size can be estimated 'manually' by direct measurement on a scanning electron microscope image resulting in pore sizes between 10 and 40 μ m [Garcia-Jaldon, 1992]. A more systematic approach has been developed by ENTPE based on a radio imaging technique called tomography. Essentially a shiv particle cross section is photographed and image analysis determines the pore sizes and the porosity of the particle. This procedure has concluded that shiv pores are cylindrical and that they traverse the entire thickness of the particle. Pore sizes ranged between 70-400 μ m [Gourlay, 2008]. Hustache & Aranud [2008] hypothesis that the differing values between investigations may have resulted from differences in cultivation techniques, climatic conditions and the position and height of the particle in the stem.

Water ingress and egress from shiv may be in the form of liquid or vapour; when in the form of vapour, shiv is susceptible to considerable mass increases of up to 35% depending on the relative humidity of the environment [Garnier, 2000] as shown in Figure 2.4. Garnier concluded that under environmental conditions of 20-21°C and 50-60%RH the moisture content of shiv ranged between 10-12%.

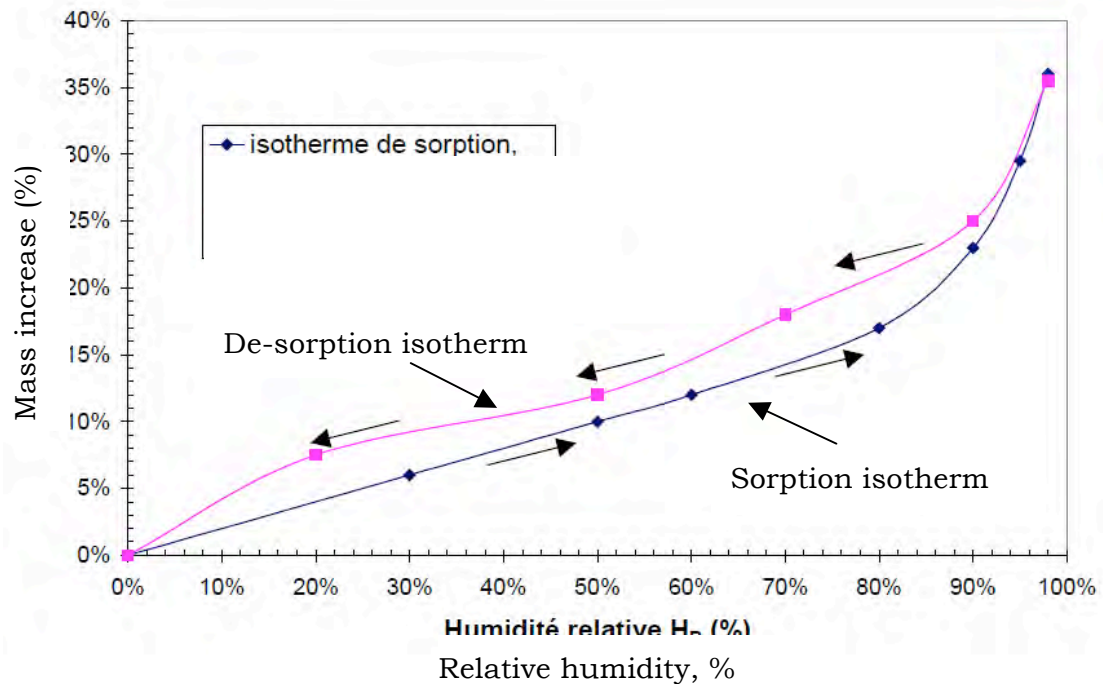


Figure 2.4 – Sorption and de-sorption isotherms of shiv at 20°C [Garnier, 2000].

No work has currently been carried out to determine the sorption-desorption characteristic of shiv from different origins; the different particle densities may result in varying porosity measurements and hence a different sorption-desorption curve. Considering that the moisture content of the shiv is instrumental to the hygro-thermal characteristics of the material [Evrard, 2008] this could essentially give different thermal characteristics for hemp-lime composites in different countries.

Gourlay [2008] determined the total liquid water absorption characteristics of ten shiv sample to within a 'confidence level of 98%'. One litre of shiv (one test for each origin) was immersed in a bucket containing 3 litres of water and placed in a vacuum oven at 78°C; at pre-determined time periods the shiv was poured through a sieve placed over another bucket to recover the wet particles; the difference in mass between the buckets of water provided the mass of water absorbed by the shiv. Figure 2.5 shows the absorption curves for four of the samples tested including UK shiv (formerly from the Hemcore company).

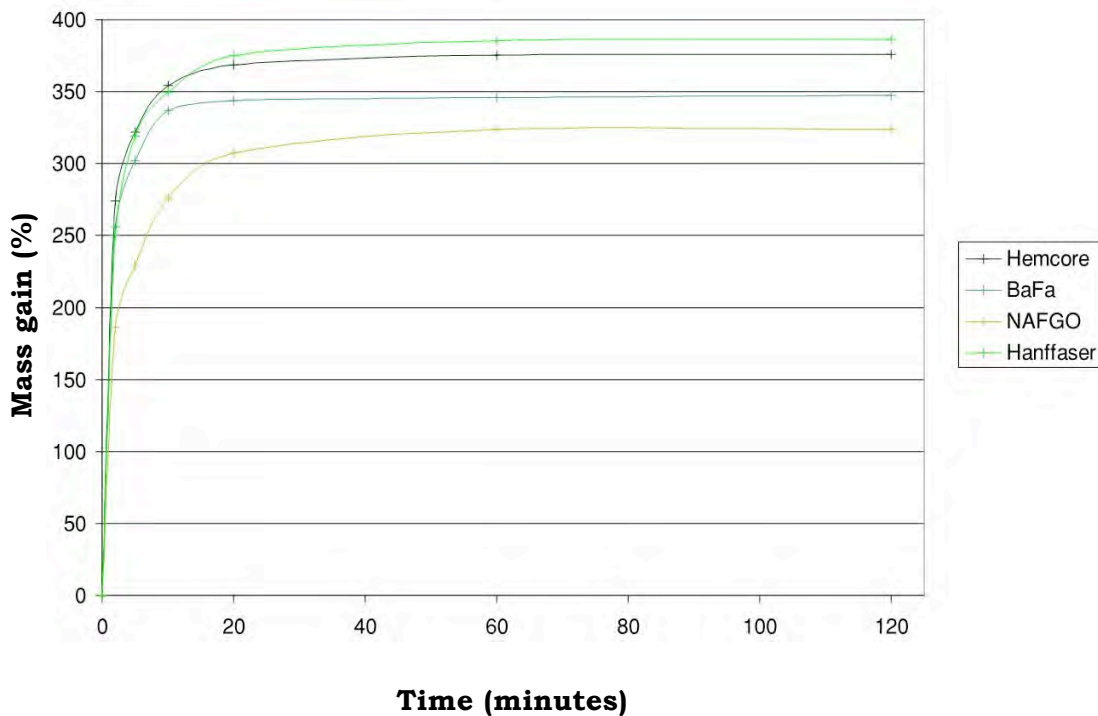


Figure 2.5 – Water absorption of shiv in vacuum oven at 78°C, [Gourlay, 2008].

The total mass gained from the ten different samples ranged between 300-385% with the UK shiv attaining 375%. After a period of 10 minutes 95% of the total absorption had occurred and 98% after 20 minutes immersion. The curves display differences in both rates and total amounts of water absorbed. This may be due to the different porosities of the shivs which were derived from different origins and growing conditions.

Problems in the testing methodology were identified, firstly when the shiv particles were drained in the sieve, small amounts of water were still found to be trapped in-between the individual particles resulting in an over-calculation of the amount of water physically absorbed by the shiv. By using a larger diameter sieve and hence spreading the shiv apart the readings were reduced by 5-7% but it was not made clear if the problem had been eliminated. Secondly, small amounts of water would stay in the bucket from which the shiv was being poured from. Gourlay accepted these variables as it was assumed they were constant for all samples under test.

The justifications for using a vacuum oven at 78°C were not made apparent. Although using a vacuum oven is most probably effective at ensuring total water absorption into the shiv particle, it does not provide representative absorptions rates compared to water absorption under normal atmospheric pressure which in all probability takes longer.

Absorption tests were also carried out by Cerezo [2003] which compared favourably with Couedel [1998] (Figure 2.6).

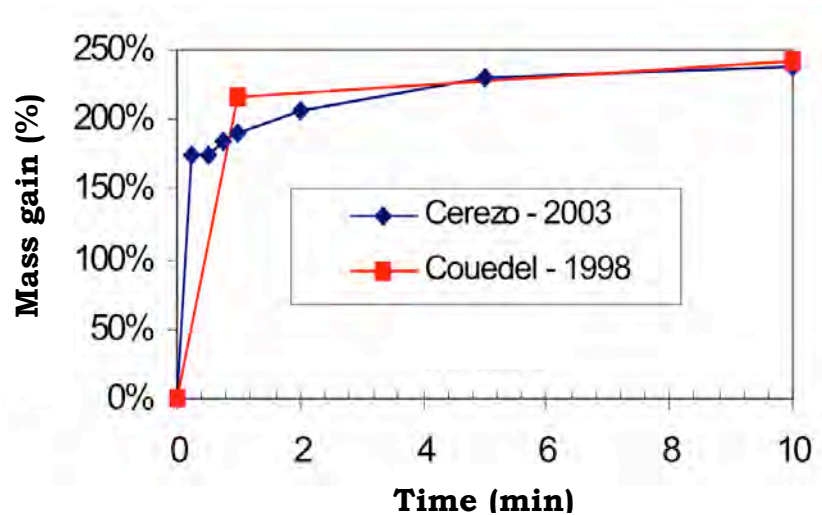


Figure 2.6 – Mass gain of immersed hemp shiv aggregate [Cerezo, 2005].

Cerezo concluded that the average time required to reach 95% saturation was 5 minutes with a total saturated mass gain of 230%. Interestingly, the slope of the graph between 5-10 minutes still indicates an increase in mass however there is no indication the test carried on beyond 10 minutes of immersion.

2.3.6 Thermal conductivity

The porosity of hemp shiv influences the overall thermal characteristics of hemp-lime [Evrard, 2003 & 2008]. Furthermore, the degree of thermal conductivity increases linearly against density [Cerezo, 2008]. Measurements of thermal conductivity have, to date, only been carried out of shiv

originating from France. Figure 2.7 shows the thermal conductivity (λ) of shiv particles compared to increasing levels of compactness (density).

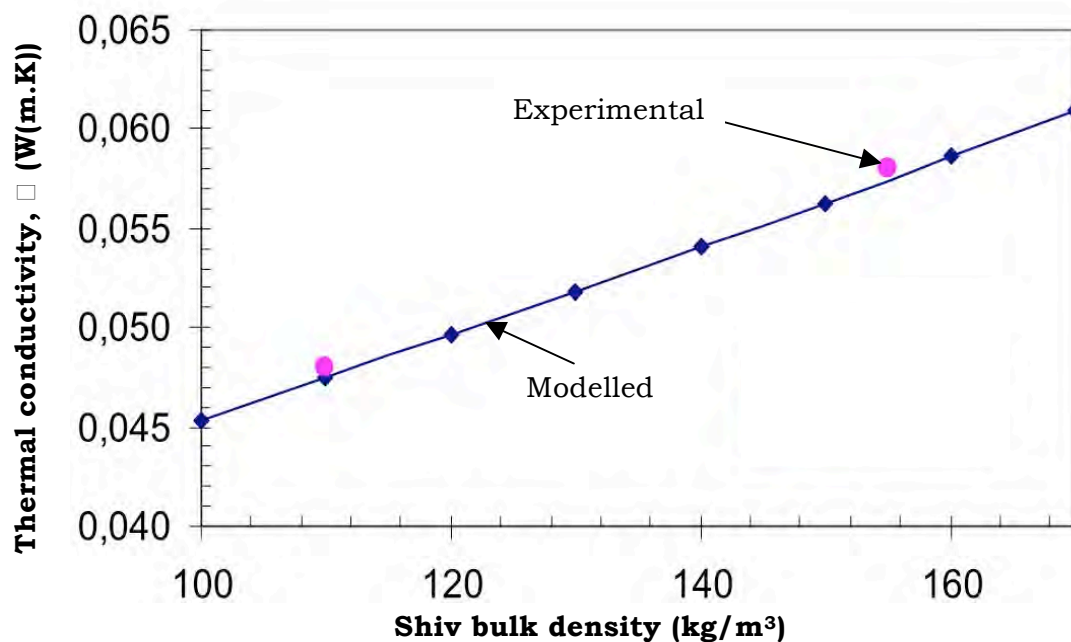


Figure 2.7 – Thermal conductivity of hemp shiv as a function of bulk density [Cerezo, 2005].

The figure illustrates that an increase in bulk density results in an increase of thermal conductivity, ultimately increasing the energy costs of the household. It is therefore favourable to investigate the liability of low density mixes and bulk densities as it directly affects the lowering of energy costs.

2.4 Binder

2.4.1 Pre-formulated binders

Modern binders used with hemp shiv are described as binders consisting of varying proportions of air lime and/or hydraulic lime (including natural hydraulic lime) and pozzolanic materials with the possibility of a small quantity of additives [RP2C, 2006]. It is also stated that manufactured pre-formulated binders should be specifically recommended for use with hemp

shiv. Table 2.4 presents the different binders used in different investigations along with the claimed constituent ratios.

Table 2.4 – Binders used in current literature [Lawrence, unpublished; Hustache & Arnaud 2008].

Publication	Binder	Constituent ratio (%wt)				
		Hydraulic Lime	Air Lime	Sand	Pozzolan	Additives
Cerezo, 2005	Tradical PF70	37	63	0	n/a	n/a
Cerezo, 2005	Tradichanvre	22	58	20	n/a	n/a
Evrard, 2008	Tradical PF70	15	75	0	10	0.5
Evrard, 2008	Tradichanvre	10	55	35	0	0.8
Evrard, 2008	Alpha 63	0	100	0	0	0
Evrard, 2008	Eclat	0	100	0	0	0
Collet et al, 2008	Tradichanvre	15	85	0	0	n/a
Collet et al, 2008	Tradical 70	15	70	0	15	n/a
Elfordy et al., 2008	Tradical 70	15	70	0	15	n/a
Nguyen et al., 2008	Tradical PF70	15	75	0	10	n/a
Samri, 2008	Tradical PF70	37	63	0	n/a	n/a
Samri, 2008	Tradichanvre	22	58	20	n/a	n/a
De Bruijn, 2008	Various proportions of cement, NHL, air lime, gypsum and silica	-	-	-	-	-

Cerezo [2005] and Evrard [2008] both used Tradical PF70 and Tradichanvre (render) in their respective investigations however both stated different constituent ratios for each formulated binder. The reasons for this inconsistency are not immediately apparent from the literature.

2.4.2 Carbonation and hydration of limes and cements

In order to design and justify the programme of work with the intent of fulfilling the aim and objectives of the investigation, an understanding of the chemistry of the binders was needed. Two main reactions take place when considering lime binders and cement, namely carbonation and hydration.

2.4.2.1 Carbonation

When calcined air lime contains no argillaceous (clay) impurities, therefore carbonation is the only way the binder will set and harden. Carbonation occurs when, on exposure to air and moisture (wetting water, rain and/or water vapour) Ca(OH)_2 reacts with the atmospheric CO_2 to form CaCO_3 according to the following reaction:



Carbonation is a slow process which can take many months or even years depending on the density, porosity and availability of air and moisture to the Ca(OH)_2 [Lawrence, 2006].

Carbonation is a diffusion related process [Van Balen & Van Gemert, 1994] as Ca(OH)_2 can only be accessed by the CO_2 in its dissolved state [Johannesson & Utgennant, 2001; Radonjic et al, 2001; Beruto et al, 2005]. The physical stages of carbonation have been summarised by Lawrence (2006) and give an indication into the processes involved;

1. Diffusion of gaseous CO_2 through the pores of the mortar.
2. Dissolution of Ca(OH)_2 in the pore water;



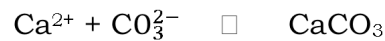
3. Dissolution of the CO_2 in the pore water;



4. Chemical equilibration of dissolved CO₂ in the pore water;



5. Precipitation of CaCO₃



The rate of carbonation increases once the initial wetting water has dried off as water effectively blocks access of atmospheric CO₂ to un-carbonated Ca(OH)₂. However, pore water is also essential to the process of carbonation. If the RH is below 20%, no carbonation will occur as there is insufficient water for CO₂ to dissolve [Van Balen, 2005]. On the other hand, if the RH is above 90%, the ingress of CO₂ is greatly inhibited as less than 50% of the pore surface is available for carbonation [Arandigoyen et al, 2004] and the diffusion of gases in a liquid is about 10,000 times slower than in air [Houst, 1996]. Therefore optimum carbonation occurs between 20-90% RH.

2.4.2.2 Lime hydration

When the calcined lime contains argillaceous impurities, the binder is capable of setting under water and is referred to as a hydraulic lime. Therefore, hydraulic limes set using a combination of hydration and carbonation. The hydraulic set is a reaction of anhydrous compounds with water which yield a new compound - a hydrate - which is both a chemical and physio-mechanical change to the system [Hewlett, 1998]. The hydraulic set primarily involves the reaction of belite (2CaOSiO₂ [C₂S]) with water to form calcium silicate hydrate (3CaO.2SiO₂.3H₂O [C-S-H]) according to the following formula:



The hydrates form over a period of between 2 days and 28 days producing a relatively rapid initial hardening [Oates, 1998]. Hydraulic limes which are

produced from naturally argillaceous limestones are referred to as Natural Hydraulic Limes (NHL). They are classified into three categories according to the cementation index [CI]- NHL2 (feebly hydraulic) CI = 0.3-0.5; NHL3.5 (moderately hydraulic) CI = 0.5-0.7; NHL5 (eminently hydraulic) CI = 0.7-1.1. The compressive strengths at 28 days (N/mm²) are typically **2-7** for NHL2; **3.5-10** for NHL 3.5 and **5-15** for NHL5, with the number after the 'NHL' being the minimum expected 28 day compressive strength of the lime paste.

2.4.2.3 Cement hydration

Chemically, the hydration of Portland cement consists of a series of reactions between individual clinker minerals, calcium sulphate, and water, which proceed both simultaneously and successively at different rates and influence each other [Hewlett, 1998]. The principal minerals in Portland cement clinker are listed in Table 2.5.

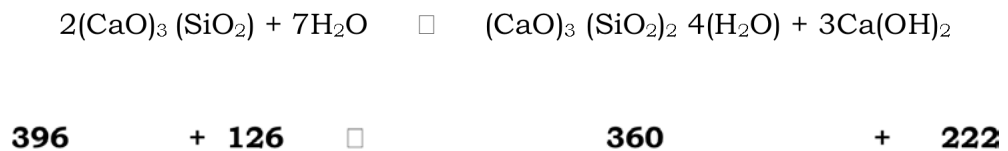
Table 2.5 – Mineral content of ordinary Portland cement.

Mineral	Cement notation	Chemical name	Chemical notation
Alite	C ₃ S	Tricalcium silicate	3CaO.SiO ₂
Belite	C ₂ S	Dicalcium silicate	2CaO.SiO ₂
Aluminate	C ₃ A	Tricalcium aluminate	3CaO.Al ₂ O ₃
Ferrite	C ₄ AF	Tetracalcium Aluminoferrite	4CaO.Al ₂ O ₃ .Fe ₂ O ₃
Gypsum	3C□H ₂	Calcium sulphate dihydrate	CaSO ₄ .2H ₂ O

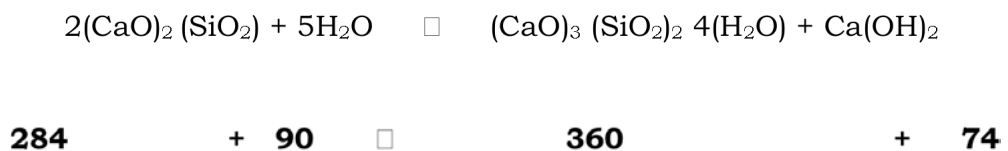
The two calcium silicates, C₂S and C₃S, typically constitutes about 75% of Portland cement by mass [Taylor, 1964]. Once water is mixed with the clinker minerals, of the four clinker phases, C₃A reacts the most rapidly, followed by alite, then belite, and finally the ferrite phase. Upon hydration, 16 to 20% of PC is converted to Ca(OH)₂ [Wild & Khatib, 1996].

Alite – Alite is the mineral in cement responsible for setting and development of "early" strength. Alite is more reactive because of its higher calcium content, and the presence of an oxide ion in the lattice. When mixed

with water, the C₃S particles hydrate to form crystalline calcium hydroxide, Ca(OH)₂, and a gel of hydrated Calcium Silicate Hydrates (C-S-H). Calcium Silicate Hydrates grow as a mass of interlocking needles that provide the strength of the hydrated cement system. The hydration reaction for alite (and molar masses below) can be described as follows:



Belite – Belite contributes to "late" strength due to its lower reactivity. Commonly found in four different crystalline forms namely □, □', □ and □ the □ form is the most desirable form to be found in cement as it reacts very slowly (about 20 times slower than C₃S) with water. Belite also forms a thickening gel of C-S-H on the surface of the cement particles. The hydration reaction of belite can be described as follows:



Tricalcium Aluminate – The most reactive of the cement mineral phases. Its uncontrolled hydration can lead to the phenomenon of "flash set" (instantaneous set) where a large amount of heat is generated. To avoid this, cements include a small addition of Gypsum whose sulphate ions initially lead to the formation of an insoluble layer of ettringite over the surface of the aluminate crystals, passivating them. These hydrates contribute little to strength development. As hydration proceeds the ettringite breaks down into monosulphates as the relative proportion of alumina to sulphate increases. The hydration reaction of tricalcium aluminate with gypsum can be described as follows.



Calcium Aluminoferrite – Its effects on cement properties are little more than those of a diluent, decreasing the viscosity of the fresh cement and increasing time of workability. Its reaction is similar to C_3A both in the presence and absence of Gypsum and the higher the Iron content the slower the hydration [Gani, 1997]. The iron content contributes to the grey colour of the cement.

2.5 Hemp-lime

2.5.1 Fabrication and curing methodologies

The constituent mix proportions of hemp-lime have varied many times since its first use. In conjunction with that variation, the mix proportions used in empirical investigations has varied greatly to either represent current practice or investigate new mixes which may offer more favourable characteristics.

Table 2.6 collates all the important aspects of the major empirical investigation on hemp-lime including constituent proportions, fabrication methodologies, specimen dimension and curing regimes.

Table 2.6 – Constituent ratios, fabrication and curing methodologies from previous publications.

Publication & sample reference	Proportions			Mixing regime	Specimen dimensions	Fabrication & de-moulding regime	Curing regime
	Hemp (kg)	Binder (kg)	Water (lts)				
Lime Technology current practice	1	1.5	1.82	Hemp, binder, water. Mix time: 5 minutes	N/A	N/A	N/A
Cerezo, 2005. A4-1.5 A3-0.75 A3-1 A3-1.5 A3-2	1 1 1 1 1 1	1.73 2.59 1.80 2.41 3.61 4.83	3.05 3.36 3.12 3.35 3.82 4.29	1. Dry hemp 2 minutes. 2. Pre-wetting 5 minutes. 3. Binder 2 minutes. 4. Binder water 5 minutes. Mix time: 14 minutes	~160ø (200cm ²) x 320mm waxed cardboard moulds for compression testing.	Tamped in 80mm layers at 0.05MPa (1kN over 200cm ²). Kept in moulds until testing. Stored horizontally with both ends exposed.	20°C ; 50% RH until testing at 21 days, 3, 6, 9, 12, 15, 18, and 24 months.
Evrard, 2008. Wall	1	2	3	No mixing details. Mix for ~4 minutes	190ø x 35mm	Loose dropped into moulds and surface struck off. 3 to 5 days.	Kept at 20°C ; 100% RH for 3 to 5 days, then at 23°C ; 65% RH for 1 month.

Chanvre, 2007 Roof Wall Floor Tradichanvre (render)	1 1 1 1	1 2.2 2.7 5	2 3.5 5 5	<p>Drum mixer (slow mixing rate, maximum tilt) – mix water and binder to slurry, add hemp until homogeneous.</p> <p>Pan mixer (slowest rate of rotation) –mix hemp and 1/3 of water. Progressively add binder and rest of water until homogeneous.</p>	N/A	N/A	N/A
Evrard, 2003 Roof Wall Ground Render	1 1 1 1	0.85 1.69 2.12 3.7	1.73 2.69 3.85 5.00	<p>Drum mixer (slow rotation speed) – Mix binder and 4/5 of water to slurry, add hemp and use water to adjust consistency. Remove from mixer as soon as mixture is homogeneous.</p>	~160ø (200cm ²) x 320mm		

De Bruijn, 2008. A B C D E E(2) D(2) B(2) N P R S	1 1 1 1 1 1 1 1 1 1 1 1	3.57 3.03 3.33 3.57 4.55 4.55 3.57 3.03 2.70 1.56 1.64 3.0	3.73 4.03 4.00 3.96 4.05 6.68 6.46 5.67 4.62 5.86 6.11 6.36	Mix binder and water to slurry, add hemp and then add additional water for consistency. Remove five minutes after all constituents have been added.	150x150x150mm steel moulds for compression tests. 150ø x 300mm steel moulds for splitting tests.	Tamped in 50mm layers with a 45x45mm wooden stave. Then subjected to 50Hz vibrating table for 1 minute. De-moulded after 2 days.	Phase 1 – cured in labs for 12 weeks at 20°C then in carbonation room for 40 days. Testing performed at 18 weeks. Phase 2 – stored in carbonation room for 40 days immediately after de-moulding. Testing performed at 12 weeks. Carbonation room contained 4.5% CO ₂ at 20°C and 50%RH. After 40 days carbonation CO ₂ levels reduced to 0.038% until testing.
Nguyen, 2008. C1 C2 C3	1 1 1	1.95 2.55 1.9	2.88 3.00 1.58	n/a	n/a	C1 and C2 lightly compacted	20°C ± 2°C ; 75% RH ± 15% until testing at 28 and 180 days.
St Astier Literature Wall	1	3.18	3.18-3.60	Paddle mixer 2-5 mins. Drum mixer until no lumps are present.	n/a	n/a	n/a

<i>Elfordy, 2008</i>	<i>1</i>	<i>2.1</i>	<i>n/a</i>	<i>Sprayed at 0.2kg/s at 150m/s</i>	<i>50x50x50mm cubes compression and density measurements. 100x150x300mm prisms cut for bending tests. 80ø x 25mm cylinders for thermal tests.</i>	<i>Projection distance varied between 0.5m and 3m. 1 month (then cut down to testing size).</i>	<i>No details given. Tested at 28 days.</i>	<i>Evrard, 2003 Wall</i>	<i>1</i>	<i>2</i>	<i>3</i>	<i>Hand mixed, manually filled and pressed around edges only.</i>	<i>190mmø 350mm height</i>	<i>3 to 5 days</i>	<i>Kept at 20°C ; 100% RH for 3 to 5 days, then at 23°C ; 65% RH for 1 month.</i>
----------------------	----------	------------	------------	---	---	---	---	------------------------------	----------	----------	----------	---	--------------------------------	--------------------	---

The highest and lowest ratio mixes were investigated by Chanvre (2007) with a shiv/binder/water ratio of 1:5:5 and 1:1:2 respectively. These ratio mixes were designed to be used as renders and roof insulation. When considering material designed as insulation within walls a very large selection of differing constituent ratios have been investigated. Current Lime Technology practise uses constituent ratios of 1:1.5:1.82 whereas St Astier literature specifies much larger proportions of binder and water at 1:3.18:3.18-3.60.

Overall there is a distinct lack of standardisation in relation to fabrication, demoulding and curing methodologies. This does not allow for direct comparisons. There is also no evidence of any 'round robin' testing which would help refine and confirm that fabrication methodologies are repeatable and reliable regardless of the user/tester.

2.5.2 Mechanical properties

Although widely accepted as a non-structural material investigation the mechanical properties of different constituent ratios of hemp-lime allows immediate comparisons and clear observations to be made. Furthermore there is a growing assumption that hemp-lime, when used as a wall infill material, may contribute somewhat to the structural behaviour of the primary structure as detailed by Helmich [2008].

At the time of publishing *Construire en Chanvre* [Evrard, 2003], Evrard claimed tests were being carried at ENTPE (*Ecole Nationale des Travaux Publics de l'Etat*) in Lyon on hemp-lime concretes with an addition of hemp fibres. It seems these results have not yet been made publically available although Evrard does state '*Initial results have shown a certain increase in the maximum compressive stress and permissible deformation values*'. On the other hand, the introduction of fibres may have some significant repercussions on the thermal, acoustic, and hygroscopic values. It has not yet been made clear if the introduction of fibres improves hemp-lime.

Table 2.7 collates results from a number of investigations which have focussed on the mechanical characteristics of hemp-lime.

Table 2.7 – Mechanical performance of hemp-lime from current literature [Lawrence, unpublished; Hustache & Arnaud, 2008].

Publication	Binder ratio by volume	Density (kg/m ³)	Ultimate compressive strength (MPa)	Elastic modulus (MPa)	Axial deformation at ultimate strength	Poisons ratio
Cerezo, 2005.	10% 19-29% 40%	250 350-500 600-660	0.25 0.35-0.80 1.15	4 32-95 140-160	0.15 0.05 0.06	0.05 0.08 0.16
Elfordy, 2008.	34%	291-485	0.18-0.80	5-35	n/a	n/a
De Bruijn, 2008.	30%	n/a	0.15-2.14	12-174	n/a	n/a
Nguyen, 2008.	25%		0.65-4.0	<100	n/a	n/a
Chanvre, 2007.	Roof (23%) Wall (40%) Floor (45%) Render (70%)	250 420 500 800	0.1 0.3 0.3 0.4	3 20 20 25	n/a	n/a

2.5.3 Environmental characteristics

Suppliers of hemp-lime claim the material to be ‘environmentally superior’ to modern materials such as bricks, cement and petrochemical based insulation material. The basis of this claim comes from the fact that a typical hemp-lime house will have three carbon sinks in its construction:

1. The timber frame; as a result of photosynthesis.
2. The shiv; as a result of photosynthesis.
3. The binder; as a result of carbonation of the lime content.

The use of chemicals is also comparatively very low; apart from fertiliser, hemp shiv requires no additional chemical products such as herbicides or

pesticides during its growth. Using a sustainable aggregate like hemp shiv also reduces the need for traditional quarried stone aggregate; the extraction, refinement and transport of which is energy intensive and damaging to the landscape.

Table 2.8 compares the CO₂ emissions of a typical hemp-lime wall against an equivalent wall built from 'conventional' materials. The values have been supplied by Lime Technology Ltd. As a result, the primary source of the data and how the values were calculated is not known and should therefore be treated with caution as values can vary from source to source. For example, Hammond and Jones [2006] state facing bricks, AAC blocks and mineral wool to have CO₂ emissions of 520, 280-375 and 1200kg/tonne respectively.

Table 2.8 – Carbon dioxide emissions of a typical cavity wall and a comparative hemp-lime wall [Bevan & Woolley, 2008].

Building element	Thickness (mm)	CO ₂ emissions (kg/tonne)	CO ₂ emissions (kg/m ² of wall)
		Conventional wall	
Facing brick	100	172+	29+
AAC block	140	430	50
Mineral wool	100	2606	7
Plaster	20	93	2
Cement mortar		122	9
			Total ~100
		Hemp-lime wall	
Hemp-lime	300	-333	-33
Lime render	20	23	1
Lime plaster	20	23	1
			Total -31

The holistic impacts a building material has over its life span can be studied by means of a Life Cycle Analysis (LCA). An LCA (also known as ecobalance or a cradle-to-grave analysis) is a technique to assess each and every impact associated with all the stages of a materials life (i.e., from raw materials through materials processing, manufacture, distribution, use, repair and maintenance, and disposal or recycling). The resulting data then feeds into a Life Cycle Inventory (LCI), a database where equivalent comparisons can be made between products. Examples of such databases include the Policy

Study Institute's project '*A systematic approach to estimation of life cycle carbon inventory (LCCI), carbon footprints and embodied carbon*' [PSI, 2006] and the University of Bath's Inventory of Carbon and Energy (ICE) database for building materials [Hammond & Jones, 2006]. Neither of these sources currently have hemp-lime inventoried.

INRA (The French National Institute for Agricultural Research) carried out an LCA study of hemp-lime which was commissioned by the Ministère de l'Agriculture et de la Pêche (Ministry of Agriculture and Fisheries) in France [Boutin et al., 2005]. The functional unit of the study was a 260mm thick rendered wall at 380kg/m³, cast around a timber frame and with a life span expectancy of 100 years. Table 2.9 outlines the main conclusions from the study.

Table 2.9 – 100 year potential environmental impact associated with the fabrication of 1m³ shuttered hemp-lime wall on a timber frame [Boutin et al., 2005].

Impacts	Materials		Installation	Service life	End of life	Transport	TOTAL
	Shiv	Other materials (timber, water and Tradical 70)					
Depletion of resource (kg Sb eq)	2.8x10 ⁻²	7.7x10 ⁻²	1.2x10 ⁻³	0	0	2.6x10 ⁻²	1.3x10 ⁻¹
Atmospheric acidification (kg SO ₂ eq)	5.1x10 ⁻²	4.8x10 ⁻²	1.3x10 ⁻³	0	0	5.1x10 ⁻³	1.0x10 ⁻¹
Greenhouse effect at 100 years. Carbon sequestration (kg CO ₂ eq)	-45.9 -52.2	23.1 -9.9	0.2	-13.6 -13.6 (lime)	0	6.7x10 ⁻¹	-35.5 -75.7
Destruction of the ozone layer (kg CFC eq)	7.1x10 ⁻⁷	3.3x10 ⁻⁶	3.4x10 ⁻⁷	0	0	5.7x10 ⁻⁶	9.9x10 ⁻⁶
Formation of photochemical ozone (kg C ₂ H ₄ eq)	7.1x10 ⁻⁴	4.2x10 ⁻³	5.0x10 ⁻⁵	0	0	3.8x10 ⁻⁴	5.4x10 ⁻³
Non-renewable energy (MJ)	52.3	265.8	19.9	0	0	56.3	394.2
Air pollution (m ³)	674	207.2	14.6	0	0	128.2	1024
Water pollution (m ³)	4.3	2.2	6.1x10 ⁻²	0	0	1.1x10 ⁻¹	6.7
Waste production (kg)	6	-	0.9	0	98		104.9

Boutin et al. [2005] concludes that hemp-lime walls absorb 35.5kg of CO₂ per square meter of built wall. However, there is an intrinsic degree of uncertainty into this conclusion due to the lack of empirical data to back up the assumptions and theoretical calculations used within the study.

One area in which the LCA is lacking is when considering the end of life phase of the material. The study classified the used hemp-lime material and the timber frame as a waste product which would be sent to a Class II technical buried disposal site (CET II). In this case the sequestered CO₂ in the material may be returned to the atmosphere as CH₄ (methane) as the material decomposes which has a greenhouse potential 20 times greater than CO₂. Hustache [2008] suggests that the timber frame may be incinerated to recover its energy whilst Courgey [2003] proposes the hemp-lime could be used in composting operations, as backfill or as a soil improver. Currently, no investigations have been carried out into optimising the use of hemp-lime at the end of its useful life.

2.5.3.1 Sequestration from shiv content

Minimal work has been carried out to specifically and empirically determine the carbon content and CO₂ sequestration of industrial hemp and only those presented by Garci-Jaldon [1992] have been peer-reviewed. However by combining the information from different publications it is possible to estimate a range of sequestered CO₂ by considering the molecular structure of hemp shiv. Industrial hemp shiv primarily consists of Cellulose, Lignin and Hemicellulose. Chemical analysis by Garcia-Jaldon [1992] at CERMAV (Centre de Recherche sur les Macromolécules Vegetales, Grenoble) determined the elemental composition of the whole industrial hemp plant which is presented in Table 2.10.

Table 2.10 – Chemical composition of hemp shiv [Carcia-Jaldon, 1992]

Element	Cellulose	Hemicellulose	Lignin	Ashes	Waxes	Pectin	Proteins
Composition (%)	48	12	28	2	1	6	3

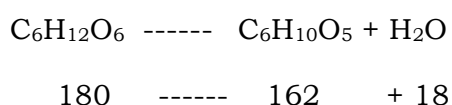
Overall the hemp shiv was composed of 7 different groups of elements. Cellulose constituted 48% of the shiv's mass whilst lignin and Hemicellulose accounted for 28% and 12% respectively. In total these three elements made up 88% of the plants mass. The carbon contents of Cellulose, Lignin and Hemicellulose account for 45, 48 and 40% of their molecular masses [Hons, 1996, unpublished], consequently one tonne of dry shiv material contains 0.398 tonnes of sequestered carbon from the atmosphere. The molecular mass of Carbon is 12 compared to 44 for CO₂; this equates to 1.46 tonnes of atmospheric CO₂ being absorbed in every tonne of UK harvested industrial hemp shiv material.

Shiv acts as a carbon sink due to the process of photosynthesis during its growth. Calculations carried out by Ian Pritchett at Lime Technology Ltd. suggest that CO₂ sequestration in the shiv can be estimated using the following formulae:

Photosynthesis:



Glucose to cellulose:



$$\frac{6\text{CO}_2}{\text{C}_6\text{H}_{12}\text{O}_6} = \frac{264}{162} = 1.63$$

In other words 1.63g of CO₂ is required to produce 1g of dry hemp shiv matter.

According to Boutin et al. [2005] the quantity of CO₂ required for the dry matter of the hemp is calculated as follows:

$$\mathbf{Q_{co_2} = (Q_{MS} \times P_{CMS}) \times (MM_{co_2}/MM_C)}$$

Q_{co₂}: The unit mass of CO₂ needed for a unit mass, **Q_{MS}**, of dry matter.

Q_{MS}: Mass of dry matter.

P_{MS}: Proportion of carbon in dry matter. Hemp dry matter is 45.9% carbon [ADAME, 1998].

MM_{co₂}: Molar mass of CO₂ = 44 g.mol⁻¹

MM_C: Molar mass of carbon = 12 g.mol⁻¹

Applying the above formula indicates that about 1.7g of CO₂ is needed to create 1g of dry matter. The report from Hons [1996, unpublished] calculates that 1.62g of CO₂ is required to produce 1g of dry matter.

Although it is possible to estimate the carbon sequestration of hemp shiv these calculation should not however be taken as a definite figure for CO₂ sequestration. As shown by Bouyer [2008], the biological make-up of shiv depends on a number of factors. Resultantly, the amount of CO₂ sequestered by hemp grown in the UK could differ from the same variety grown in France as it may be assumed that the growth rates, crop yield and particle densities of the crop could differ.

Considering the shiv is the largest carbon sink in the material [Boutin et al., 2005], it is surprising to find little surety into how much CO₂ is actually absorbed

What cannot be ignored, however, is how well hemp-lime compares to 'conventional' building materials such as bricks and concrete blocks which, for the foreseeable future, will always have a net carbon emission associated to them. It is a promising sign to find a 'modern' construction material with a net negative carbon emission which has the potential to be widely implemented in modern construction.

2.5.3.2 Sequestration from binder

The carbon dioxide released during the calcination of lime is claimed to be reabsorbed during carbonation, however it is hard to find out exactly how much is reabsorbed and over what time period. In their database Hammond and Jones [2008] state that the total embodied carbon in lime is 0.74 kgCO₂/kg (cradle to gate) but also mentions that lime releases approximately 0.48 kgCO₂/kg of lime produced. If the full amount of carbon dioxide is reabsorbed over a number of years, as some people claim, only 0.26 net kgCO₂/kg is actually released in total from the fossil fuels burnt during production. Carbonation is not an immediate effect and takes many years, therefore it difficult to know which values should be used when analysing the environmental impacts of the binder.

The rate of carbonation is highly variable as, although currently unknown, the thickness, type and porosity of the render effects the diffusion of CO₂ into the hemp-lime. Predominant weather conditions also vary the rate of carbonation, therefore, two identical walls built in different countries will almost certainly carbonate differently. Clearly, much work into the affect these variables have on the carbonation of hemp-lime needs to be carried out.

Boutin et al. [2005] states, *'by using the carbonation formula, the proportion of CO₂ absorbed by the lime content in the binder has been estimated by the lime experts of the work group (BCB-Lhoist) to be 249 kg/metric tonne of Tradical 70 or 13.6kg/m². The speed of re-carbonation is even higher if the process is not slowed by the presence of a rendering.'* The LCA does not, however, go into any more detail about which assumptions were made in calculating this value. It is understood by the author that the hemp-lime industry and the

scientists associated with the research in the LCA assume 100% carbonation of the lime content although there is a lack of empirical data to confirm this assumption. Furthermore the LCA does not include the process of rendering the hemp-lime wall. This process will have high impact on the greenhouse gas emissions and non-renewable energy inputs.

A life cycle analysis is only as valid as its data, therefore, it is crucial that data used for the completion of a life cycle analysis is accurate and current. When comparing different life cycle analyses, it is essential that equivalent data is available for either products or processes in question. If one product has a much higher availability of data, it cannot be justly compared to another product which has less detailed data [Trusty, 2010].

2.6 Measurement of carbonation

2.6.1 Chemical staining

A wide range of methods are available for the measure of carbonation [Lawrence, 2005], however, the traditional method of detecting this process is to spray a freshly broken surface of mortar with phenolphthalein [Lawrence 2006]. Phenolphthalein is an organic compound of the phthalein family and is the most common indicator used to detect carbonation in both lime mortars and concrete [RILEM, 1998]. Phenolphthalein is colourless below pH 8.3 but attains a deep fuchsia hue above pH 10.0. When applied to a freshly broken specimen of hemp-lime or mortar, a stained area is seen which marks the 'un-carbonated' material as illustrated in Figure 2.8. This method offers a quasi-quantitative method for determining the 'carbonation depth' as work by Lawrence (2006) demonstrated that even un-stained areas of mortar may not be considered as fully carbonated, however, as a method for determining and comparing the main carbonation front between different specimens this method provides extremely quick reliable results.

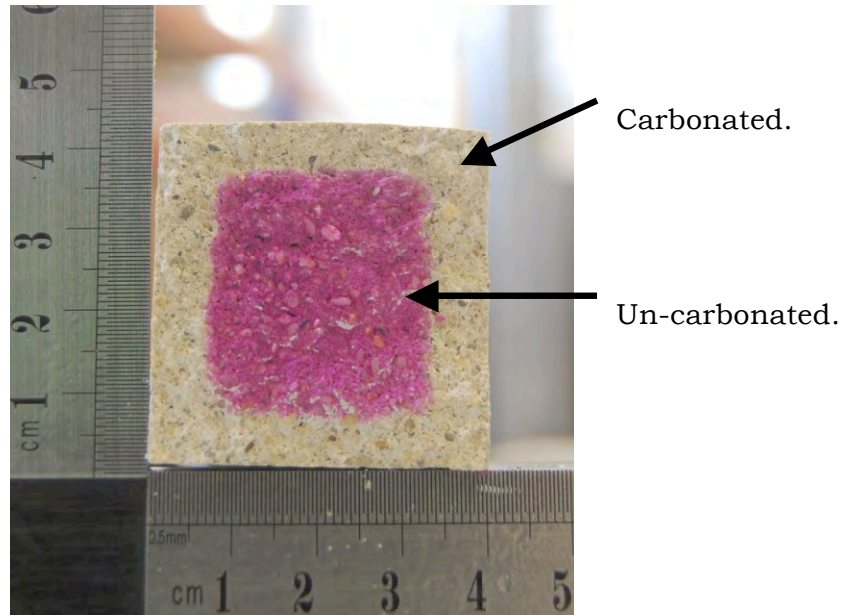


Figure 2.8 – 180 day old THB-52.5R mortar specimen

Parrot [1990] carried out work comparing various chemical solutions on the detection of carbonation working up from a pH of 6.6 to 13.0. Phenolphthalein was found to produce the most apparent visual results with the other indicators producing less visible boundaries (**Error! Reference source not found.**).

Table 2.11 – Chemical solutions used to indicate carbonation [Parrot, 1990].

Indicator solution	pH (range)	Colour changes
Nitrazine yellow	6.6 (6.4-6.8)	Yellow > blue
Phenol red	7.3 (6.4-8.2)	Yellow > red
Diphenol purple	7.8 (7.0-8.6)	Yellow > violet
Cresol red	7.9 (7.0-8.8)	Yellow > violet/red
□-naphtholphthalein	8.0 (7.3-8.7)	Yellow > blue
m-cresol purple	8.2 (7.4-9.0)	Yellow > violet
Phenolphthalein	9.0 (8.3-10.0)	Colourless > magenta
Thymolphthalein	9.9 (9.3-10.5)	Colourless > blue
Brilliant orange	11.3 (10.5-12.0)	Yellow > red
Tropaeolin O	11.9 (11.1-12.7)	Yellow > red
Titan yellow	12.5 (12.0-13.0)	Yellow > red

2.6.2 Thermogravimetric analysis

Thermogravimetric analysis (TGA) is frequently used for the mineralogical analysis of materials as TGA measures the weight loss resulting from the thermal decomposition of different minerals in a material [Earnest, 1988; Dollimore, 1992]. TGA determines change in weight in relation to change in temperature and is a technique that, although limited in scope to those reactions taking place with a change in weight, gives results that are intrinsically quantitative [Lawrence, 2006]. TGA has successfully been used for the mineralogical analysis of both cements and lime mortars and the accuracy of thermal analysis for the quantitative determination of Ca(OH)_2 and the conformity with chemical titration for the quantitative speciation of calcium in lime have been demonstrated [Valenti & Cioffi, 1985; Balcerowiak, 2000].

In pure lime binders, such as those investigated by Lawrence [2006], the quantification of Ca(OH)_2 and CaCO_3 by TGA is less complex as no hydraulic phases are present. However, Tradical® hemp binders, Batichanvre and NHL5 all contain hydraulic phases, the TGA analysis of which is more complex since the hydraulic elements break down at lower temperatures and overlap [Ubbriaco & Tasselli, 1998; Ellis, 2000]. Furthermore, measurement of the amount of Ca(OH)_2 in cement and some hydraulic limes can be understated when the material also contains tricalcium silicate (C_3S) as is the case with hemp-lime binder. This is because C_3S and Ca(OH)_2 partially synthesise at a temperature of around 320°C , resulting in lower weight losses at the dehydroxylation temperature of Ca(OH)_2 of $\sim 470^\circ\text{C}$ [Valenti & Cioffi, 1985]. Table 2.12 presents different heating regimes used in previous investigations.

Table 2.12 – TGA regimes followed by different researchers [Lawrence, 2006].

Author(s)	Material	Temperature range	Heating rate	Atmosphere
Dheilly et al, 1998	Lime	20°C - 850°C	0.67°C min ⁻¹	Dry O ₂
Thomas et al, 1996	Cement	20°C - 900°C	10°C min ⁻¹	?
Strydom et al, 1996	Lime	20°C - 800°C	5°C min ⁻¹	Dry N ₂
Balcerowiak, 2000	Lime	20°C - 950°C	24°C min ⁻¹	Dry Air
Ubbriaco & Tasselli, 1998	Lime	20°C - 950°C	?	Dry Air
Lanas & Alvarez, 2004	Lime	20°C - 1200°C	20°C min ⁻¹	Dry Air
Valenti & Cioffi, 1985	Cement	20°C - 700°C	10°C min ⁻¹	?
Stepkowska, 2005	Cement	20°C - 1000°C	1°C min ⁻¹	Dry Air
Alvarez et al, 2000	Lime	20°C - 1100°C	10°C min ⁻¹	Dry Air
Montoya et al, 2003	Lime	20°C - 1050°C	20°C min ⁻¹	Dry Air
Bruno et al, 2004	Lime	20°C - 1000°C	5/10°C min ⁻¹	Dry Air
Ingo et al, 2004	Lime	20°C - 1000°C	20°C min ⁻¹	Dry Air
Riccardi et al, 1998	Lime	20°C - 1300°C	10°C min ⁻¹	Dry Air
Moropoulou et al, 2004	Lime	20°C - 1000°C	10°C min ⁻¹	Dry Air
Gualtieri et al, 2006	Lime	20°C - 1000°C	20°C min ⁻¹	Dry N ₂ /Air
Maravelaki-Kalaitzak, 2005	Lime	20°C - 1000°C	10°C min ⁻¹	Dry Air
Paama et al, 1998	Lime	20°C - 900°C	10°C min ⁻¹	Dry N ₂ /Air
Bakolas et al, 1998	Lime	20°C - 1000°C	10°C min ⁻¹	Dry N ₂

Table 2.13 presents the different decomposition temperatures of the different hydrate phases commonly found in hydraulic binders. These data can then be used to quantify the mass of hydrates that have formed during hydration.

Table 2.13 – Thermal decomposition temperatures of hydrated compounds [Ellis, 2000; Ubbriaco & Tasselli, 1998].

Compound Name	Formula (S =SO ₃ ; S=Si; A=Al; C=Ca)	Temperature °C
Calcium Silicate Hydrates	CSH Types 1 and 2	95-120
Ettringite	C ₄ A SH ₁₂	125-135
Monosulphate	C ₆ A SH ₃₂	185-195
Syngenite	K ₂ Ca S ₂ H	265-275
Gypsum (dihydrate)	C SH ₂	160-186 (2 peaks)
Calcium Sulphate Hemihydrate	C SH _{1/2}	185
Calcium Aluminates	CAH ₁₀	110-130
	C ₂ AH ₈	175-185
	C ₃ AH ₆	280-320

2.7

2.8 Summary of findings

As a result of the review of literature the following gaps in research have been identified:

1. Design of standard fabrication and testing techniques for hemp-lime as a composite
2. Comparison of different curing regimes
3. Comparison of different densities and mixes currently used in the UK with the new binder
4. Quantification of how much the binder carbonates
5. Carbonation rates of the composite under laboratory conditions
6. Amount of hydration products in the binder
7. The setting times of the binders
8. Compressive and flexural strength comparisons of the different binder previously and currently available.
9. Empirical CO₂ sequestration of shiv
10. CO₂ sequestration of shiv from different origins.

Little work has been carried out focussing on the standardisation of fabrication and testing techniques of hemp-lime under laboratory conditions and there is little empirical evidence to support the carbon sequestration values connected to the use of hemp-lime in the UK construction industry.

CHAPTER 3 - EXPERIMENTAL PROGRAMME

3.1 Introduction

This chapter outlines the design and development of the experimental programme of work, including justification of the variables investigated, procedures used for specimen fabrication and preparation, and the testing methodologies used in this study. To fulfil the aim and objectives set out in Chapter 1 a total of 166 cylindrical specimens were prepared and tested to determine mechanical properties and chemical characteristics up to a 360 day period after casting. To compare the mechanical performance of the hemp-lime composite against that of the binder, 75 mortar prisms were fabricated to map the flexural and compressive strength development of the binder over the same period. Test results are reported in Chapters 4, 5 and 6.

3.2 Selection of materials

The main materials used in this investigation were selected to reflect UK hemp-lime construction industry practice between 2007 and 2010. At the same time a comparison of UK materials was made with materials in common use elsewhere in Europe.

3.2.1 Binders

Tradical® is the Lhoist Group brand name for their range of air lime based construction products. The following four binders were used in this investigation:

1. **Tradical® HB-42.5N:** Tradical® HB-42.5 formulated binders almost identical to the Tradical® PF70 binder however Tradical® HB(a) is based on UK produced high purity CL90 air lime manufactured to BS EN 459-1:2001 with the addition of selected cementitious, hydraulic and inorganic materials to improve porosity and consistence [Rizza, 2005]. Within this investigation this binder has been named THB42.5N.
2. **Tradical® HB-52.5R:** Tradical® HB-52.5R formulated binders are based on UK produced high purity CL90 air lime manufactured to BS EN 459-1:2001 with the addition of selected cementitious, hydraulic and inorganic materials to improve porosity and consistence [Rizza, 2005]. Tradical® HB(b) uses CEM I 52.5R cement which provides a faster hydraulic set than CEM I 42.5N. This change in formulation seeks to extend the temperature range in which the binder can be used to suit the UK's colder climate. Within this investigation this binder has been named THB52.5R.

The precise constituent composition of the above binders is not publically available; however, the patent does specify mass ranges of constituents as follows:

Air lime: 50 – 80%

Hydraulic binder: 10 – 70% such as hydraulic lime or cement

Pozzolanic filler(s): 5 – 10%

In addition the chemical composition of the set binders is later explored using TGA.

- 3. St. Astier Batichanvre (BC):** Batichanvre formulated binders are air lime based hemp binders produced by French lime producers St. Astier (www.c-e-s-a.fr) and distributed in the UK by Womersleys Ltd. (www.womersleys.co.uk). The basic composition of this binder is 70% air lime, 30% hydraulic and pozzolanic binders plus specific additives [BC, 2013].
- 4. Natural Hydraulic Lime (NHL5):** When the practise of using hemp-lime began in France, NHL was widely used as the binder due to its natural hydraulicity but still provide flexibility and vapour permeability to the material. NHL is produced by calcining limestone that contains natural clay and other impurities. Calcium reacts in the kiln with the impurities to produce silicates that enable the lime to set without exposure to air. Calcium oxide is then slaked to form calcium hydroxide. NHL5 was chosen within this investigation as it is the most eminently hydraulic NHL commonly available.

For the purposes of this investigation THB-52.5R was set as the control binder to which comparisons are made as it is currently the most widely used binder in the UK.

3.2.2 Bio-aggregates

Four different plant based bio aggregates have been used in this investigation:

Tradical® HF: Tradical® HF is sourced from industrial hemp grown and harvested in the UK and processed, bagged and distributed by Hemp Technology Ltd. specifically for construction purposes. Approximately 2400 hectares of industrial hemp were cultivated in 2003 in the UK with an

average yield of 6.4 tonnes of shiv per hectare [DEFRA, 2005]. The processing of the hemp removes the fibre and chops, grades and de-dusts the shiv. During this investigation the processing of hemp was moved from an existing plant to a new multi million pound processing plant in Halesworth, Suffolk. During characterisation of the shiv, batches of hemp from both plants were compared.

To investigate the influence of fibre inclusion in the shiv on properties of the composite hemp-lime a series of parallel tests were conducted within the main series of testing using shiv which had had its fibre content removed. In preparation for the fabrication of these specimens a total of ten kilograms of shiv was sieved through a 10mm screen. These specimens have been named 'SH-275' with SH signifying 'sieved hemp'.

Hemp Technology horse bedding: Processing is identical to that used for construction except for the addition of citronella, used to neutralise the odour of horse urine. This shiv was used within preliminary testing of the composite material and during grading of the shiv for constituent characterisation also.

Chanvribat® (CB): CB is the French equivalent of Tradical® HF and is processed and distributed by La Chanverie de L'Aube in the Champagne Ardenne region. Approximately 10,000 hectares of hemp are processed annually in France [CenC website]. This shiv was only used for comparison purposes during grading of the shiv.

Rapport® oil seed rape (OSR): Rapport is the Hemp Technology brand name for OSR straw, which is produced using the softened stem of the oil seed rape plant (Figure 3.1). A total of 581,000 hectares of OSR was harvested in 2003 in the UK [DEFRA, 2005] providing a more ready supply of material if demand increases. Rapport is processed in an identical manner to shiv and commonly used for animal bedding. An initial feasibility study into its possible use either as a replacement or supplement with hemp binder was completed as part of this investigation.



Figure 3.1 – Shiv (left) and Oil Seed Rape straw (right).

3.3 Safety during handling and preparation of materials

Natural hydraulic limes or air limes are not classified as a "dangerous substance" according to the European Commission's 67/548/CEE directive [Lime Technology]. However, due to its alkaline qualities in solution, precautions must be taken whilst using it. Lhoist supply data sheets for Tradical® products prepared in accordance with directive 2001/58/EC [Lime Technology]. The following points were taken into account when using the binders:

- Lime is an irritant to the eyes, respiratory tract and mucous membranes and there are risks of ocular lesions in the case of contact with powder or paste in the eye.
- Prolonged contact with the skin can cause dermatitis.
- In case of ingestion (of a significant quantity), lime is caustic to the digestive tract and may cause burns to the mouth, oesophagus and stomach.

Gloves and eye protection were worn at all times during handling, fabrication and testing of all specimens. When using the binder in dry form dust levels were kept to a minimum and appropriate dust masks were worn at all times. When mixed with water the resulting strong alkaline solution can cause chemical burns without pain being felt at the time. Full body overalls were worn during fabrication of all specimens and any solution which came into contact with the skin was washed away immediately.

3.4 Characterisation of binders

In response to lime's other construction uses (mortars, plasters, renders) various standards have been developed for the empirical testing and characterisation of lime binders. Characterisation and testing procedures of lime binders often rely on mixes utilising silicate sand aggregate, therefore, to compare the mechanical performance of the different binders, a series of standard-sand mortar prisms were fabricated, cured and tested according to the following standards:

- BS EN 196-1:2005 – *Methods of testing cement. Determination of strength*
- BS EN 459-2:2010 – *Building lime. Test methods*
- BS EN 1015-11:1999 – *Determination of flexural and compressive strength of hardened mortars*

3.4.1 Bulk density

At each mortar testing age, the bulk density of each prism was calculated in accordance with BS EN 1015-10:1999 – *Methods of test for mortar for masonry*. This gave a basic indication of the density increase caused by carbonation in the binder.

3.4.2 Setting times and consistence of binders

The comparative setting times of the different binders in this investigation were determined in accordance with BS EN 196-3:2005 – *Cements: determination of setting times and soundness* with the use of the Vicat apparatus as illustrated in Figure 3.2.



Figure 3.2 – Vicat apparatus for determining standard consistence and setting times (www.controls-group.com).

Vicat testing works on the theory that the distance penetrated by the needle will decrease as the hydrates in the binder begin to set. Primarily, the standard consistency of each binder needed to be determined. A series of trial and error tests were conducted to determine the amount of distilled water needed to create the standard consistency when mixed with 500g of binder in accordance with the standards. Table 3.1 shows the mass of water required to achieve standard consistency for each binder.

Table 3.1 – Mass of distilled water required to achieve standard consistency for VICAT testing.

Binder	Mass of binder (g)	Mass of water (g)	Water binder ratio
THB-52.5R	500	208	0.416
THB-42.5N	500	209	0.418
Batichanvre	500	188	0.376
NHL5	500	190	0.380

The four tests for initial setting times were performed simultaneously, requiring four moulds which fell within the specifications set out by the standards. Mixing of the pastes was carried out using a Controls 65-L0006/AM automatic mortar mixer as shown in Figure 3.3.



Figure 3.3 – Automatic mortar mixer [www.controls-group.com].

The preparation and testing procedure was as follows:

- 500g of binder was weighed and placed in the mixing bowl. The correct amount of distilled water was weighed into a plastic cup.
- With the mixing bowl in the mortar mixer the water was introduced into the bowl and the mixer started on a low speed for a period of 90 seconds.

- During the next 30 seconds, any paste adhered to the wall and bottom of the mixing bowl was removed using a palette knife and placed in the middle of the bowl.
- The mixer was restarted for a period of 90 seconds.
- Each mould was placed on a glass base-plate and filled with paste of standard consistence. The mould and base-plate were then placed in a plastic container and filled with distilled water so that the top surface of the paste was submerged to a depth of at least 5mm.
- Every 15 minutes, the assembly was placed under the VICAT needle. The needle was positioned on the surface of the paste and then released.
- The integrated scale indicated the distance from the needle to the base-plate.

The initial setting time for the binder occurs when the distance between the needle and the base-plate is (6 ± 3) mm to the nearest five minutes.

3.4.3 Flexural and compressive strength

For each binder type and testing age three mortar prisms of 40x40x160mm were fabricated totalling 75 prisms. For comparison an extra series of prisms were fabricated using water steeped with OSR for a period of 24 hours to explore whether the minerals present in the organic aggregate leached into the water and had an effect on the setting and strength of the binder. At each testing age the three mortar prisms were tested in flexure and each resulting half was tested in compression to create average values for both properties. CEN (European Commission for Standardisation) standard sand was used as an aggregate in all the mortars. Table 3.2 gives the particle size distribution of CEN standard sand. It is necessary to use sand aggregates to characterise binders as pure lime pastes are problematic to fabricate due to high shrinkage during drying and curing.

Table 3.2 – Particle size distribution of CEN standard sand in accordance with BS EN 196-1:2005.

Square mesh size (mm)	2.00	1.60	1.00	0.50	0.16	0.08
Cumulative sieve residue (%wt)	0	7 ± 5	33 ± 5	67 ± 5	87 ± 5	99 ± 1

As a result of the review of literature, Tradical® hemp binders were treated as air lime/cement mortars with cement mass not exceeding 50% of the total binder mass. Therefore the mortar mixes were mixed in accordance with BS EN 196-1:2005 but then moulded in accordance with BS EN 1015-11:1999.

The proportions by mass of the constituent parts were one part hemp binder (450±2g), three parts CEN standard sand (1350±5g) and one half part of water (water/binder ratio 0.50) (225±1g). Distilled water was used throughout with the exception of the ‘OSR’ series of mortars where the water which has been steeped with OSR.

An automatic mortar mixer was used throughout. Initially the dry binder was placed into the mixing bowl where the distilled water was added and the mixer started at a low speed (Table 3.3) for a period of 30 seconds. The sand was steadily added during the next 30 seconds of mixing after which the mixer was switched to high speed and mixed for an additional 30 seconds. After 90 seconds the mixer was stopped, during which the mortar adhering to the sides of the bowl was scraped off, by means of a palette knife, and placed in the centre of the bowl. Finally the mortar was then mixed for a further 60 seconds at high speed.

Table 3.3 – Speed of mixer blade according to BS EN 196-1:2005.

	Rotation (min⁻¹)	Planetary rotation (min⁻¹)
Low speed	140 ± 5	62 ± 5
High speed	285 ± 10	125 ± 10

Each mixed batch consisted of sufficient material to fabricate three test specimens. The prisms were cast in steel moulds as illustrated in Figure 3.4.



Figure 3.4 – Steel mould used for casting mortars [www.controls-group.com].

To facilitate de-moulding, the steel moulds were lightly coated with mineral oil. The prisms were cast in two layers; each subjected to 25 tamps using an acrylic prismatic rod with a cross-section of 12x12mm in order to minimise voidage in the mortar. After compaction of the second layer any excess mortar was removed using the straight edge of a palette knife and the top surface smoothed. The steel moulds were then sealed in polythene bags to provide a relative humidity environment of $95\% \pm 5\%$ and placed in the conditioning room (20°C and 65%RH). After five days the prisms were de-moulded by disassembling the steel moulds and lightly hammering any steel pieces which were still attached to the prisms. The prisms were then placed in the polythene bags once again for a further two days before being removed and placed on wire shelving in the conditioning room for drying and curing until the prisms were due for testing. Mechanical testing on mortars was carried out on a DARTEC 100kN testing rig coupled with automatic data acquisition software. Figure 3.5 shows typical testing setups for flexural and compressive mortar tests. Preliminary tests concluded that a displacement rate of 0.2mm/min for both flexural and compressive testing resulted in load rates within requirements set out by the standards.



Figure 3.5 – Typical mortar flexure and compressive test.

3.4.4 Moisture absorption

In general the shiv was stored in the departmental concrete laboratory with varying environmental conditions (approximately 15-20°C and 45-55% relative humidity). However, previous publications state that shiv is very susceptible to changes in relative humidity due to the open pore structure of the shiv [Evrard, 2003; Cerezo, 2006]. To determine if this was the case two nominally identical opened bales of shiv were stored in two different locations; one in the concrete laboratory (heated but otherwise uncontrolled) and the other in a the conditioning room. Additionally 100g of shiv were taken from each bale and placed in a sieve to ensure free flow of air to all surfaces of the shiv particles; one sieve was also placed in each location. The aim was not to carry out an in-depth study into shiv behaviour in changing environmental conditions but to determine whether different locations in a typical laboratory setting would have a significant effect on the moisture content of the shiv before it was mixed with the other constituents. After a period of 7 days 100g of material was taken from the top and the bottom of each bale, together with the materials from the sieves the six samples' respective masses were measured before and after oven drying allowing determination of moisture contents.

The initial competition for water between the binder and shiv is intrinsic to the resultant properties of the composite material as shiv has the ability to absorb up to 4.5 times its own mass in water [Evrard, 2003]. Furthermore

the formulated binders also have specific water demands for hydration and setting reactions. Knowledge of the absorption rate and total water absorption properties of shiv is therefore important to determine. To establish the rate of water absorption a novel methodology was developed within this investigation. A total of 50 grams of shiv was placed within two ordinary kitchen sieves which were tied together creating a sphere allowing free flow of water from all directions once submerged. The sphere was weighed and then submerged into a container of water over increasing periods of time up to a total of 14 days; at each time interval the sphere was removed from the container and excess water removed by vigorous shaking. The sphere was subsequently weighed and any increase in mass was attributed to water absorption. The water absorption at 14 days was presented as the total water absorption potential of UK shiv.

3.4.5 Particle grading

Quantifying the ratio of hemp fibres, shiv and dust is an important step in fundamentally characterising the shiv as it allows immediate physical comparisons between shivs from differing origins. Particle grading of the shiv was determined by sieving method (BS EN 993-1:1995) using an electromechanical sieve shaker of the sort shown in Figure 3.6. A column of nine soil grading sieves (with decreasing apertures of 28, 20, 14, 10, 8, 4, 2, 1, 0.5 and 0.25mm) were vibrated on the electromechanical shaker for a period of 10 minutes. All aggregates were subjected to particle grading; three 100g samples of shiv were selected of each aggregate to create an average distribution curve.

In an attempt to understand the movement imparted on the shiv particles inside the grading sieves, preliminary testing consisted of sieving one batch of material whilst the grading sieve column was locked down but otherwise uncovered. It was observed that the movement imparted was not a random bouncing whereby the particles jumped up and down. The movement was more like 'shuffling' whereby the particles remained lying flat on the sieve grate throughout the whole process and moved around the sieve in a circular motion. This only caused the particles to fall through a sieve grade if the

length of the particle was less than the aperture size. This therefore indicates that the particle grading of shiv via the sieving method is a reliable way of ascertaining length particle distribution data.



Figure 3.6 – Electromechanical sieve shaker, [www.controls-group.com].

3.5 Main programme of work for composite testing

In the majority of cases hemp-lime is not used as a structural material. Despite this, compression testing provides an effective comparison tool for the composite testing of hemp-lime. In the first instance it allows the mechanical parameters of different binders to be directly compared. Furthermore it allows comparison against previous empirical investigations which have used the same mechanical technique and allows basic assessment of the integrity and robustness of the material; the material must display sufficient robustness during processes such as shuttering

removal and plastering when on site. It is also important to have a value of the maximum compressive strength and elastic modulus of the material as when cast around a primary structure it is necessary for the material to withstand a certain amount of wind and shear loading as it spans across the studwork. The tests used measured the development in mechanical parameters over a 360 day period culminating in values of ultimate compressive strength and elastic modulus. A total of 141 hemp-lime specimens were fabricated for compression testing. The specimens were sub-grouped into four different binder types, three different bulk densities, and two different curing regimes and then tested at six different age intervals.

3.5.1 Composite specimen design

Minimizing the number of unwanted fabrication, curing, testing and material variables in empirical investigations hopefully provides reliable and repeatable results. This section examines and justifies the variables used in this investigation as a result of the review of literature and through preliminary testing.

3.5.1.1 *Constituent ratios*

Hemp-lime is made up of three constituent materials whose relative proportions change depending on the use and placement in a building (see Chapter 1). This investigation concentrated on hemp-lime when used as an insulative infill material for walls. During the length of this investigation the constituent proportions used in practise varied a number of times and in many cases the constituent proportions are determined as a result of considering the individual factors at each construction site including the season in which construction is taking place, the predominant weather conditions, method of material application, whether shuttering is permanent or not and the required final dry density. However, by reducing the formulated binder content it is possible to reduce material costs, carbon footprint and the density (improving thermal insulation) of hemp-lime. The UK hemp-lime construction industry is currently implementing low density materials, as a result, this investigation evolved from focussing on higher

density hemp-lime composites to novel, lower density mixes, using constituent proportions which had not been previously empirically tested.

Hemp-lime wall mixes have typically used two parts (by mass) of binder to one part of shiv, mixed together with around 3 parts of water. This mix, when correctly tamped on site, produces a dry density of around 330kg/m³. By reducing the proportion of binder and limiting the degree of material compaction the final density of the material can be reduced. Current practice specifies 1.5 or 2 parts of binder to 1 part of hemp, combined with around 2 parts of water, producing a final dry density of 275 or 330 kg/m³.

This investigation compares the performance of 275 and 330kg/m³ mixes. In addition tests were carried out on mixes of one part binder to one part hemp by mass, producing a final density of approximately 220 kg/m³ to investigate whether this could be a viable mix for use in future wall construction. Figure 3.7 shows the constituent proportions, by percentage mass, relative to each density.

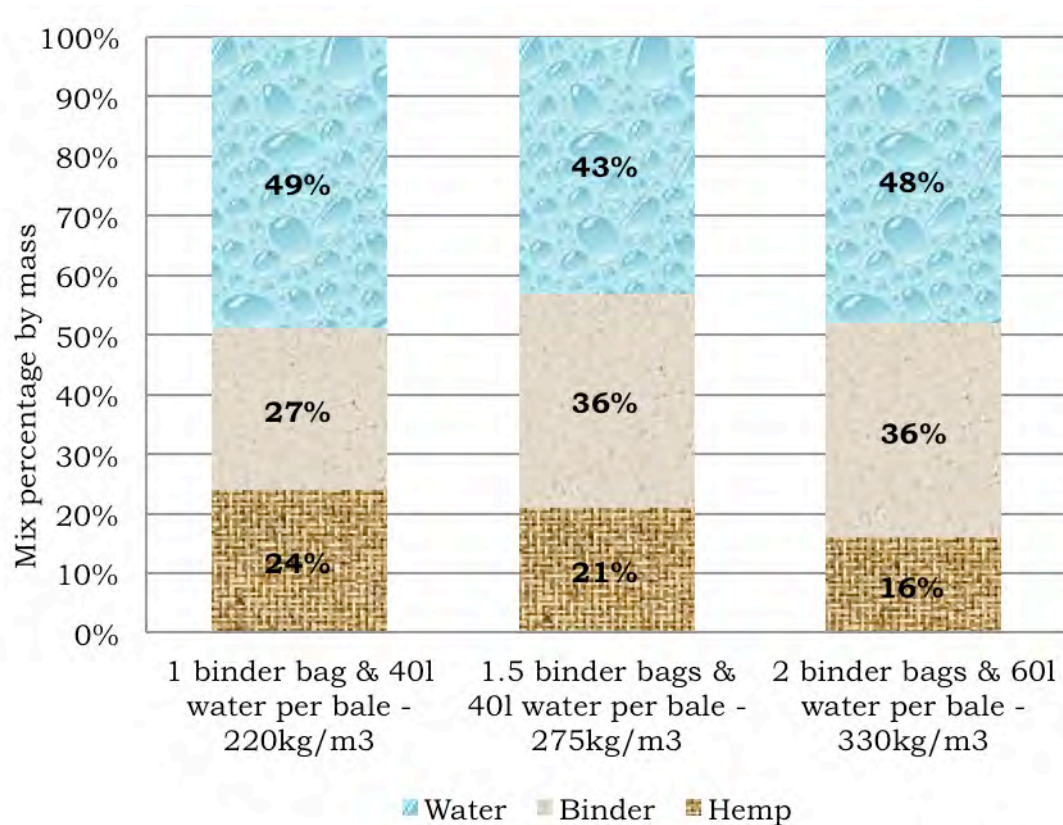


Figure 3.7 – Mix proportions by percentage mass of the three mixes studied

These mix proportions provide water/binder ratios of 1.8, 1.2 and 1.3 for 220, 275 and 330kg/m³ respectively, higher when compared to normal water binder ratios for concretes (typically 0.3 – 0.6).

One of the main objectives of this investigation was to have a specimen fabrication methodology whereby the final air dry density of the material could be reliably and consistently achieved. The air dry density refers to the anhydrous density of the specimen with the addition of 4-7% moisture content [Evrard, 2003]. Previous publications [Evrard, 2003; Cerezo, 2006] fabricated specimens by systematically inserting between 80-100mm of wet hemp-lime material into the mould and then applying a compressive force to that layer. This process was repeated until the specimen mould had been filled. The hypothesis was that applying a constant compressive force to each layer would produce specimens with consistent densities. However large

density variations were observed in specimens cast to the same regime as previously discussed in Chapter 2.

To initially understand the relationship between how much wet material was required to get the desired air dry density a series of specimens were fabricated using the three different material ratios for 220, 275 and 330kg/m³ material. For each mix three cylinders were fabricated, one cylinder where the wet material was gently placed into the cylinder without any levelling or tamping, another where the material was placed, levelled and gently tamped by hand and a third cylinder where the material was placed, levelled and firmly tamped by hand. Thus a total of nine cylinders were fabricated for each series.

After a period of 24 hours the specimens were de-moulded and placed in an oven at 105°C to remove the moisture. When no further changes in mass had been observed, the specimens were removed from the oven and weighed to determine the anhydrous density of the specimens. By then looking at the mass relationship between the wet density and the anhydrous density (Appendix I) and adding an air dry moisture content of 7%, the mass of wet material required to achieve the desired final air dry densities of 220, 275 and 330kg/m³ could be determined. A moisture content of 7% was chosen for the following reason; carbonation of the binder would add to the mass gain of the material over time, however, it was not possible to precisely calculate its contribution as the constituent proportions in the binder blend were not known. This assumption of 7% MC, when used in the calculations lowered the amount of wet material needed to cast the specimens, thereby allowing the mass increase due to carbonation to add to the final air dry density to the desired values. Table 3.4 shows the wet densities and the resultant dry densities for each mix along with the mass of wet material needed to achieve the desired air dry densities for the specimens tested in this investigation.

Table 3.4 – Wet and dry cylinder masses and densities

Mix ratio Density (kg/m³)	Wet mass (g) Density (kg/m³)			Anhydrous mass (g) Density (kg/m³)			Anhydrous mass + 7% MC (g) Density (kg/m³)			Wet material mass required for casting (g)
	Specimen			Specimen			Specimen			
	1	2	3	1	2	3	1	2	3	
2:1 330	2762 521	3434 648	4116 777	1415 267	1745 329	2093 395	1597 301	1970 372	2363 446	3036
1.5:1 275	2144 405	2503 472	2863 540	1190 237	1387 276	1599 318	1343 253	1566 295	1805 341	2328
1:1 220	2003 378	2346 443	2689 507	990 187	1180 223	1324 250	1118 211	1332 251	1495 282	2080

As a result of these tests it was determined that 3036, 2328 and 2080g of wet material was needed to create air dry densities of 220, 275 and 330kg/m³ respectively. The hypothesis behind this methodology is that, if the material has been homogenously mixed and specimens have the same mass of wet material when cast, the densities of the specimens should be consistent at the different testing ages, providing a significantly more reliable methodology of producing consistent and comparable specimens.

3.5.1.2 Specimen dimensions

Evrard [2003] and Cerezo [2006] carried out compressive tests on hemp-lime specimens with dimensions of 110mm diameter and 220mm length. This created end surface areas of 10000mm² and an aspect ratio of 2:1. 150mm and 300mm diameter specimens were chosen for this study for the following reasons:

1. The cylinders had the same aspect ratio (2:1) as previous tests carried out in France.
2. The specimen dimensions are the same as those for standardised concrete cylindrical strength tests in BS EN 12390-1:2012.

3. Batches of hemp from the old processing plant occasionally contained shiv particles up to 50mm in length. With reference to a note in section 5.1 of ASTM C 31/C 31M-98 which states that '*the diameter of any cylinder shall be at least three times the nominal maximum size of the coarse aggregate in the concrete*' the diameter of 150mm was determined. This minimises the effect large particles may have on the global mechanical performance of the specimen.

Specimens fabricated for chemical testing had dimensions 100mm diameter and 200mm length. The rate of carbonation through different densities of hemp-lime is not currently known. It was assumed that carbonation would not progress through the full cross-section of the specimen as carbonation in lime mortars is a very slow reaction [Lawrence, 2006] therefore a 100mm diameter specimen was deemed sufficient.

3.5.1.3 Testing ages

There is no standardised time frame for the testing of hemp-lime as a composite material. However, the testing regime followed that set out by the standards for lime mortar testing. The testing ages were also based on a number of other factors:

1. It was desirable to ascertain strength and elastic modulus values as early as possible to determine the strength contribution purely as a result of the hydration in the binder. It was not possible to reliably test the specimens at the de-moulding age as they were too friable to go through the testing preparation process therefore the earliest testing age was set at 14 days.
2. It was necessary to be able to directly compare the mechanical parameters of the material with previous empirical investigations.
3. The time frame needed to fit within the time limits of this investigation.

With these factors in mind testing ages for mechanical and chemical testing of the composite material were 14, 28, 91, 180 and 360 days.

3.5.1.4 Specimen curing

There were two main decision drivers into designing the curing regimes used in this investigation:

1. It was important to allow uniform carbonation across the whole surface area of the specimens in order to minimise the effect un-even carbonation may have had on the mechanical characteristics of the material.
2. It is advantageous to be able to use the same curing regimes as have been used in previous empirical investigations.

All specimens were cured in the conditioning room to remove environmental variables. Two curing regimes were chosen to be compared:

1. Specimens were de-moulded after a period of seven days and placed on wire mesh in the conditioning room, providing a 4mm gap between the shelf and the bottom of the specimen to facilitate uniform carbonation

Specimens were kept in their moulds until the day of testing to mimic the conditions used on empirical tests carried out in France [Evrard, 2003; Arnaud, 2009; Cerezo, 2006]. This methodology more closely resembles the drying and carbonation dynamics of the material when used on-site where the length of the specimen can be considered to be the depth of a wall and the two ends the interior and exterior surface of the cast material after the shuttering has been removed. This series of specimens was named the 'French regime' (FR) specimens.

3.5.2 Specimen fabrication matrix

Table 3.5 outlines, in a simple manner, the variables investigated, the number of large and small specimens and the total number of specimens fabricated for the purpose of this investigation.

Table 3.5 – Composite specimen fabrication matrix.

Specimen fabrication matrix								Number of specimens
Binder, aggregate or curing regime	THB-52.5R	THB-42.5N	BC	NHL5	SH	FR	0.3OSR, 0.6OSR & OSR	-
Densities (kg/m ³)	220, 275 & 330	275	275	275	275	275	275	-
Testing ages	14, 28, 91, 180, 360	28, 91, 180, 360	28, 91, 180, 360	28, 91, 180, 360	28, 91, 180, 360	28, 91, 180, 360	28, 91, 180, 360	-
Large specimen at each testing age	3	3	3	3	3	3	3	-
Small specimen at each testing age	1	1	1	1	1	1	1	-
Total No. large specimens	45	12	12	12	12	12	36	141
Total No. small specimens	15	4	4	4	4	4	12	37
Total								198

3.5.3 Specimen fabrication

3.5.3.1 Mixing

When mixed on site, the shiv and binder are combined first before the desired amount of water is added. This order is necessary due to the type of mixer that is used. The order used in this investigation varied slightly, however, this does not change the handling or performance characteristics of the material. Test batches confirmed that the pan mixer used within this investigation produced very homogenously mixed material and, based on visual observations the shiv was evenly coated with the slurry.

The water and dry binder were initially mixed together to create a uniform slurry and to reduce lime dust. The shiv was then added and mixed for up to five minutes until a homogenous blend was created. The material was mixed in batches of 35kg, slightly below the maximum volume capacity of the mixer. Figure 3.8 shows the pan mixer, the weighed constituent parts and the wet material after mixing.



Figure 3.8 – Pan mixer, weighed constituent materials and mixed material.

3.5.3.2 Casting

One of the main objectives of casting was to produce cylinders with homogenous material distribution and with minimal density variation along the height of the specimen. To achieve constant distribution of the wet material one handful was inserted at a time (each handful contained between 230-270g of wet material) before being manually levelled off around the whole cross-section of the cylinder. It was the case, with all three mixes, that no tamping was required for the calculated wet mass of material to be inserted in the mould. This may suggest that walls currently being constructed in practise may be of higher densities than designed (reducing the thermal performance of the material) as tamping is a regular occurrence on the building site.

The wet material was cast in wax dipped cylindrical cardboard moulds manufactured and supplied by Curran Packaging (www.curran.co.uk). Cardboard was chosen, instead of plastic moulds, as cutting the cardboard moulds (either using a table saw or by hand with a Stanley knife) was found to be much easier and less likely to damage the hemp-lime cylinder. The wax prevented any take-up of water from the wet mix and prevented any material from sticking to the mould which aided de-moulding.

When cast on-site the material is placed between layers of removable shuttering which is left in place for a period of 24 hours to allow the hydraulic phases in the binder to set sufficiently so the material is self supporting once the shuttering has been removed. To replicate this process in the laboratory, plastic caps (supplied by Curran packaging) were used to cover the ends of the specimens during casting and for the first 24 hours of specimen curing (Figure 3.9).

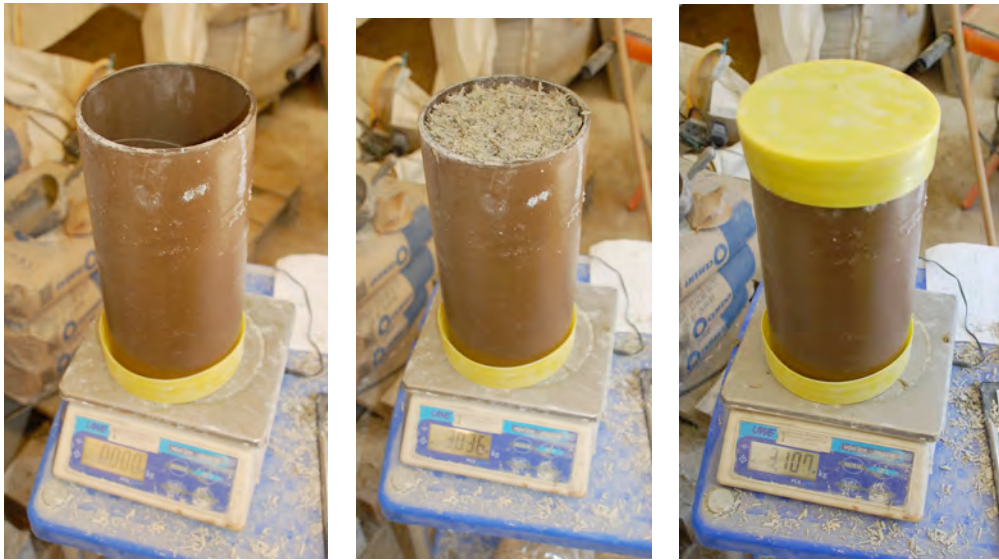


Figure 3.9 – Casting procedure for fresh hemp-lime material

3.5.3.3 De-moulding

Freshly cast specimens were placed in the conditioning room in the vertical position to ensure the specimen retained its circular cross-section. After a period of 24 hours the plastic caps were removed and the specimens laid on their sides to allow air to flow to the ends, Figure 3.10. The specimens were left in the cardboard moulds for a further six days to allow hydration of the cementitious content in the binder and to allow the specimens to become robust enough for handling; de-moulding after 24 hours produced specimens which, although self-supporting, were not robust enough to be handled. This methodology is similar to classical methods set out for curing of mortar and concrete samples as set out by empirical standards.



Figure 3.10 – Capped and un-capped composite specimens.

Removal of the moulds was carried out using a small table circular saw with the saw adjusted to the depth of the cardboard moulds (5mm). Three cuts allowed the cardboard to be easily removed as is shown in Figure 3.11.



Figure 3.11 – De-moulded composite specimen.

After de-moulding the specimens were returned to the conditioning room and placed on shelves. The shelves had a layer of wire mesh which allowed free air flow underneath the specimens by standing the approximately 5mm above the surface of the shelves (Figure 3.12). The specimens were also spaced with a 30-40mm gap between adjacent specimens to allow free air flow and to give enough room for handling.



Figure 3.12 – De-moulded composite specimens standing on mesh.

3.5.4 Testing methodology

At each testing age, three specimens of each binder type, density and testing regime were randomly chosen from the conditioning room, weighed and prepared for testing. From these three tests, an average value for the density, moisture content and mechanical parameters of the material at that testing age were obtained.

3.5.4.1 Capping

Upon de-moulding the specimens it became apparent that the bottom surface of the specimens was level as a result of it being cast against one of the bottom plastic caps, however, the top surface displayed heterogeneities. In order to apply a homogenous uniaxial stress across the entire cross section of the specimen it was necessary to prepare the ends of the specimens so that they were flat and parallel to each other. Cerezo [2006] concluded that using a batt of hemp fibre between the platen and the top of the specimen was insufficient in distributing an even stress. Consequently, sawing of the specimen ends, using a large stone cutting saw was used successfully to produce flat specimen ends. The same methodology was trialled during preliminary tests in this investigation using both a band saw and a stone cutting saw. Due to the lower density of these specimens compared to those tested by Cerezo, the saws did not produce flat ends, rather, they tore at the material producing unsatisfactory results as shown in Figure 3.13.



Figure 3.13 – Composite specimen end cutting using a band saw (left) and stone cutting saw (right).

The decision was made to cap the specimen ends using rapid hardening dental plaster immediately before testing. The capping methodology was as follows:

- A white board was wiped with release oil to allow easy removal of the capped specimens.

- Dental plaster was mixed with water until the desired consistency was achieved.
- Using a palette knife, dental plaster was smoothed over one end of the specimen. Preliminary tests had shown this part of the methodology to eliminate air bubbles from the capping process.
- Three palette knives of dental plaster was placed on the white board and the plastered specimen end was placed on the mound of plaster and pressed down until excess plaster was seen to flow from the edges.
- A tri-axial spirit level was placed on the vertical face of the specimen to ensure verticality (Figure 3.14).
- The excess plaster around the edge was removed by sliding a finger around the edge.
- The plaster was left to set for 10-15 minutes.
- The process was repeated for the second end (Figure 3.15).

Upon completion of capping the overall length of the specimen was recorded to determine the thickness of capping and for strain calculations.



Figure 3.14 – Equipment for capping (left) and use of tri-axial spirit level for the capping of the first end.



Figure 3.15 – Capped composite specimen.

3.5.4.2 Strain measurements

An accurate measure of axial strain is necessary when determining the Elastic Modulus of a material. To ascertain whether or not end effects and/or confinement of the material had any effects on strain measurements between the ends of a specimen and those measured across the central span of the specimen a series of tests were designed to compare these differences using four different strain measurement methods. The automated data acquisition software coupled to a DARTEC 100kN electromechanical testing rig measured the strain from the end platen as a constant displacement rate of 3mm/min was applied. Hall Effect Transducers (HET), Linear Variable Differential Transducers (LVDT) and Demountable Mechanical Strain Gauges (DEMEC) were used to determine the strain measurements across the central span of a specimen. HET's work by measuring the change in magnetic field as two magnets slide over each other; this change in magnetic field is consequently changed into a distance measurement using calibrated software. LVDT's are a common and well accepted type of electromechanical transducer which converts the rectilinear motion into a distance measurement. Unlike HET's and LVDT's which are automated, DEMEC's

manually record any change in distance and consist of a standard or a digital dial gauge attached to an Invar bar. A fixed conical point is mounted at one end of the bar, and a moving conical point is mounted on a knife edge pivot at the opposite end. The pivoting movement of this second conical point is measured by the dial gauge.

In order to directly compare the strain measurement methods across the central span, a capped prismatic specimen was prepared. This allowed HET's to be placed on two of the vertical faces, LVDT's on the other two faces and the DEMEC's on all four faces. The specimen was loaded and at regular displacement intervals, the test was paused to allow manual recording of the DEMEC points. Figure 3.16 indicates that there is little difference in the strain measurements between the end platens and the central span of the specimen and between the different measurement techniques considered. Due to the manual interaction when taking DEMEC readings, the results seem irregular compared to the other methods, however, they generally agree well with the automated recording apparatus. Therefore, for the purposes of this investigation, end platen readings were used for strain calculations; this minimised human error and increased the rate of specimen testing due to decreased pre-testing specimen setup.

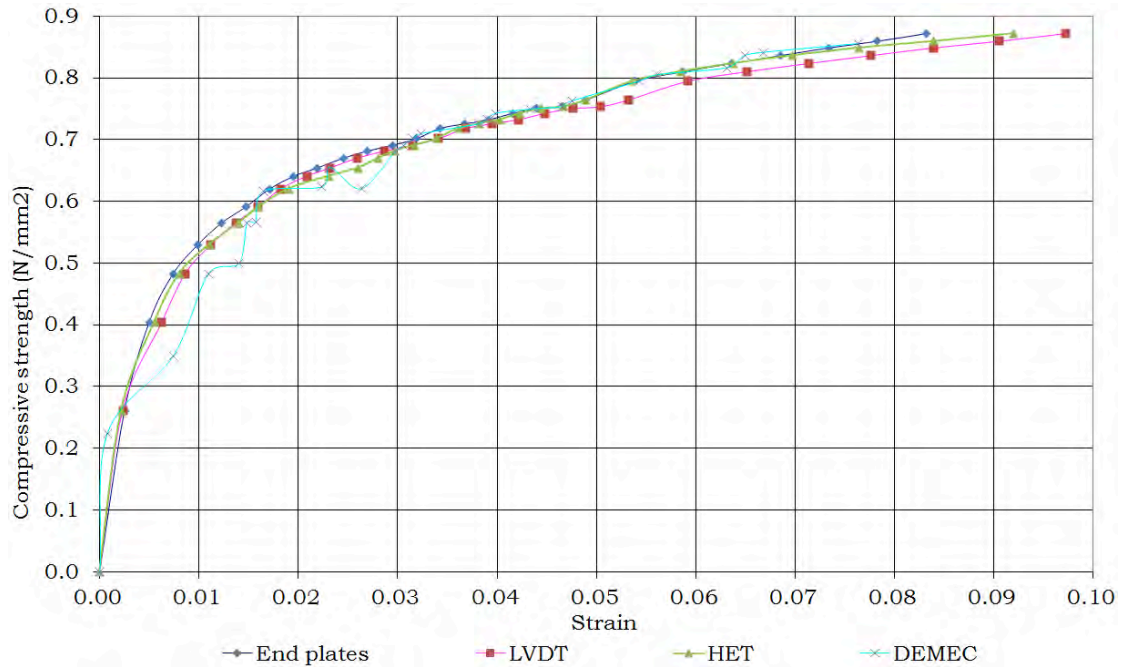


Figure 3.16 – Stress vs. Strain comparison of different strain measurement techniques.

3.5.4.3 Compression testing

Compression testing of the composite specimens was carried out on a DARTEC 100kN electromechanical testing rig with automatic data acquisition software. The platens provided with the rig measured 150mm in diameter. As the majority of specimens measured fractionally more than 150mm in diameter, square platens were attached to the rig to provide complete coverage of the specimen ends.

A displacement rate of 5mm/min was used whilst loading the specimens. This value was determined by analysing the speed of loading on the deformation of specimens [Couedel, 1998]. Furthermore, Cerezo [2006] applied three different loading rates: 0.25 mm/min, 2.5 mm/min and 5 mm/min to three different specimens. In all three cases, the increase in loading was parallel. The value of the slope (the modulus of elasticity E) is therefore independent of the choice of loading rate over range tested. A higher displacement rate was not chosen however as the role of water on the mechanical behaviour of hemp-lime needs to be limited. Tests may otherwise have been principally measuring the compressive response of water as 14

day specimens still contained a large amount of free water. Figure 3.17 presents a typical compression test specimen setup.



Figure 3.17 – Typical compression test setup.

The displacement of the platen $d(\text{mm})$ and the force applied $F(\text{kN})$ as a function of time was recorded by the data acquisition software which then allowed the determination of the mechanical parameters of the material.

3.6 Programme of work for chemical testing

This section describes and justifies the investigative techniques and testing methodologies used to evaluate the chemical characteristics of the binders and the composite material at each testing age. Mortars were subjected to phenolphthalein staining to visually determine the carbonation front at each testing age, concurrently thermogravimetric analysis was used to provide a more detailed insight into the mineralogical development of the binder in the composite as carbonation occurred.

3.6.1 Phenolphthalein indicator

At each testing age, a small hemp-lime and/or standard sand mortar specimen was split in half over a bolster. One half of the freshly split specimen was sprayed with phenolphthalein and photographed against a scale ruler (Figure 3.18). The image was then introduced into a CAD program and scaled to 1:1 by reference to the scale rule on the image. It was then possible to measure the depth of carbonation with great accuracy by taking a number of readings, producing an average which was used as the carbonation depth.

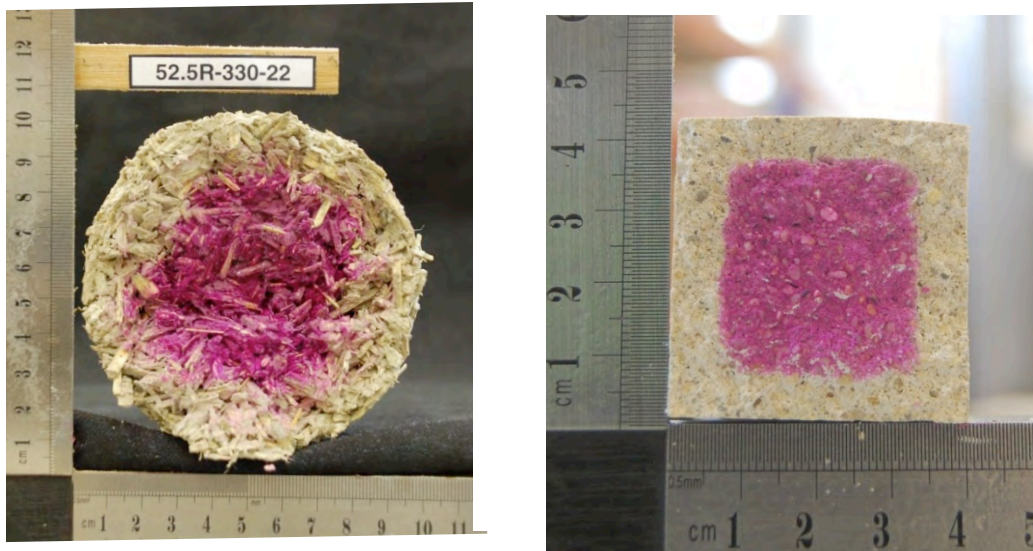


Figure 3.18 – Respective phenolphthalein stains on 28 day and 180 day old THB-52.5R hemp-lime and mortar specimen.

3.6.2 Thermogravimetric analysis

In this investigation, TGA was used to determine the quantitative differences in hydration and carbonation products between the edge and the core of hemp-lime specimens at different ages. This series of testing was carried out with the following objectives in mind:

- To determine the rate of carbonation relative to the density of hemp-lime.
- To determine the total amount of CO_2 which was absorbed by the binder during the carbonation process.
- To determine whether 100% of the $\text{Ca}(\text{OH})_2$ originally present in the bagged binder was converted into CaCO_3 during the carbonation process.
- To ascertain how much $\text{Ca}(\text{OH})_2$ was produced by the cement content in the Tradical® hemp binder compared to the theoretical amount.

- To quantify the development of the hydraulic phases within the binder as hydration takes place.

This investigation used a Setram TG-92 high resolution thermogravimetric analyser. The accuracy of this equipment was measured by Lawrence (2006) who determined the machine had a slight tendency to underestimate the amount of Ca(OH)_2 present. The absolute errors are below 0.3% which produces a relative error of the order of 3-4% when calculating the measured content of Ca(OH)_2 in the sample.

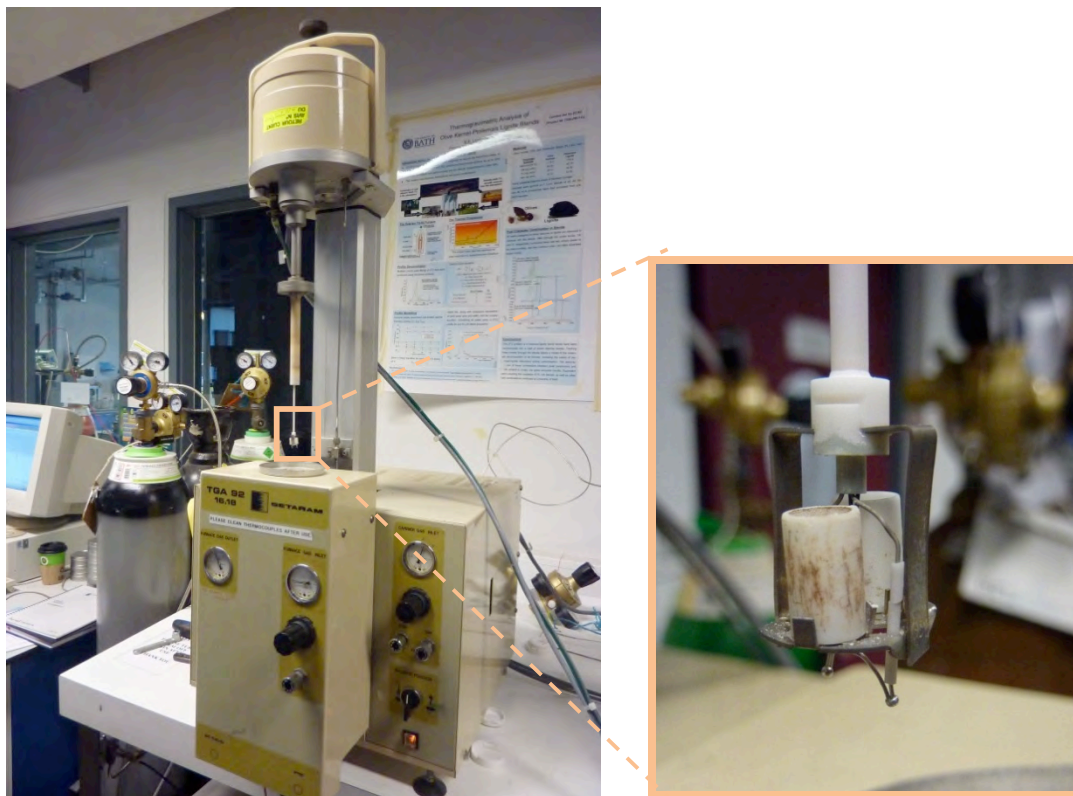


Figure 3.19 – Setram-92 high resolution TGA/DTA analyser with expanded view of crucibles.

Figure 3.19 shows the TGA equipment used in this investigation with the microbalance raised showing the alumina crucibles in which the powdered samples are placed.

Figure 3.20 shows a typical TGA plot for a partially carbonated sample of hemp binder. The graph illustrates three important mass loss phases. A steady mass loss can be seen between $\sim 100^{\circ}\text{C}$ and $\sim 400^{\circ}\text{C}$. This is due to the loss of the hydrates from the hydraulic phases of the binder. The loss between $\sim 400^{\circ}\text{C}$ and $\sim 470^{\circ}\text{C}$ is due to the thermal decomposition of $\text{Ca}(\text{OH})_2$ (dehydroxylation) into CaO and H_2O , and the final loss between $\sim 600^{\circ}\text{C}$ and $\sim 800^{\circ}\text{C}$ is due to the thermal decomposition of CaCO_3 (decarboxylation) into CaO and CO_2 . By knowing the mass of H_2O and CO_2 which has been thermally broken down from the sample, an accurate quantification of the mass of minerals originally present in the sample can be made using stoichiometry.

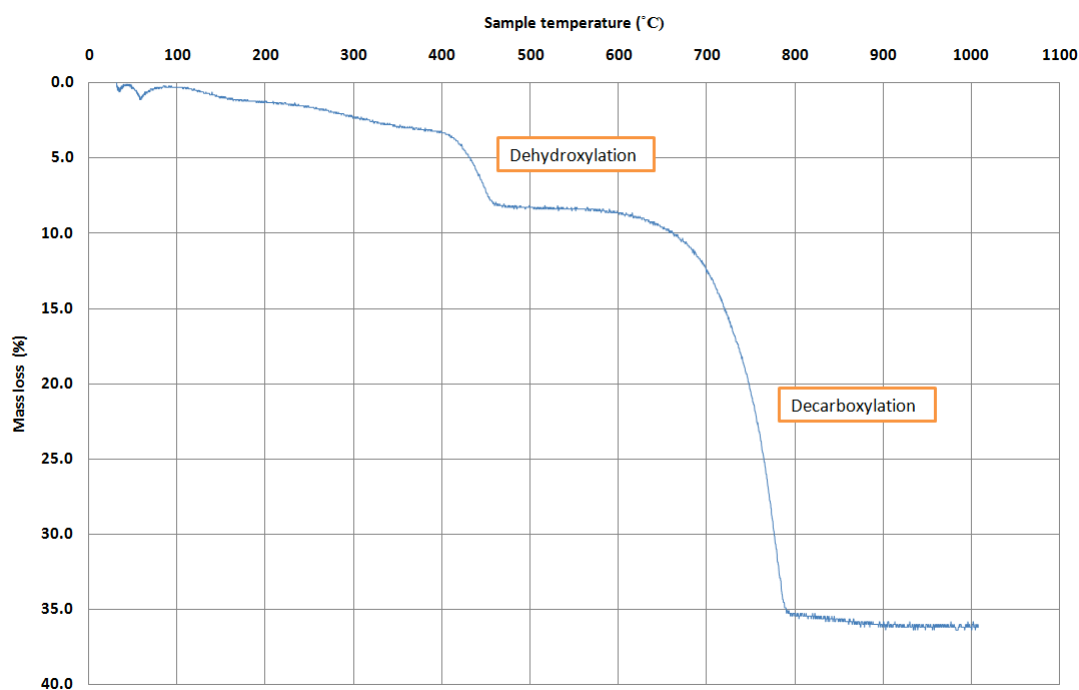


Figure 3.20 – Typical TG plot for a partially carbonated sample of hemp binder.

Any increase in CaCO_3 between cured specimens compared to the fresh binder can only be caused by absorption of CO_2 from the atmosphere. An ultimate value of CO_2 sequestration per bag of binder can then be calculated. The increase of CaCO_3 will come from the carbonation of Ca(OH)_2 . The Ca(OH)_2 will come from the air lime, however, as cement hydrates a certain amount of Ca(OH)_2 is produced from the hydration reaction. This extra Ca(OH)_2 will also carbonate and contribute to the total CO_2 sequestration of the binder.

3.6.2.1 Composite specimen sample preparation

At each testing age, small specimens from each binder type, density and curing regime were randomly removed from the conditioning room for chemical characterisation. Shiv particles were removed from the outer surface of the specimens using tweezers. The specimen was then split in half and the tweezers were again used to remove shiv particles from the core (from within 1cm radius of the centre) of one half of the specimen. The other half was used for phenolphthalein testing. The edge and core samples were then separately ground using a pestle and mortar to remove the binder from the surface of the shiv particles. By then passing the material through a 125 micron sieve the shiv was separated from the powdered binder. The binder was then placed into small glass jars and in an oven at 70°C for a period of 3 days to remove any free water which may have been present. It was important to maintain the oven at 70°C as CSH's begin to thermally decompose at temperatures of 95°C [Ubbriaco & Tasselli, 1998; Ellis, 2000]. The bottles were then filled with nitrogen and sealed in order to avoid the carbonation process continuing [Dheilly et al, 2002]. Storage was in glass bottles since Thomas et al [1995] demonstrated that CO_2 penetrates plastic vials or bags. TGA was also carried out on fresh samples of THB52.5R, THB42.5N, BC and NHL5 straight from the bag to establish a base line for the amount of calcium hydroxide and calcium carbonate originally present.

3.6.2.2 Binder paste fabrication

As the hydraulic constituents in the binder hydrate calcium hydroxide is produced. In order to quantify the amount of calcium hydroxide produced

binder pastes were fabricated and cured in polythene bags so carbonation could not occur. Two different water binder ratios of 0.4 and 0.5 were used for a parallel series of tests to determine if the change in water content had an effect on the amount of calcium hydroxide produced. To observe the progression of the hydraulic compounds, samples were taken from the paste at five different curing ages of 6 hours, 24 hours, 3, 7 and 28 days, therefore a total of ten TGA tests were carried out for the two water binder ratio mixes. The following methodology was employed when mixing the pastes:

- 250g of THB52.5R binder was prepared in a mixing bowl.
- 100g (for 0.4 w/b ratio) of distilled water was weighed into a plastic cup.
- The mixing bowl was placed in the Controls automated mixer, the water introduced into the bowl and the mixer started at a fast speed for a period of two minutes.
- Ten polythene bags were labeled with their respective w/b ratio and testing ages.
- Equal amounts of paste were placed into each bag, the air pressed out and the bags sealed.
- To ensure there was no access of air to the paste the bag was placed in another polythene bag in case of punctures.

The polythene bags were stored in the conditioning room to ensure a constant temperature regime during curing. At each testing age, the required paste was removed from the polythene bag, sprayed with acetone and stored in a vacuum dessicator in order to stop the hydration reaction.

3.6.2.3 Testing regime

There is no standardised testing regime for the thermal analysis of lime mortars, cements or hemp formulated binders and previous investigations have used widely varying regimes as previously discussed in Chapter 2.

Within this investigation, the following heating regime was employed:

- A heating rate of $50^{\circ}\text{C min}^{-1}$ between experiment start temperature and 70°C was set.
- An isotherm at 70°C was set for a period of five minutes. This was defined as the drying period whereby any free water left over from the sample preparation was evaporated.
- A heating rate of $10^{\circ}\text{C min}^{-1}$ was set between 70°C and 1000°C .

For each test, between 10-15mg of material was placed in the alumina crucible.

CHAPTER 4 - PROPERTIES OF CONSTITUENT MATERIALS

4.1 Introduction

This chapter presents and discusses the experimental results from constituent material characterisation tests described in Chapter 3. Results are presented for the hemp shiv (moisture content, grading and water absorption tests) and lime binder (physical, mechanical performance and carbonation tests) over different ages. Relationships between the individual tests are then discussed and the data used to develop an improved understanding into the constituent materials. The results of the constituent tests are then linked in later chapters against the composite tests in an attempt to find relevant relationships.

4.2 Hemp shiv

4.2.1 Moisture content

Table 4.1 below presents the moisture contents from the six hemp shiv samples tested according to the methodology set out in Chapter 3.

Table 4.1 – Comparison of shiv storage conditions.

Sampling	Moisture content (%)	Storage conditions
Top of bag	12.2	20°C and 65%RH
Bottom of bag	11.8	
Grading sieve	11.6	
Top of bag	12.0	Departmental laboratory
Bottom of bag	11.6	
Grading sieve	11.7	

Overall the samples stored under two different conditions presented very similar moisture contents. The average moisture content from all six samples was 11.8%, varying between 11.6% for both shiv from the controlled and concrete laboratory environment and 12.2% for shiv from the top of the bag in the controlled environment. Hemp from the top of the bag in the laboratory and the conditioning room contained just 0.4% more moisture than hemp from the bottom of the bag. This confirmed that each batch of hemp shiv could be treated as a consistent constituent and did not require special storage prior to use. Furthermore the shiv did not seem to be especially sensitive to different storage conditions which may be found within typical laboratory environments provided that it is kept indoors and dry. Simultaneously, taking into consideration that between 40-60 litres of water is mixed per bale of hemp shiv, it did not seem necessary to store the shiv in a controlled environment. Variations in shiv moisture content under different laboratory ambient conditions are also unlikely to have any significant influence on its initial water absorption properties.

The results relate well when compared to the isotherm and moisture content data from previous investigations. Isotherm data produced by Garnier [2000]

showed that at a relative humidity of 60% at 20°C the hemp shiv displayed a moisture content of 11.4%. Gourlay [2008] also concluded that UK shiv had an average moisture content of 11% when stored under laboratory conditions.

4.2.2 Hemp shiv grading

Shiv particle grading was carried out in order to characterise the consistency of the hemp shiv particle size used in this investigation. The average percentage of material which passed through each sieve grade, together with the range of results, is shown in Table 4.2 below.

Table 4.2 – Mean percentage of material passing each sieve.

Sieve grade (mm)	Average % of material passed (range)			
	Tradical HF OPP	Tradical HF NPP	Hemp Technology horse bedding HB	Chanvribat CB
28	100.0	100.0	100.0	100.0
20	100.0	100.0	100.0	100.0
14	99.3 (99.0 – 100)	100.0	100.0	100.0
10	98.0 (98.0 – 98.0)	95.3 (94.3 – 95.9)	89.0 (86.7 – 91.2)	94.4 (90.7 – 98.1)
8	87.8 (85.5 – 91.0)	83.8 (82.8 – 84.7)	79.6 (79.0 – 80.1)	84.9 (80.1 – 89.7)
4	59.7 (53.0 – 68.0)	27.0 (26.5 – 27.6)	26.4 (26.3 – 26.5)	40.0 (38.2 – 41.8)
2	18.7 (16.0 – 22.0)	4.1 (3.7 – 4.5)	3.6 (3.4 – 3.7)	6.0 (5.7 – 6.3)
1	2.0 (1.0 – 3.0)	0.5 (0.4 – 0.7)	0.3 (0.3 – 0.3)	0.5 (0.5 – 0.5)
0.5	0.0	0.1 (0.1 – 0.1)	0.0	0.1 (0.1 – 0.1)
0.25	0.0	0.0	0.0	0.1 (0.0 – 0.1)

Overall the use of the electromechanical sieve method provided a consistent and reliable basis for comparative analysis of shiv from different origins and from varying processing procedures. Tests carried out on hemp shiv from the new processing plant, both NPP and HB, displayed close correlation and small percentage differences from the mean. Respective average percentage differences of 1.3 and 1.2% from the mean were displayed for results between sieve grades of 28 and 2mm's which correspondingly constituted 95.9 and 94% of the total material tested for each sample. In the instance of the materials collected on the 10mm sieve from the OPP sample, there was no percentage difference from the mean between the three tests; however, OPP also displayed the largest average percentage difference from the mean of 6.4% between sieve grades of 28 to 1mm which constituted 98% of the total mass of material. The values for CB fell within these two.

The particle distribution curves for hemp shiv from the old and new processing plant is presented in Figure 4.1. The average distribution curves for the four different hemp shiv aggregates are presented in Figure 4.2.

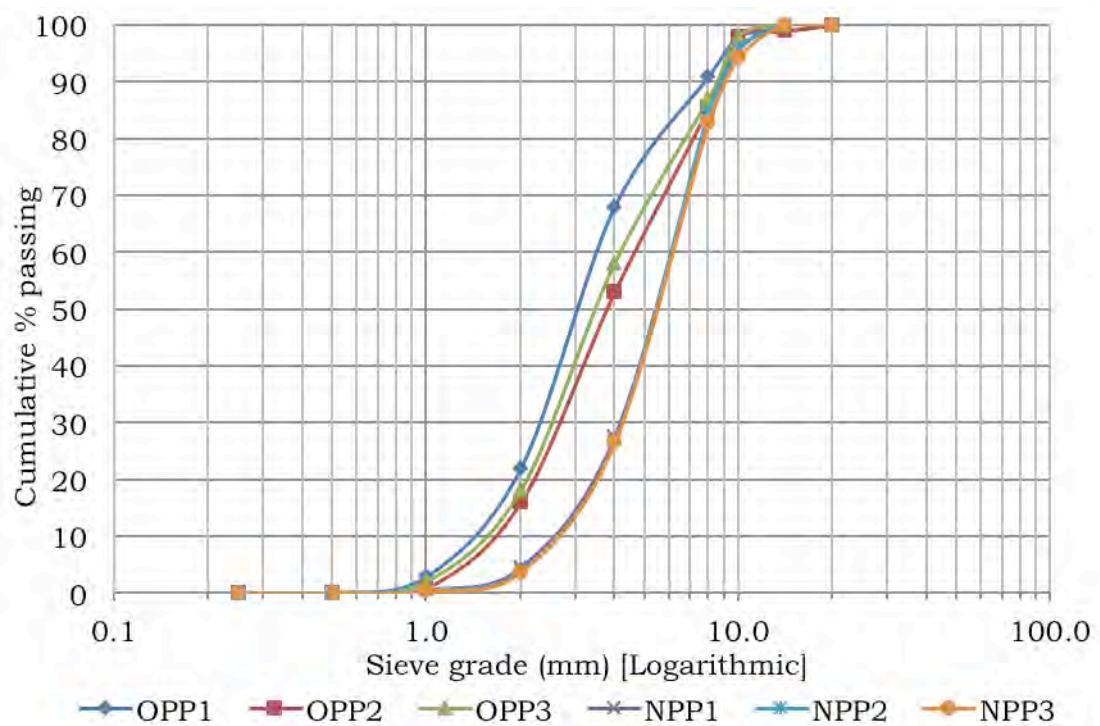


Figure 4.1 – All particle distribution curves for OPP and NPP samples.

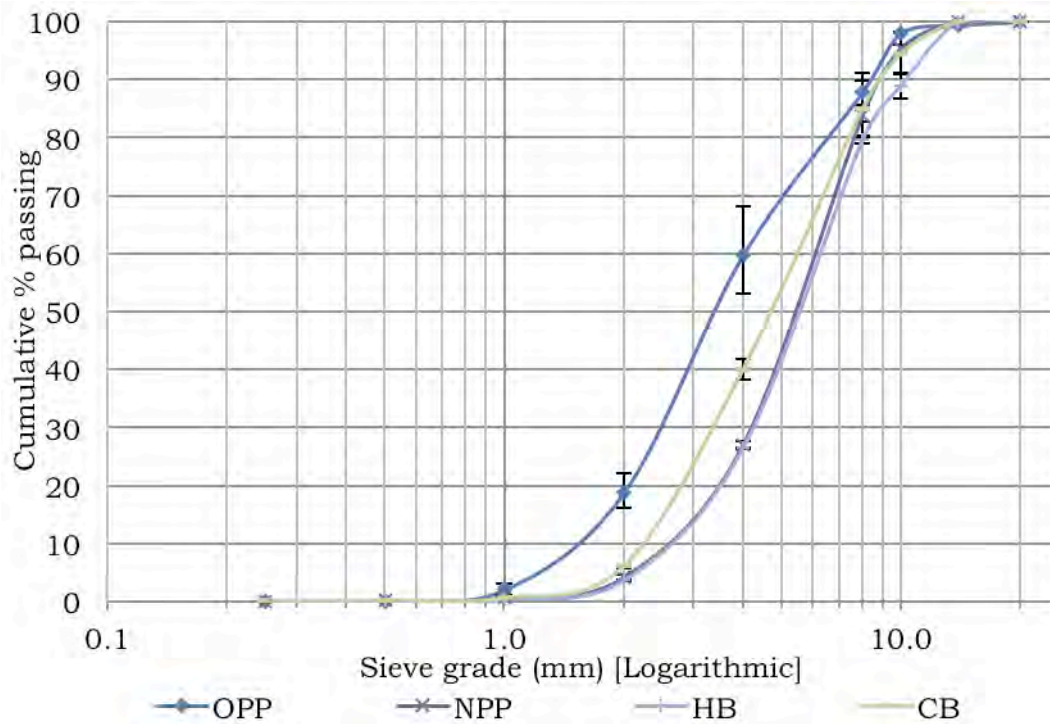


Figure 4.2 – Average particle distribution curves for OPP, NPP, HB and CB samples.

Hemp shiv from Hemcore’s old processing plant (OPP) was notably different to the other samples. The material was generally finer but also had a wider spread of particle sizes compared to the other three samples. NPP showed the smallest variation in particle distribution. In all cases 100% of the hemp shiv passed through a 20mm sieve. The material collected on the 10mm sieve typically constituted bundles of fibres (with a few trapped hemp shiv particles) as shown below in Figure 4.3.



Figure 4.3 – Typical hemp fibre material from material grading process.

No regulatory guidelines or standards currently exist for the standard fabrication and grading of hemp-shiv for construction purposes however, the draft French standard for the construction of hemp-lime building elements [RP2C, 2006] specifies particles in a parallelepiped form with widths between 1 and 5mm and lengths of 1 to 30mm. Furthermore, granulometric tests (by the sieve method) should not display more than 5% by mass of material passing a 0.5mm sieve, approximately 90% by mass should pass between 1 and 4mm and less than 3% by mass should exceed 4mm. All samples displayed masses less than 5% passing the 0.5mm sieve, however, none of the samples fell within the recommendation of 90% of the material mass between 1 and 4mm; this also included the French produced Chanvribat shiv. All samples fell outside of the 3% limit for material above 4mm. There could be two reasons for this occurrence. Firstly the shiv getting caught up in bundles of fibre above the 10mm grading sieve will contribute largely to the mass percentage above 4mm. Secondly it could indicate that the holistic process of harvesting and processing for distribution still needs further refining to achieve an even more consistent material. Conversely, no empirical evidence has been found by the author into why these particular guidelines specify the given ranges. Further analysis of work carried out by Gourlay (2008) demonstrated that none of the ten samples tested fell within the guidelines set out by the draft standard. However the four samples

originating from the same processing plant in the l'Aube region of France fell closest to the guidelines with an average of 85% of the mass of material falling between 1 and 4mm grading sieves.

A comparison between the sieving technique used here and the optical technique used by investigators in France is difficult to establish as there are currently no published empirical papers detailing the technique, its effectiveness and accuracy. However, it would provide verification of this methodology's effectiveness in determining the grading characteristics for the length of shiv particles.

4.2.3 Hemp shiv water absorption characteristics

There are currently no recommended empirical standards or guidelines to characterising the water absorption characteristics of organic aggregates such as hemp shiv. Absorption tests were carried out on three different batches of NPP hemp shiv in order to characterise the water absorption properties of the material currently used in the UK and to determine water absorption capacity. The experimental water absorption curves are presented in Figure 4.4.

The total immersion time for the hemp shiv was almost 14 days. By seven days the shiv samples had reached saturation capacity, where subsequent slight variations in mass seemed dependent on the technique employed for the removal of free water. Prior to immersion in the container of water the average initial moisture content of the hemp shiv was 11%. After seven days immersion an average mass increase of 396% was observed. There was a very rapid uptake of water during the first minute of immersion, where an average of 38% of the total water absorption occurred. After 15 minutes the hemp shiv had absorbed an average of 200% its own mass in water which increased to 224% after 64 minutes (Figure 4.5).

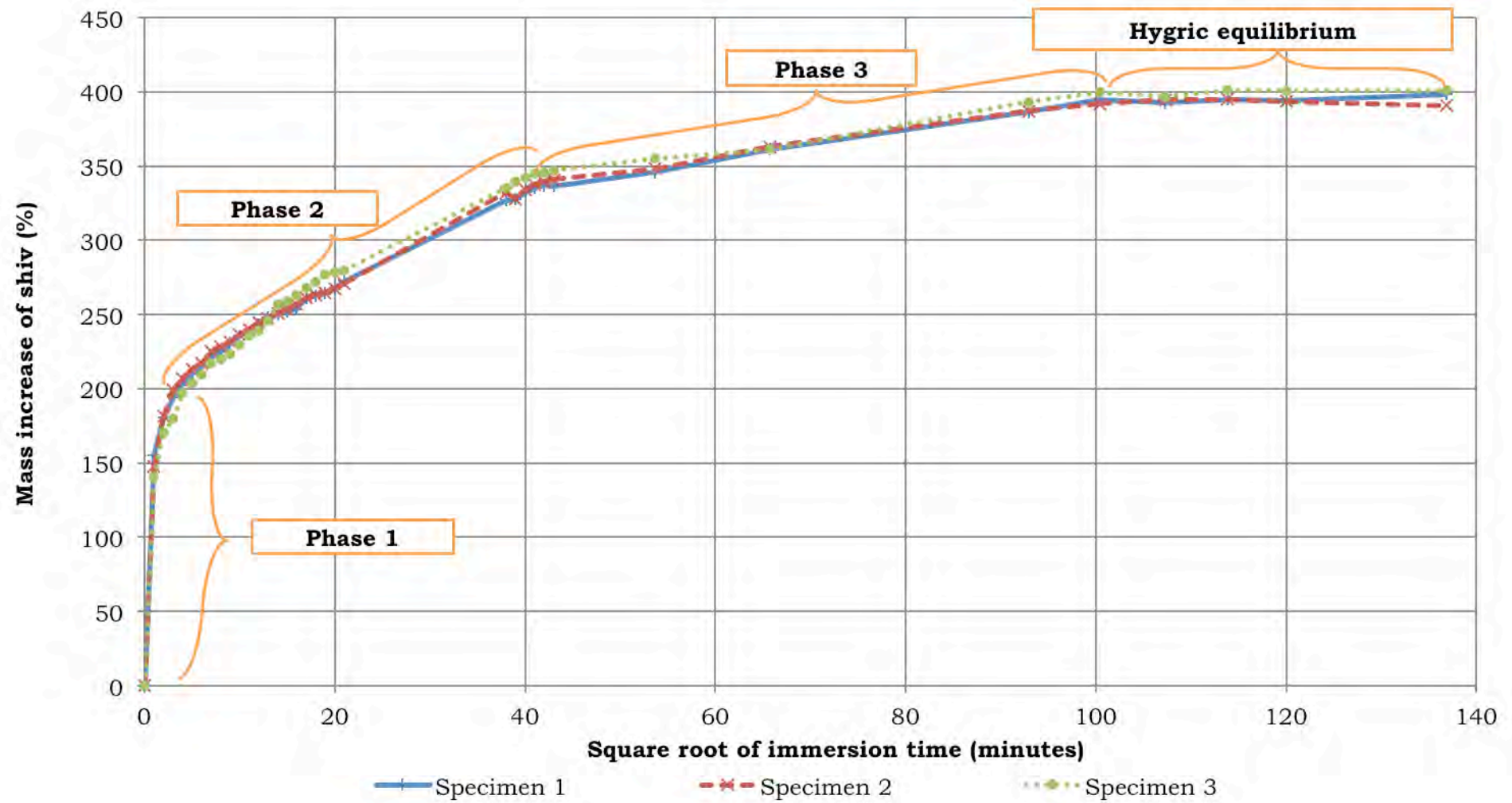


Figure 4.4 – Water absorption curves for NPP hemp shiv

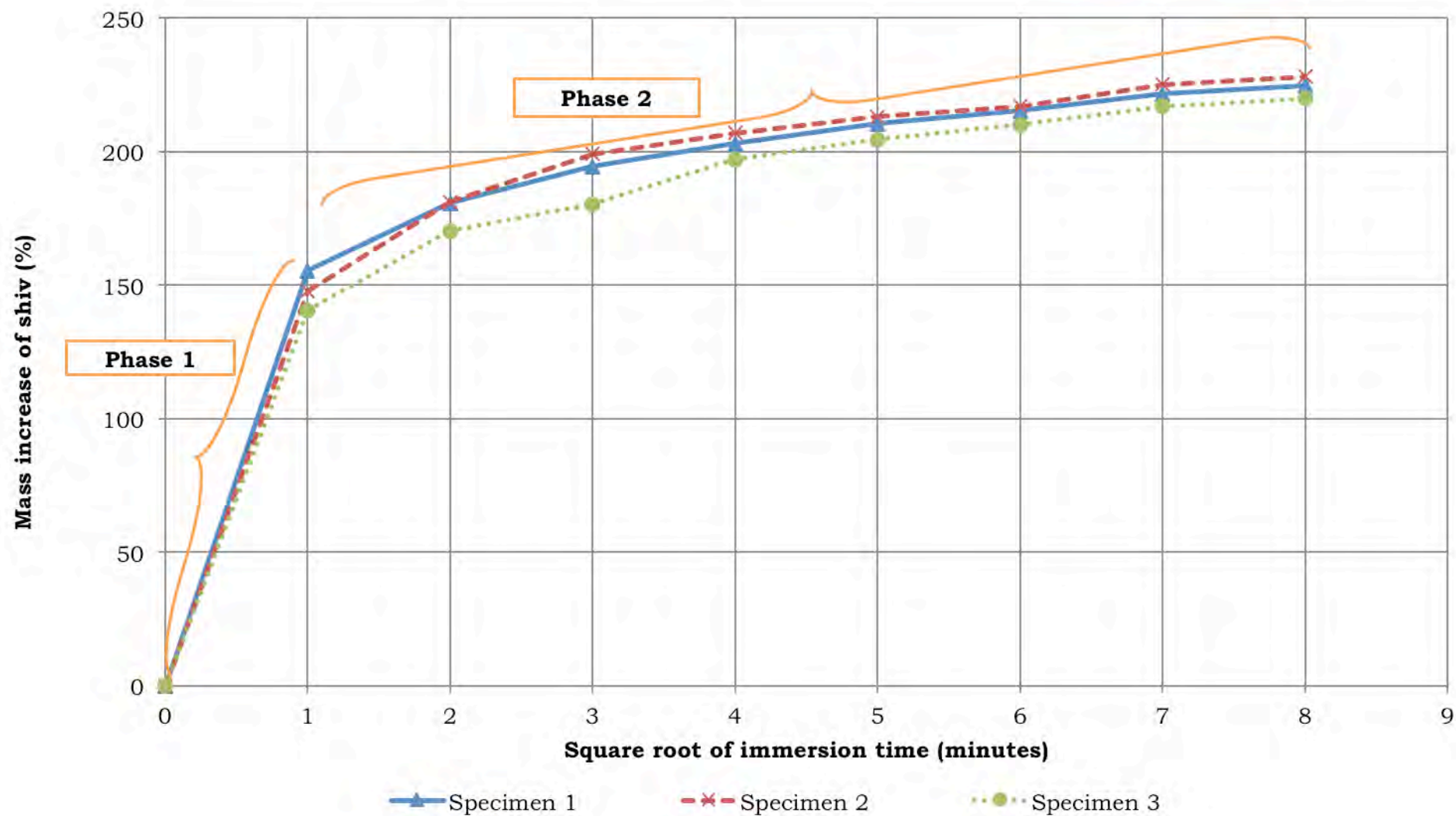


Figure 4.5 – Water absorption curve of first hour of immersion for NPP shiv.

It is possible to identify three distinct absorption phases, with three different approximately linear rates of absorption, as illustrated in Figure 4.4. The rapid rate of absorption observed in the first minute may be attributed to the absorption of water into the macro pore structure. The rate of water absorption within this period was on average 74gmin^{-1} which equates to $1.48\text{gmin}^{-1}\text{g}^{-1}$ of hemp shiv. A transitional period between phase 1 and 2 occurs between one and two and a half minutes after immersion. Between two and a half minutes and 1600 minutes after immersion the absorption curve can be approximated to a linear rate of absorption which displayed an average rate of absorption of 0.059gmin^{-1} . This slower rate of absorption may be attributed to micro pore absorption and to a lesser extent cellular absorption. The rate of absorption in phase three, between 1600 and 10080 minutes (7 days) was 0.004gmin^{-1} . This much slower final rate of water absorption may be attributed to cellular absorption as osmosis takes place across the cell membrane.

Within the first minute the three samples displayed an average mass increase of 148%. By integrating the results from this series of testing into the absorption behaviour of the hemp shiv when mixed with the other constituents, interesting observations were made. When considering the constituent proportions of 275kg/m^3 specimens (21% hemp shiv, 36% binder and 43% water) this indicates that within the first minute almost all the water that was mixed has been absorbed by the shiv; i.e. a 1kg specimen of hemp-lime would have initially contained 210g hemp shiv whose mass after one minute would increase to 520g and then 630% after 15 minutes; this suggests that almost all the water is absorbed into the shiv. This was clearly not the case when the fresh material was mixed and may indicate that there are differences in absorption behaviour when hemp shiv is immersed in water compared to a water/binder slurry due to the higher viscosity of the slurry. The higher viscosity may be altering the capillary dynamics inhibiting and/or decreasing the rate of absorption into the pores of the shiv particle. Furthermore the particle sizes within the slurry may be larger than the pore sizes of the hemp shiv.

The validity and repeatability of the test methodology has been primarily confirmed by the three test results carried out within this investigation and also comparing the average results to other investigations; the same methodology was adopted by Woods (2008) and good correlation between the two investigations was achieved. The method of swiping the sieve assembly ten times to remove the free water from the sample before recording the mass gain proved in general to be a reliable and consistent step in determining the moisture content of the hemp shiv; differences in results varied between 1.6% and 19% with an average difference of 8.4%.

Due to the difference in testing methodologies it is not possible to directly compare these results against those obtained by Gourlay [2008]. However there are inconsistencies when compared to the results obtained by Cerezo [2003]. Cerezo claimed 95% of the saturation had occurred within the first 5 minutes of immersion followed by a total saturated mass gain of 230% after 10 minutes immersion. This investigation experienced 95% saturation at approximately 1 hours immersion time and a final saturated mass gain of 396%. Just under 50% saturation was displayed after 15 minutes. This may be the result of studying shiv from different origins (Cerezo solely investigated shiv from la Chanvrière de l'Aube). However, the author hypothesises that the final saturation stated by Cerezo may not be conclusive as the mass gain slope was still increasing at the point of finalising the test signifying that the final saturation value may indeed have been greater.

4.3 Binder characterisation

This section presents and discusses the results from the tests undertaken to mechanically and chemically characterise the different binders within this investigation.

4.3.1 Initial setting times

Vicat testing was carried out on each of the binders to investigate and compare the setting times of the different binders used within this investigation. The initial setting time is defined as the elapsed time, to the nearest five minutes, at which the distance between the penetrating needle and the glass base-plate is (6 ± 3) mm [BS EN 196-3:2005]. Table 4.3 presents the recorded initial setting times for the binders under test along with the water binder ratios determined from tests carried out and describes in Chapter 3.

Table 4.3 – Vicat test results for initial setting times.

Binder	Initial setting time (mins)	Water binder ratio
THB-52.5R	110	0.42
THB-42.5N	155	0.42
BC	80	0.38
NHL5	175	0.38

BC displayed the fastest initial setting time of 80 minutes, 33% higher than the lower limit value set out by BS EN 197-1:2011 for CEM I 32.5N cements. This result was expected due to the assumption of higher cement content in the binder compared to the other binders. NHL5 displayed the slowest initial setting time of 175 minutes validating the conformity of the NHL5 binder as the initial setting time is greater than the 60 minute lower limit value set out by BS EN 459 – 1. The 29% faster setting time of the THB – 52.5R compared to the THB – 42.5N binder is in keeping with the use of CEM I 52.5R cement in the blended binder.

4.3.2 Bulk density

The mass and volumetric dimensions of each standard sand mortar prism were recorded prior to testing in accordance with the methodology set out by BS EN 1015-10:1999 to determine their respective bulk density.

Table 4.4 presents the development of the bulk densities of the mortars at the different testing ages. Bulk densities generally increase with time as a result, initially, of the hydration process and longer term as a result of carbonation of the remaining calcium hydroxide. The results presented are arithmetic means taken from three mortar prisms fabricated for each binder for each testing age.

Table 4.4 – Bulk density development of all standard sand mortar specimens from 14 to 360 days.

Binder	Bulk density (kg/m³) (range)				
	14 days	28 days	91 days	180 days	360 days
THB52.5R	1849 (1843-1859)	1886 (1884-1887)	1913 (1886-1963)	1948 (1928-1963)	1997 (1987-2012)
THB42.5N	1553 (1539-1579)	1709 (1697-1726)	1820 (1805-1829)	1902 (1888-1914)	2008 (1990-2021)
BC	1985 (1971-2002)	2002 (1997-2014)	1981 (1964-2005)	2017 (2013-2022)	2032 (2026-2042)
NHL5	1976 (1938-2000)	1981 (1971-2001)	2073 (2062-2083)	2091 (2068-2118)	2119 (2114-2128)
THB52.5R – OSR	1780 (1746-1813)	1799 (1779-1813)	1836 (1806-1867)	1877 (1840-1909)	1914 (1881-1945)

All binders exhibited increasing bulk density over the testing period. An average density variance within each series of just 0.9% from the mean bulk density confirmed a reliable and repeatable fabrication process. The bulk density increase between 14 and 360 days varied between 2% and 29%, the BC binders displaying the lowest increase and the THB42.5N binders the highest. This small increase may indicate that BC binders contain a higher proportion of cement compared to THB binders as there seems to be little density increase due to lime carbonation. The similarity in the rate of density increase between the THB52.5R and OSR mortars may indicate that the minerals in the organic aggregate may not have any adverse effect on the chemical and pore structure development of the hydrates and carbonates.

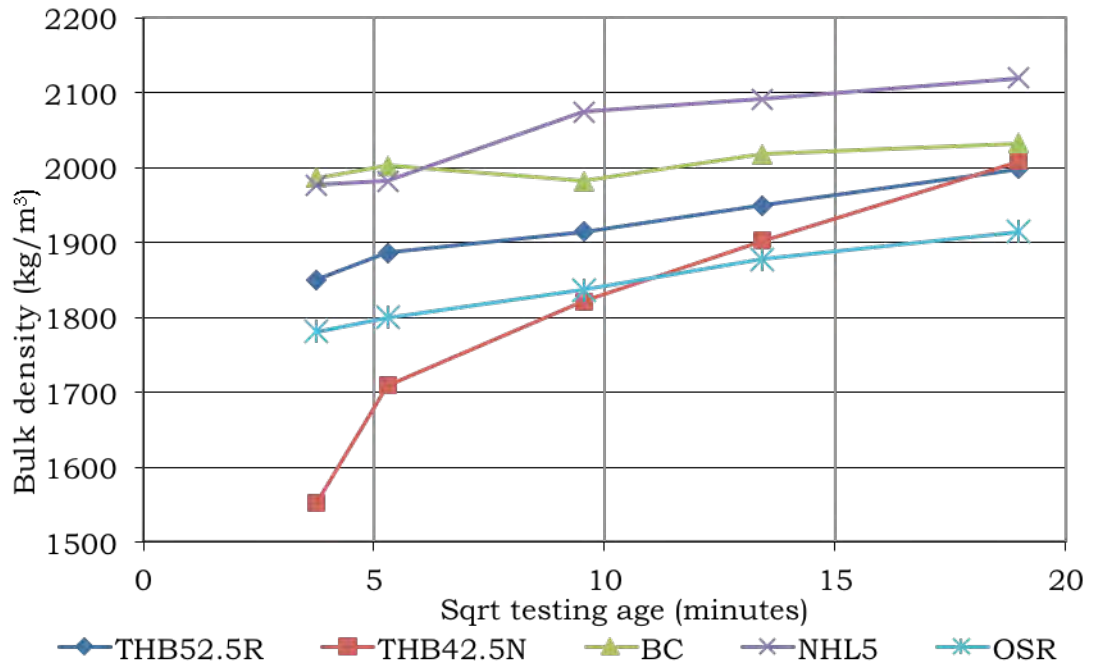


Figure 4.6 – Bulk density development over time of standards sand mortar prisms.

A striking result is the difference in density increase between THB52.5R and THB42.5N. THB52.5R binders displayed an 8% density increase over the testing period compared to 29% displayed by THB42.5N binders. This may be down to a significant difference in the constituent make-up of the binder indicating that THB42.5N may contain a larger percentage mass of CL90 air lime compared to THB52.5R and thus displaying larger density increases as a result of the lime carbonation reaction; this is explored later using TGA testing.

4.3.3 Flexural and compressive strength

Flexural and compressive strength testing were carried out to compare the mechanical characteristics of all the binder mortars used within this investigation. The compressive tests were carried out in accordance with BS EN 196-1:2005 with modifications from BS EN 459-2:2001 which suggested different loading rates for lime mortars compared to pure cement mortars. The flexural strength, R_f , was determined using the following equation:

$$R_f = \frac{1.5 \times F_f \times l}{b^3}$$

Where F_f is the maximum load at fracture, l is the distance between the supports in mm's and b is the side of the square section of the prism in mm's. The flexural strength test results were calculated as the arithmetic mean of the three individual results for each binder type at each testing age.

The compressive strength, R_c , was determined using the following equation:

$$R_c = \frac{F_c}{1600}$$

Where F_c is the maximum load at fracture in Newtons and 1600 is the area of the platens applying the load in mm². The compressive strength test results were calculated as the arithmetic mean of the six tests carried out on the halved prisms created by the flexural test. However, if one result within the six individual results varied by more than $\pm 10\%$ from the mean, that result was discarded from the results and a revised arithmetic mean was calculated from the five remaining results. This process, as set out by BS EN 196-1, was repeated until all results fell within the variation limits. Within this investigation all experimental recorded results fell within the variation limits, indicating good consistency in material preparation, performance and testing. Table 4.5 presents the average values of flexural and compressive strength for each mortar at each testing age along with the range of experimental values obtained.

Table 4.5 – Flexural and compressive strength results for all mortar specimens at all testing ages.

THB52.5R	Flexural strength (range) (N/mm²)	Compressive strength (range) (N/mm²)	Flex/Comp ratio
14 Day	3.6 (3.5 – 3.7)	11.1 (10.8 – 11.6)	3.0
28 Day	4.5 (4.4 – 4.7)	14.0 (13.3 – 14.3)	3.1
91 Day	4.4 (4.3 – 4.6)	15.8 (14.9 – 16.3)	3.6
180 Day	4.8 (4.6 – 5.0)	18.5 (16.8 – 19.3)	3.9
360 Day	5.5 (5.1 – 5.8)	20.8 (20.5 – 21.2)	3.8
THB42.5N			
14 Day	2.5 (2.3 – 2.6)	5.0 (4.7 – 5.5)	2.0
28 Day	3.5 (3.3 – 3.8)	9.3 (8.8 – 10.0)	2.6
91 Day	4.0 (3.5 – 4.2)	13.2 (12.2 – 14.3)	3.3
180 Day	5.2 (5.1 – 5.4)	18.1 (17.7 – 18.9)	3.5
360 Day	5.9 (5.2 – 6.7)	15.9 (13.7 – 17.6)	2.7
BC			
14 Day	5.2 (5.1 – 5.4)	24.3 (23.6 – 25.0)	4.7
28 Day	7.2 (6.9 – 7.5)	30.1 (29.6 – 30.8)	4.2
91 Day	6.2 (6.1 – 6.3)	29.7 (28.8 – 30.4)	4.8
180 Day	6.3 (6.0 – 6.8)	31.6 (30.3 – 33.1)	5.1
360 Day	7.0 (6.95 – 7.13)	32.9 (31.2 – 33.8)	4.7
NHL5			
14 Day	1.7 (1.5 – 1.9)	5.4 (5.1 – 5.9)	3.2
28 Day	1.9 (1.6 – 2.0)	6.3 (6.1 – 6.6)	3.4
91 Day	2.8 (2.7 – 2.9)	8.3 (6.1 – 8.8)	3.0
180 Day	3.3 (3.0 – 3.4)	11.1 (9.6 – 11.7)	3.4
360 Day	3.1 (3.0 – 3.3)	14.8 (13.6 – 15.6)	4.7
OSR			
14 Day	2.1 (1.7 – 2.3)	9.1 (8.8 – 9.3)	4.3
28 Day	4.3 (4.2 – 4.6)	13.5 (13.3 – 14.0)	3.1
91 Day	4.8 (4.5 – 5.1)	16.3 (15.0 – 17.6)	3.4
180 Day	5.6 (4.9 – 6.4)	18.1 (9.4 – 19.2)	3.2
360 Day	5.4 (5.2 – 5.7)	20.2 (18.8 – 21.5)	3.7

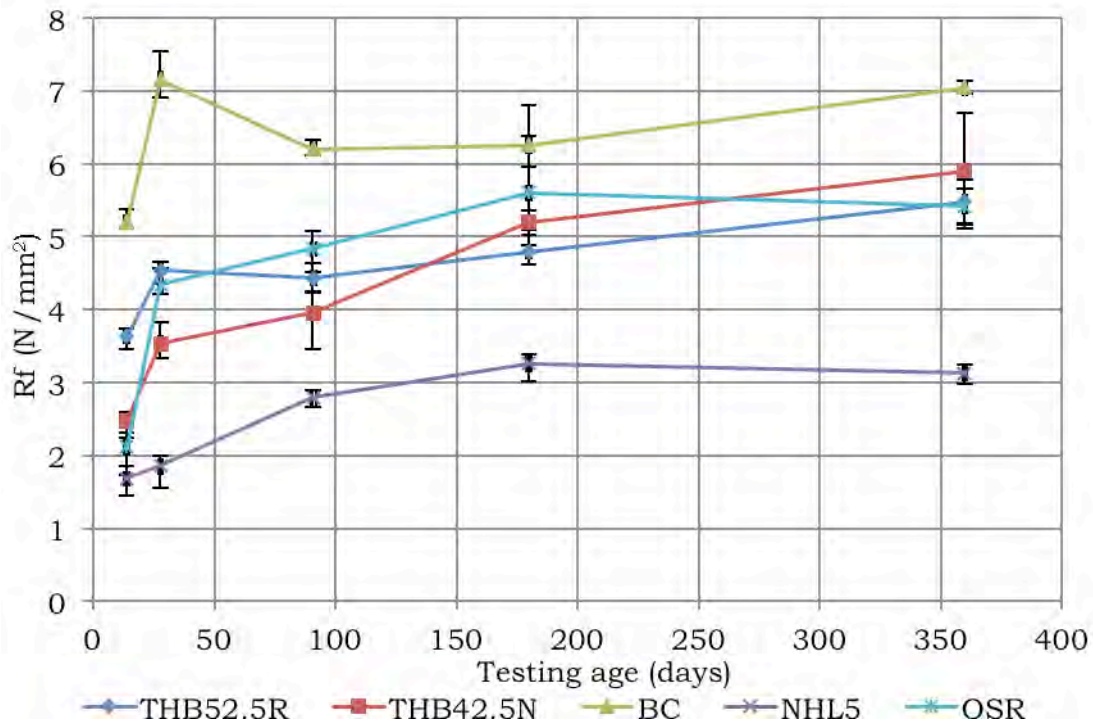


Figure 4.7 – Flexural strength of all binders at all testing ages.

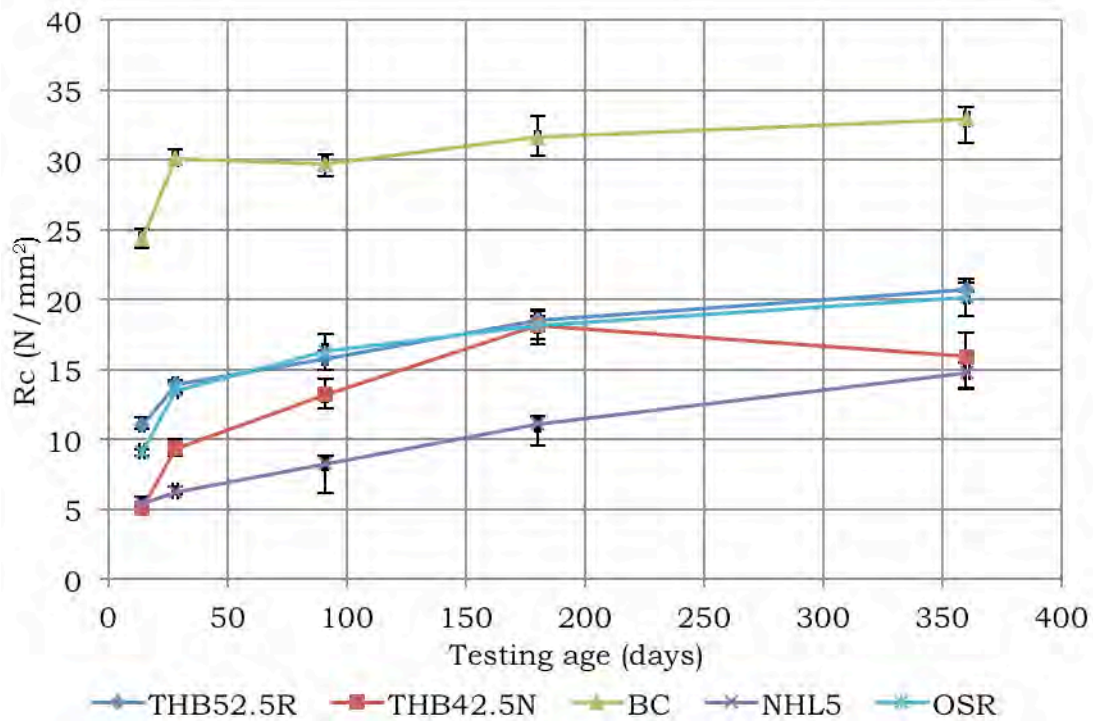


Figure 4.8 – Compressive strength of all binders at all testing ages.

The compressive strengths showed notable differences of the mortar specimens across the five binder types. The most striking result was the difference in compressive strength between BC and NHL5 binders. At 14 days the strengths ranged from 5.4 N/mm² for NHL5 to 24.3 N/mm² for BC mortars. However, by 360 days the strengths increase to 14.8 N/mm² for NHL5 to 32.9 N/mm² for BC mortars. The strengths for THB-52.5, THB-42.5 and OSR mortars fall in between the other two binders with respective 14 and 360 day compressive strengths of 11.1/20.8 N/mm², 5.0/15.9 N/mm² and 9.1/20.2 N/mm². Compressive strength is related to the degree of hydraulicity of the binder and the extent of carbonation which has taken place during curing as all other variables in the fabrication, curing and testing have been minimised. These results may indicate that there is a large degree of cement in BC; CEM I 32.5 is manufactured to display a minimum 28 day compressive strength of 32.5N/mm². Furthermore, following 28 days of curing there was no significant gain in strength indicating that the majority of the BC binder may be cement. There is no clear difference between THB-52.5 and OSR mortars, indicating the minerals in the organic aggregate may not have any effect on the strength of the binder. The 28 day compressive value of 6.27N/mm² for NHL5 confirms the materials conformity to the standard strength requirement in BS EN 459-1:2010.

Currently there is no empirical investigation or commercial literature available which states the flexural or compressive strengths for THB Tradical binders or St Astier Batichanvre binder. Taking into consideration that the manufacturer literature states the respective binders to be based on CL90 air lime (for THB binders) and NHL5 (for Batichanvre) it makes sense to compare the strength results from the binders against standardised laboratory results for CL90 and NHL5. As described in Chapter two, the average 28 day compressive strength of CL90 air lime standard sand mortar prisms tested in accordance with standards can range between 1 and 3N/mm². It must be stated however that the standard fabrication and curing methodology for air limes varies slightly to those used in this investigation, nevertheless these values can still be used as a base point with which to compare the THB binders.

4.3.4 Binder carbonation

The development of the carbonation boundary of the mortars was determined at each testing age using indicator methods. Following flexural testing, where the specimen had been split in half, the face of one half of the specimen was sprayed with phenolphthalein, pictured and the carbonation depth measured using computer software. The carbonation profile of the other half of the specimen was assumed to be identical.

Figure 4.9 and Figure 4.10 illustrate the methodology used for the determination of the carbonation depths in the mortar specimens and show the phenolphthalein staining of NHL5 mortars at 91 and 180 days respectively (all available photographs relating to the phenolphthalein staining of mortar specimens can be found in Appendix IV). The picture was scaled to 1:1 and the depth established by overlaying four lines from the edge of each face to the stained boundary. The average length of the four lines specified the carbonation depth for that specimen at that age to an accuracy of 0.1mm.

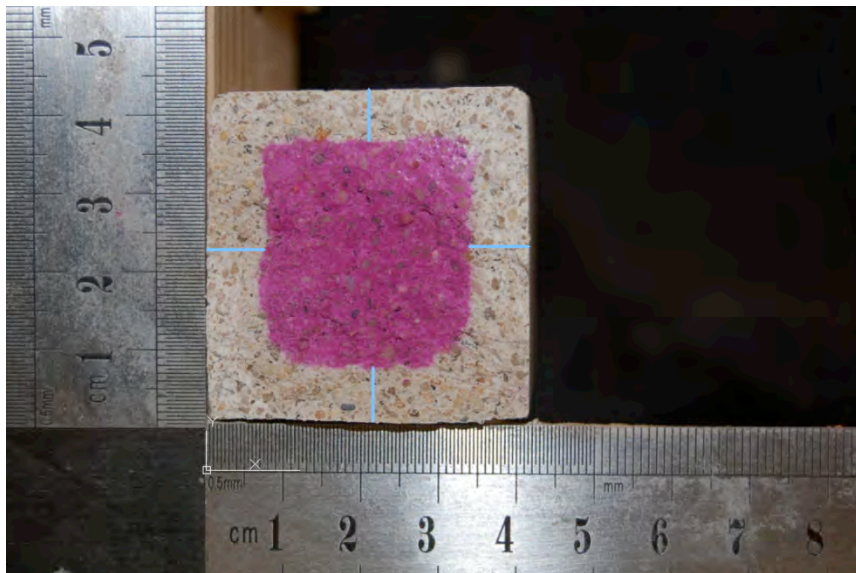


Figure 4.9 – Mortar carbonation depth analysis for a 91 day old NHL5 specimen.

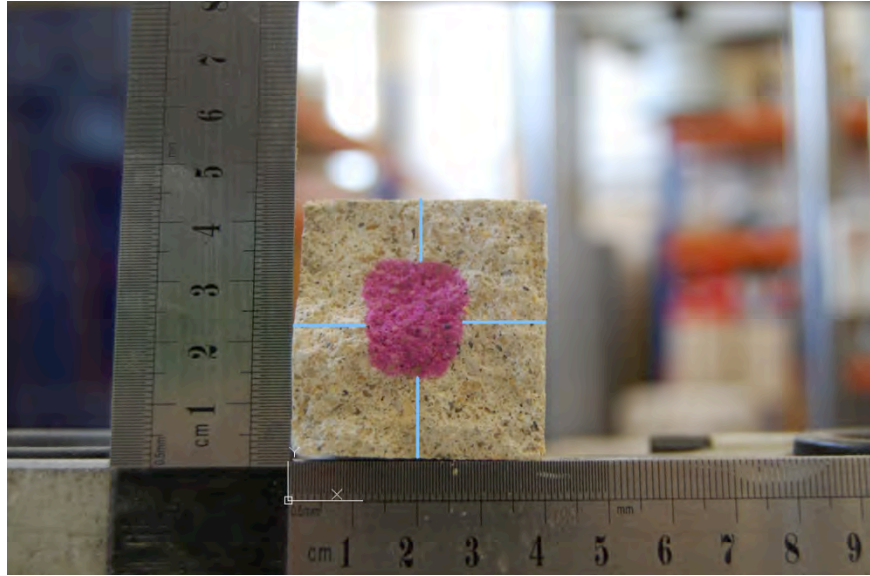


Figure 4.10 – Mortar carbonation depth analysis for a 180 day old NHL5 specimen.

The average carbonation depths along with range of results for all mortar specimens at the different testing ages are presented in Table 4.6. Furthermore, the average carbonation rate, between 14 and 360 days, is also presented. Overall the boundary between carbonated (un-stained) and un-carbonated (stained) material was observed to be very well defined. This allowed precise positioning of the measurement lines and a degree of accuracy down to 0.1mm.

Table 4.7 presents the interval carbonation rates for each binder, i.e. the rate of carbonation between each testing age. This allows analysis of the change in carbonation rate compared to curing time and also compared to the development of the bulk density of the mortars.

Table 4.6 – Average carbonation depth, range of results and average carbonation rate for all mortar specimens.

Binder	Average carbonation depth (mm) (range)					Average carbonation rate (mm/day)
	14 days	28 days	91 days	180 days	360 days	
THB-52.5R	0.9 (0.5-1.1)	1.5 (1.2-1.8)	3.4 (3.0-3.8)	6.1 (5.2-6.8)	7.4 (6.1-8.5)	0.02
THB-42.5N	1.4 (1.0-1.9)	1.8 (1.5-2.1)	3.7 (3.0-4.3)	6.5 (6.1-7.4)	7.9 (6.5-8.7)	0.02
BC	0.7 (0.5-1.1)	1.3 (1.2-1.3)	3.1 (2.7-3.4)	5.4 (5.0-5.9)	6.7 (5.3-7.2)	0.02
NHL5	1.5 (0.9-1.9)	3.4 (3.2-3.7)	6.9 (5.7-7.6)	11.3 (8.6-12.7)	15.8 (12.7-18.3)	0.05
OSR	0.6 (0.4-0.9)	1.4 (0.8-1.9)	3.4 (2.5-4.1)	4.4 (3.7-5.3)	6.7 (6.1-8.2)	0.02

Table 4.7 – Interval carbonation rates of all binders.

Binder	Carbonation rate (mm/day)				
	7 – 14 days	14 – 28 days	28 – 91 days	91 – 180 days	180 – 365 days
THB-52.5R	0.127	0.041	0.030	0.031	0.007
THB-42.5N	0.196	0.027	0.031	0.032	0.008
BC	0.101	0.040	0.028	0.026	0.007
NHL5	0.208	0.141	0.056	0.049	0.025
OSR	0.08	0.059	0.031	0.012	0.013

Figure 4.11 displays the development, with time, of the carbonation depth for all binders.

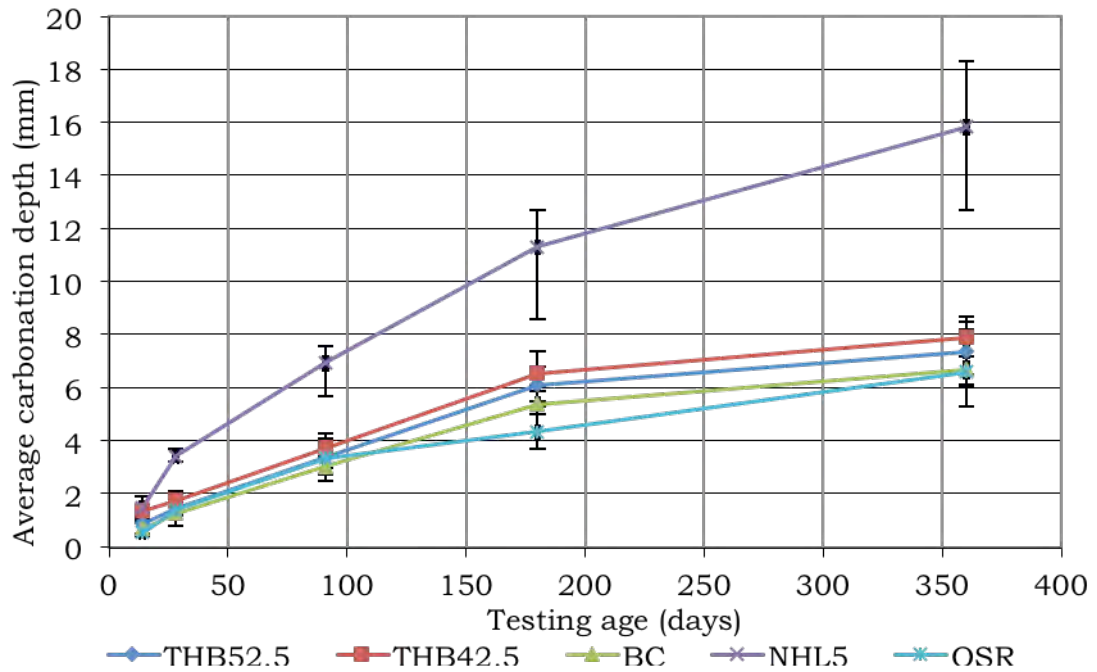


Figure 4.11 – Average carbonation depth of all mortars at all testing ages.

In all instances the rate of carbonation decreased as curing progressed. This decrease may be attributed to the reduction in porosity as a result of carbonation products inhibiting the diffusion of atmospheric gases through the mortar. The rates of carbonation for THB-42.5N, THB-52.5R and BC binders was almost identical for the duration of the testing regime. Figure 4.11 presents the carbonation rates for all binders between each testing age.

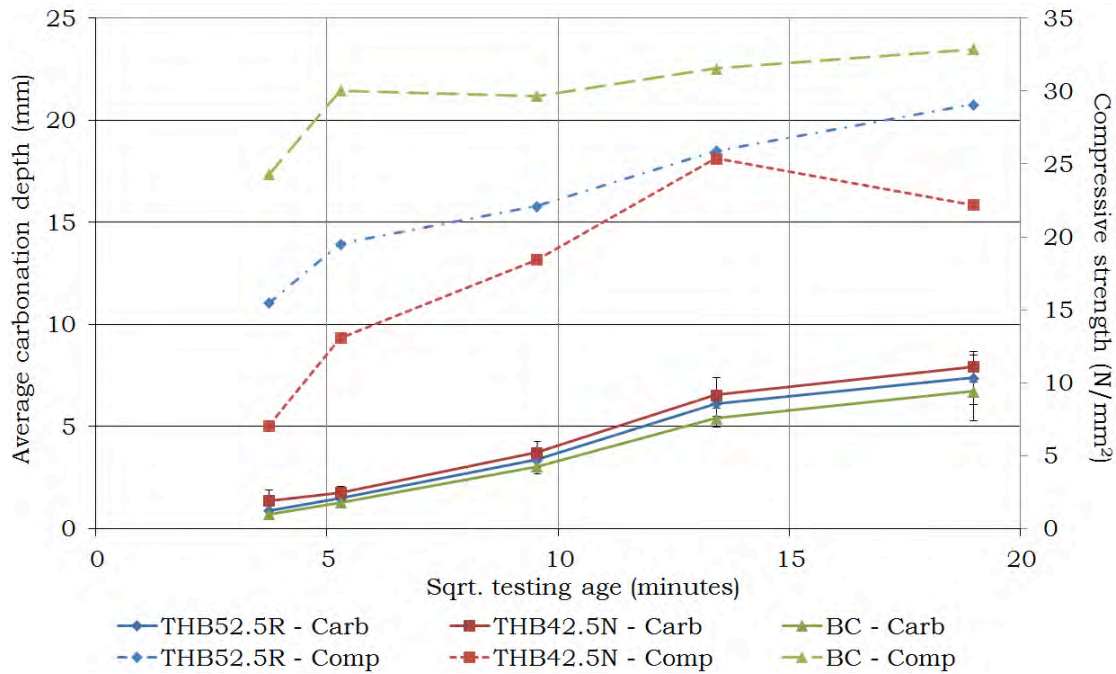


Figure 4.12 – Carbonation vs. Compressive strength over age for pre-formulated binders.

Figure 4.12 shows the compressive strength results compared to the carbonation depths for mortars made using THB-52.5R, THB-42.5N and BC for each of the testing ages.

The results demonstrate that the increase in strength of a binder is not necessarily directly related to the increase in carbonation. The compressive strength of THB-42.5N decreased between 180 and 360 days from 18.14 to 15.9 N/mm² (it may be reasonable to assume this being a testing anomaly), however, the carbonation depth increased from 6.5 to 7.9mm. Furthermore, the carbonated area of BC binders increased by almost 800% between 14 and 360 day tests whereas the strength of the binder only increased by 35%.

4.4

Summary of findings

- The new hemp processing plant delivers very well graded hemp shiv.
- The repeatability of the mortar fabrication process was confirmed through the low variability of bulk densities at each testing age.
- The carbonation depth, in conjunction with rates of carbonation, are able to be accurately distinguished through the use of phenolphthalein indicator staining on standard sand mortar specimens.
- NHL5 mortar specimens displayed the highest rate of carbonation; possibly due to the comparatively small ratio of hydraulic constituents in the binder.
- BC mortar specimens displayed the lowest rate of carbonation; possibly due to the comparatively large ratio of hydraulic constituents in the binder creating a tighter pore structure on the outer layer of the specimens during early phases on carbonation hence inhibiting the ingress of CO₂.

CHAPTER 5 - CHEMICAL CHARACTERISTICS OF HEMP-LIME

5.1 Introduction

Results from the phenolphthalein indicator staining and thermogravimetric analysis (TGA) of 57 hemp-lime specimens are presented and discussed in this chapter. A total of 114 TGA tests were carried out to detail the carbonation development of the binders between 0 and 360 days. Furthermore, a preliminary understanding into the development of hydrates in the initial stages of curing in the binder is presented along with preliminary calculations into how much Ca(OH)_2 is contributed to the overall binder mass by the setting reactions. These data are used to develop an improved understanding into the carbonation rate for hemp-lime materials, carbon sequestration characteristics and provide empirical data for future life cycles analyses.

5.2 Phenolphthalein indicator staining of composite specimens

5.2.1 Testing and analysis methodology

At each testing age and during random selection of large specimens for strength testing, one small hemp-lime specimen for each binder type and density was also randomly chosen from the conditioning room (with environmental conditions as described in Chapter 3) for the determination of the carbonation profile depth via phenolphthalein indicator staining. Specimens were weighed and measured to determine their bulk density and then split, at mid-height, over a bolster. One half was placed by scale rules, sprayed with phenolphthalein indicator and photographed within five seconds to capture the resultant stain pattern. A typical stain pattern is shown in Figure 5.1 (all available photographs relating to phenolphthalein staining of composite specimens can be found in Appendix III)



Figure 5.1 – Phenolphthalein stain on a 28 day SH-275 hemp-lime specimen within 5 seconds of spraying.

This time constraint was important; as time progressed the whole face of the specimen began to turn pink, as shown in Figure, as the phenolphthalein indicator was absorbed into the binder matrix. Previous investigations have shown that even after carbonation has apparently been completed, there are still small amounts of un-carbonated Ca(OH)_2 present. Studies of medieval mortars have revealed the continuing presence of residual Ca(OH)_2 [Adams et al, 1988]. A plausible theory is that some Ca(OH)_2 crystals can be covered by an impervious layer of insoluble CaCO_3 as carbonation takes place, thereby blocking access by CO_2 to the Ca(OH)_2 core [Dheilly et al, 1998; van Balen, 2005]. Swenson and Sereda [1968] used optical extensometry and chemical analysis to demonstrate that particles of lime can become coated with calcium carbonate. This results in moisture being trapped inside the coating. When the moisture outside the coating dries out, a moisture gradient is created which is sufficient to produce cracking. A sequence of deposition of calcite, slowing of the reaction, drying and cracking continues

until the build-up of the coating eventually stops the reaction and no further carbonation takes place, trapping some uncarbonated lime inside the coating. An analogy to this would be a Malteser which has a comparatively impervious outer chocolate shell (calcium carbonate) and a porous inner core (calcium hydroxide). Consequently what may immediately seem like carbonated material may in fact contain small amounts of Ca(OH)_2 which may never carbonate reducing the carbon sequestration potential of the material. If this were the case it could therefore be expected that small amounts of Ca(OH)_2 are still present in 365 day specimens; this would be determined by the use of thermogravimetric analysis.



Figure 5.2 – Phenolphthalein stain on a 28 day SH-275 hemp-lime specimen one minute after spraying.

The methodology used to determine the carbonation depth was similar to that set out for mortar specimens, however, it was observed upon spraying that the transition between carbonated (unstained) and un-carbonated (stained) material was not a well defined boundary as was the case with mortar specimens. To increase accuracy the depth of the carbonation profile was therefore determined by measuring at eight equidistant points around

the specimens; the arithmetic mean was then deemed to be the carbonation depth at that age. Due to the differences in curing regime for FR-275 specimens the carbonation depth was measured from the ends of the specimens. The carbonation depth measurement of specimens under both curing regimes is illustrated in Figure 5.3.



Figure 5.3 – Phenolphthalein staining on a 28 day FR-275 (above) and SH-275 specimen (below).

To determine where the measurement lines should be extended to it was necessary to consider the way phenolphthalein behaves. Chemical indicators do not suddenly change colour at one particular pH level, but rather over a narrow range. For phenolphthalein, this range is between 8.3 and 10.0 as illustrated in Figure 5.4. The objective therefore, when overlaying the lines on the picture, was to extend the measurement lines to a point where they met the lightest fuchsia colour of the stained material and after which all the material was of a fuchsia colour. It was then assumed that the majority of the material beyond this point could be considered to be un-carbonated. Other methodologies were experimented with which involved visual enhancement and/or contrast changes to the picture in an attempt to create a clearer boundary however this was unsuccessful.

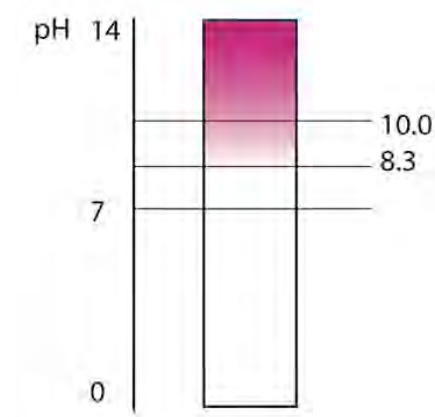


Figure 5.4 – Colour change seen in phenolphthalein according to pH level [Lawrence, 2006].

5.2.2 Carbonation results

As a result of the measurements taken from the phenolphthalein stain patterns it was possible to present average carbonation depths for each binder type and/or density for each testing age along with the range of measurements and the rates of carbonation. The carbonation rates, in mm's per day, relate to the rate of carbonation from the day the specimen was de-

moulded (seven days after fabrication) to the testing age (14, 28, 91, 180 or 360 days). Henceforth the ages of the specimens are presented as the 'carbonation age' which equates to the testing age minus the seven days before de-moulding took place (7, 21, 84, 173 and 353 days).

Overall the rate of carbonation was much faster than had been expected prior to fabrication and testing. As a consequence many cylinders which were tested at 84 days and older displayed 'fully carbonated' cross sections. In some cases it was possible to take carbonation depth measurements from spare large cylinders which had been stored under identical conditions and these reading have been included in the final results which are presented in

Table 5.1. The average carbonation rate from the time of de-moulding to the time of testing is also presented along with the interval carbonation rate; the rate of carbonation between each testing age.

In general the tests were unsuccessful in providing results from which decisive comparisons between the different binders and densities could be drawn. Furthermore the effect of the less defined boundary between unstained and stained material is clear from the large ranges compared to those for mortar specimens.

At this stage it is difficult to directly compare the results of the three densities as the constituent ratios of all three are different however a number of observations can still be made. Overall THB52.5R-220, 275 and 330 specimens displayed average carbonation rates of 2.1, 0.7 and 0.4mm/day respectively, however, when comparing the 21 day results a clear advantage in reducing the density and amount of binder in the fabrication of the specimens becomes apparent from the increase observed in the average carbonation rate for 220kg/m³ specimens compared to 275 and 330kg/m³ specimens. This indicates a threefold increase in carbonation rate for the 220kg/m³ specimens and a 60% decrease in carbonation rate for 330kg/m³ specimens when compared to the 275kg/m³ specimens.

Table 5.1 – Average carbonation depths, rates and interval carbonation rates for all composite specimens at all curing ages. * indicates readings taken from large specimens.

	Average carbonation depth (range) (mm)	Average carbonation rate (mm/day)	Interval carbonation rate (mm/day)
THB52.5R-220			
7 day	6.7 (5.4 – 9.5)	1.0	1.0
21 day	43.9 (38.9 – 47.7)	2.1	2.7
THB52.5R-275			
7 day	4.0 (3.1 – 5.3)	0.6	0.6
21 day	26.7 (24.3 – 30.3)	1.3	1.7
84 day	58.4* (53.2 – 64.8)	0.7	0.5
THB52.5R-330			
7 day	3.5 (2.5 – 4.7)	0.3	0.3
21 day	18.3 (15.7 – 20.6)	0.9	1.1
84 day	33.6 (25.8 – 38.9)	0.4	0.2
THB42.5N-275			
21 day	22.2 (17.9 – 25.5)	1.1	1.1
BC-275			
21 day	40.3 (36.2 – 43.9)	4.7	4.7
NHL5-275			
21 day	No staining	-	-
FR-275			
21 day	13.1 (12.2 – 14.2)	0.6	0.6
84 day	33.5 (27.8 – 40.4)	0.4	0.3
173 day	58.6 (52.2 – 63.5)	0.3	0.3
353 day	97.4 (94.2 – 99.4)	0.3	0.2

Only 7 and 21 day results were obtained for THB52.5R-220 specimens; large cylinders at 84 days of testing did not display any un-carbonated material upon indicator spraying indicating that full carbonation occurred between 21 and 84 days. Figure 5.5 presents the development of carbonation depth against the square root of time for all THB52.5R specimens. 220kg/m³ specimens clearly displayed the highest rate of carbonation followed by 275kg/m³ specimens. By extending the 220kg/m³ plot and also adding a

secondary extension line parallel to that of the 275kg/m³ plot it can be confidently assumed that full carbonation of the 220kg/m³ specimen occurred within the range of days where the extension lines cross the 50mm carbonation depth. In this instance the range was 24-30 days curing.

THB52.5R-275 and 330 specimens provided results up to 84 days of curing, however, only 275kg/m³ specimens provided full carbonation depth results indicating carbonation was completed after 63 days of curing. By extending the 330kg/m³ plot it was possible to determine that 193 days was the earliest possible time at which carbonation could have been completed. This implies that un-carbonated material should have been visually present at the carbonation age of 173 days however this was not the case.

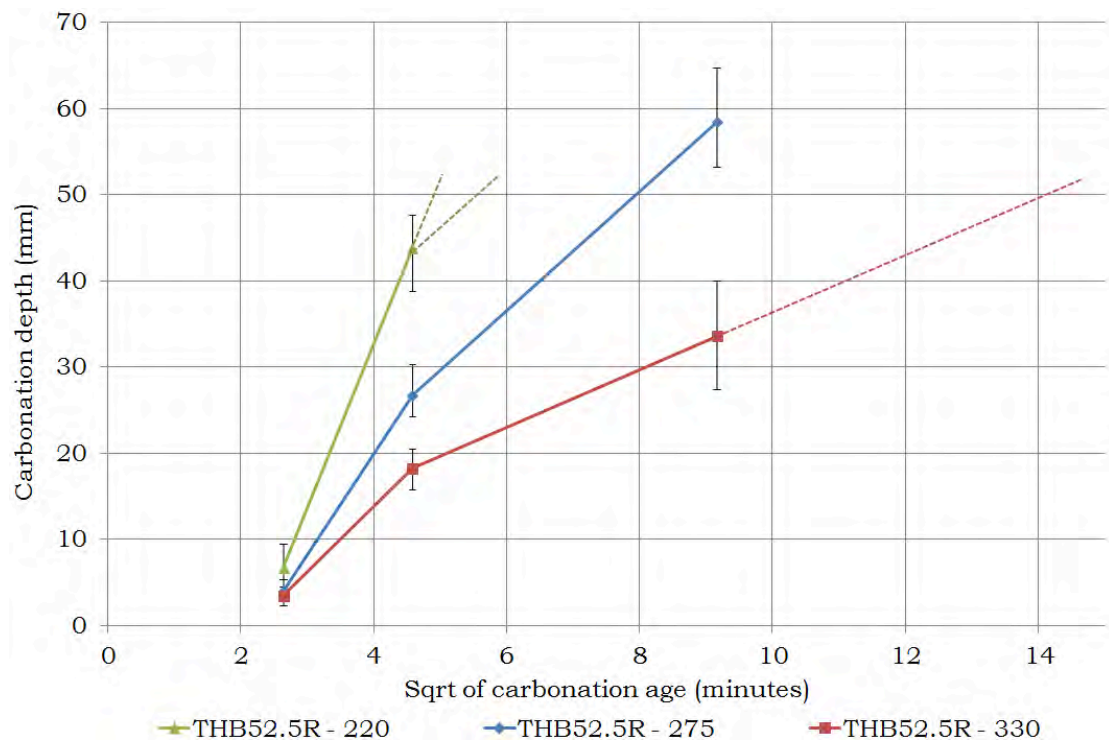


Figure 5.5 – Carbonation depth development against sqrt. of carbonation age for THB52.5R composite specimens.

THB42.5N-275 specimens only produced results at a carbonation age of 21 days with an average carbonation rate of 1.1mm/day. This binder, when

compared to the THB52.5R-275 specimens' average rate of 1.3mm/day for the same testing period, displayed a similar rate of carbonation.

Contrary to the behaviour observed from the carbonation of BC mortar specimens where the average rate of carbonation was slower than either two of the THB binder mortars, Batichanvre, when used within composite specimens, displayed a much greater rate of carbonation than the THB binder specimens. This may be explained by considering the assumed constituents of the Batichanvre binder and the differences in the make-up between mortars and composite specimens. Batichanvre is marketed as a binder predominantly composed of NHL; it is also assumed to contain an unknown but significant percentage of cement. When fabricated and cured as a mortar the cement (due to its fineness compared to air lime/NHL binders) will create a tighter micro pore structure around the outer edge of the specimen inhibiting the ingress of CO₂ which the NHL5 component of the binder needs to carbonate. When used within a composite specimen the cement is still causing a tighter pore structure within the binder matrix however the larger macro porosity of the composite specimen still allows a comparatively free flow of CO₂ to ingress for carbonation.

Surprisingly NHL5-275 specimens did not display any staining at 21 days of curing. NHL's are essentially air lime with a certain percentage of naturally occurring cementitious minerals which give the binder the ability to hydraulically set as well as hardening over time through carbonation. Stained areas of un-carbonated material were therefore expected to be found, as in the case of the mortar specimens, upon spraying of the chemical indicator. By not displaying any un-carbonated material it can be assumed that the NHL5 binder had fully carbonated within 21 days of curing. This could also be attributed to the difference in micro porosity between air lime/NHL binders and formulated binders which contain percentages of cement. In general cements are ground to a finer particle grading than air limes and NHL's. This consequently creates a tighter micro pore structure therefore inhibiting the access of CO₂ for carbonation. Indeed this property is sought after in cements as inhibiting carbonation also inhibits the corrosion of concrete and the reinforcing bars. The speed of

carbonation displayed in the composite specimens correlates well with results obtained from the phenolphthalein staining of NHL5 mortar specimens where the average carbonation rate over 353 days of curing was two and a half times greater than any of the other binders. Furthermore, detailed testing could help determine the speed and time to full carbonation for NHL5-275 specimens.

The only test series to produce a full set of results were the FR-275 specimens which were still just within the full carbonation depth of 100mm after 353 days of curing. Figure 5.6 presents the development of the carbonation depth as time progressed along with the data series trend line.

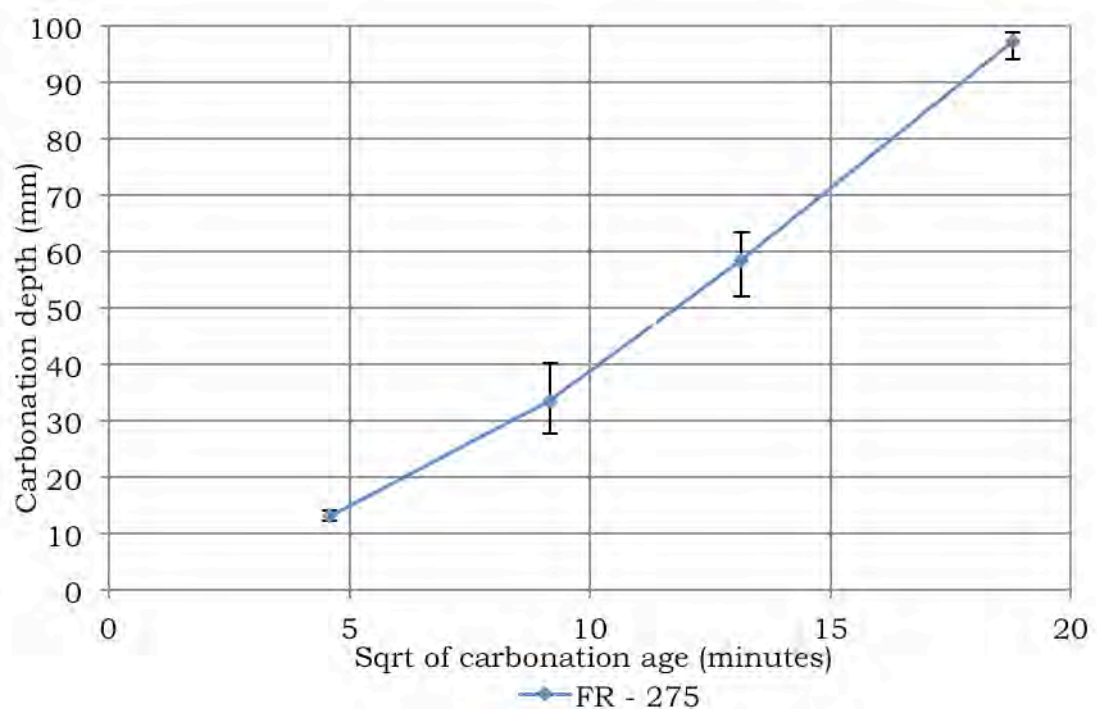


Figure 5.6 – Carbonation depth development of FR-275 specimens.

The almost linear relationship displayed by the data series correlated well with the trend line allowing confident extrapolation of the carbonation start time and the time to full carbonation as nine and 388 days respectively. 21 and 84 day carbonation depths for FR-275 specimens were 51 and 43% lower than those of THB52.5R-275 specimens. A large proportion of this would have been down to the higher moisture content in the FR-275

specimens blocking pore access to CO₂. This was purely as a result of the differing curing methods. However the FR specimens were cured in a way to mimic the curing conditions on-site and therefore produced representative results of the rates of carbonation which can be expected to be found in-situ once shuttering has been removed and before render or plaster layers are applied.

The previous graphs have provided us with an estimation of the time to full carbonation by extrapolating the data. Using results obtained from test series with two or more results across the curing ages it is also possible to estimate the time taken for ‘full’ carbonation to take place by assuming that in general, the rate of penetration of carbonation may be assumed to follow a square root law of the form that is typical of cement bound materials [Concrete Society, 2000] as shown below:

$$d = K_c \sqrt{t} \quad \text{therefore} \quad t_{50} = \left(\frac{d}{K_c} \right)^2$$

where d = carbonation depth, t = time from de-moulding to the final testing age results were obtained and K_c is the carbonation constant. By subsequently defining ‘t’ as the subject of the equation the carbonation constant can be used to estimate the age at which full carbonation (d=50mm) would have taken place.

Table 5.2 gives the carbonation constant (K_c) for all specimens the estimated time to achieve full carbonation (t₅₀).

Overall this methodology works well with specimens that produced results over two or more testing ages. For THB42.5N-275 specimens the estimated time for full carbonation was 107 days, however, no phenolphthalein stain patterns were observed at 84 days of curing.

Table 5.2 – Mean carbonation constants and time for full carbonation to take place in all binder types and densities. * indicates readings taken from large specimens.

	Last recorded carbonation depth (mm)	K_c (mm/day^{1/2})	t₅₀ (days)
THB52.5R-220			
21 day	43.9	9.6	27
THB52.5R-275			
84 day	58.4*	6.4	62
THB52.5R-330			
84 day	33.6	3.7	182
THB42.5N-275			
21 day	22.2	4.8	107
BC-275			
21 day	40.3	8.8	32
FR-275			
353 day	98.7	5.3	362

Clearly, for binder THB52.5R, the carbonation constant increases as density decreases, as shown in Figure 5.7. Consequently, the time to achieve a carbonation depth of 50mm differs from over 62 days in the case of THB52.5R-275 to around 27 days for THB52.5R-220 specimens. This result is expected as the higher porosity in the lower bulk density specimens facilitates both drying and the ingress of CO₂ for carbonation. Comparison of K_c and t_c for all three binder types at a density of 275 kg/m³ shows that hemp-lime with THB52.5R-275 carbonated more rapidly than that made with THB42.5N-275 and BC-275. It can be suggested from this that the binder paste phases of hemp-lime with these binders are less porous and less facilitating of carbonation.

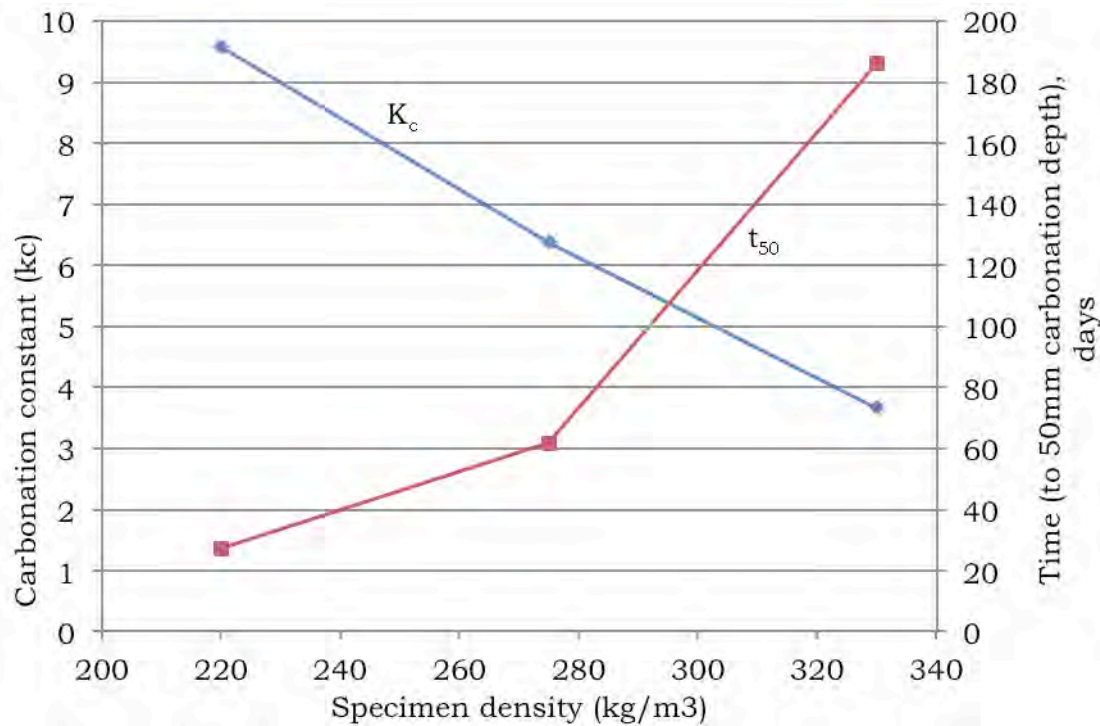


Figure 5.7 – Effect of density of hemp-lime on K_c and t_{50} for binder THB52.5R.

It is clear that the carbonation constant is affected by density variations but it will also be affected by different constituent material ratios at fabrication as this directly dictates the porosity of the specimen, therefore two specimens of the same density but of different constituent material ratios at fabrication will provide two different values of carbonation constant. The constants provided here therefore can only be applied to specimens of the same density fabricated with the same material ratios. Through continued future testing of different variables it may be possible to calculate the relationship between material ratios, density and carbonation constants. This would subsequently produce a data set of values for instant reference.

As a result of these tests it could be assumed that constructing walls with lower bulk densities would be promising due to the increased speed of carbonation and hence carbon sequestration from the atmosphere. Indeed, this holds true if the improved hygro-thermal properties are also taken into account due to the lower bulk density of the material. On the other hand,

however, a lower bulk density wall will use less hemp shiv and less binder (both of which sequester CO₂).

It must be noted however that these results can only be assumed to be indicative as the calculation of K_c is extremely sensitive to changes in carbonation depth measurements

5.2.3 Summary of findings

- NHL5 binders full carbonation within the first 21 days of testing.
- Reducing the bulk density of the specimens and reducing the constituent ratio of the binder significantly increased the average carbonation rate.
- Even at 275kg/m³ it takes 1 year for the specimens to fully carbonate under ideal environmental conditions and with no render or plaster.
- The methodologies used to estimate the time to full carbonation compared very well

5.3 Thermogravimetric analysis of hemp-lime

5.3.1 Treatment of thermogravimetric analysis results

The method of collecting and interpreting the results obtained from thermogravimetric analysis (TGA) will ultimately determine the reliability and consistency of the results. Two of the most important events in the thermal decomposition of the binders under study in this investigation are the dehydroxylation and decarboxylation phases which indicate the amount of calcium hydroxide and calcium carbonate present in the sample; these values will allow quantitative determination of CO₂ sequestration of the binder as currently used in the UK industry. To accurately determine these

values the start and end temperatures of these two phases needs to be determined with confidence. A common method used by previous authors, such as Lawrence [2006], is to study the differential of the mass loss curve, or the rate of change of the curve. This method provided a very well defined start and end temperature to the mass loss phases during Lawrence's investigation of pure air limes, however, preliminary tests in this investigation did not provide useful dTG data from which these values could be confidently determined. Figure 5.8 displays the mass loss and dTG plot for a 14 day old core sample of THB52.5R-275.

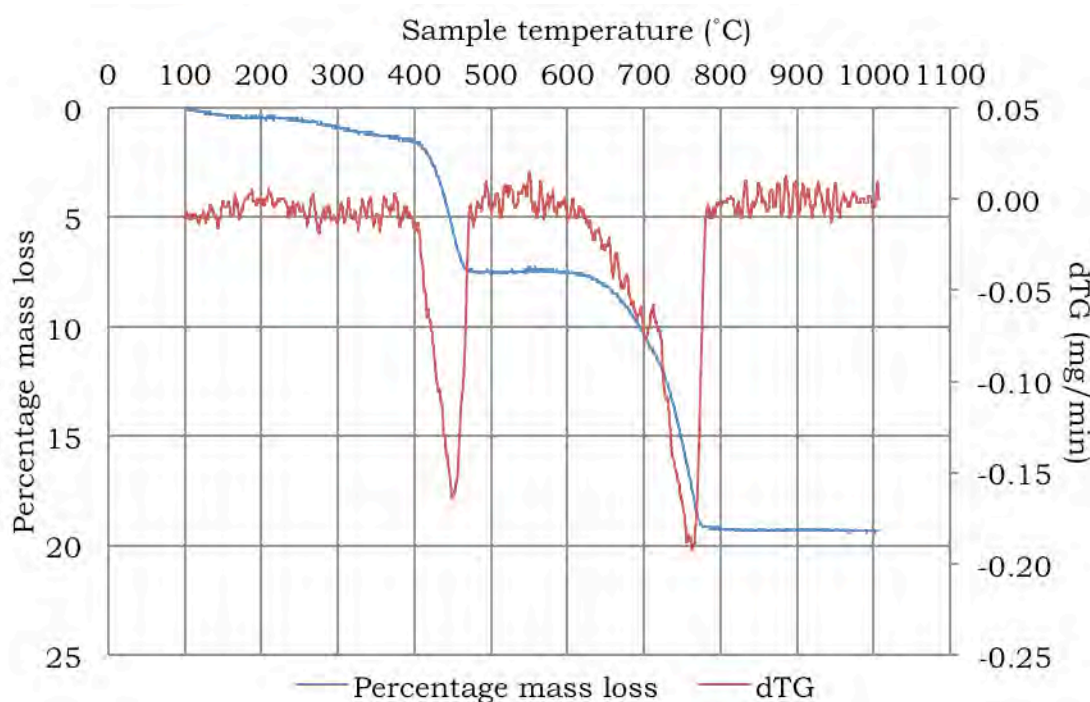


Figure 5.8 – dTGA results for core sample of 14 day THB52.5R-275.

It can be clearly observed that determining the start and end temperatures of the two different mass loss phases would have been extremely challenging considering the shape of the dTG plot. The unevenness of the curve could be explained by considering the sensitivity of the micro balance in use within the TG equipment. All tests were carried out within the calibrated range of the equipment; 5-20mg. However there was still a very small amount of

'noise' within the readings due to the sensitivity of the micro balance. This noise only ranged between $\pm 0.01\text{mg}$, however the noise was exaggerated once the differential was calculated.

A second possible methodology for the determination of the start and end temperatures was to analyse the heat flow during the test, i.e. the rate of heat being applied to the system to keep the heating rate of $10^\circ\text{C}/\text{min}$ constant irrespective of exothermic or endothermic reactions taking place within the sample. However this also presented similar problems as displayed in Figure 5.9 below.

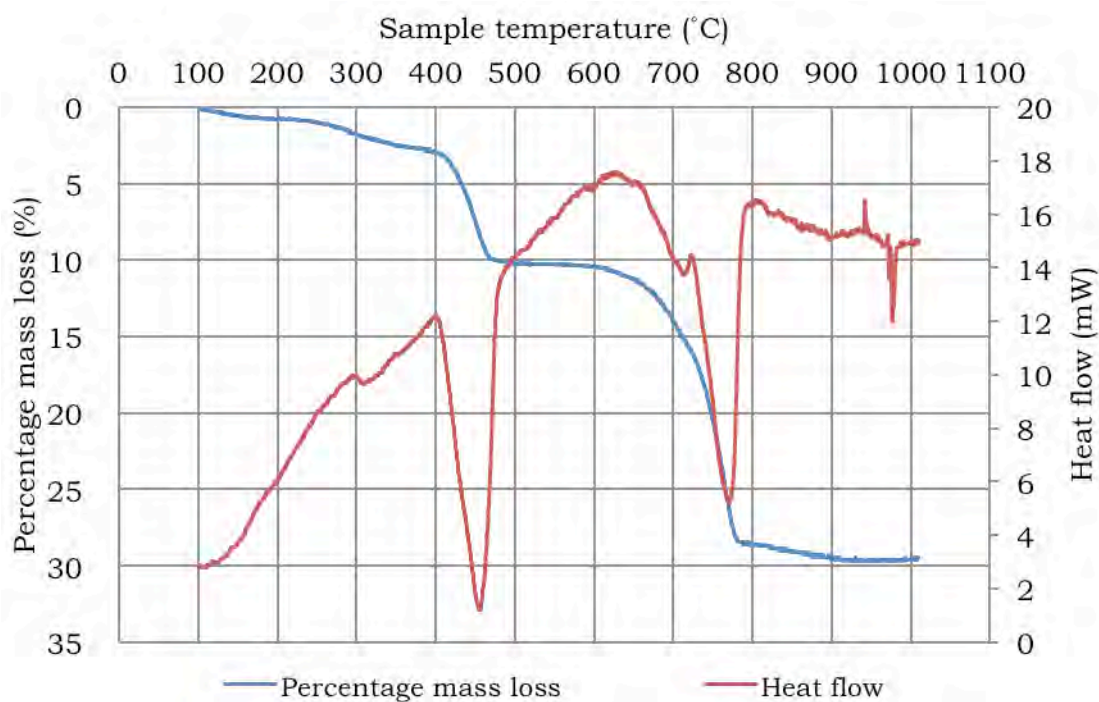


Figure 5.9 – Heat flow chart of 14 day THB52.5R-275.

A lower degree of noise was displayed via this method, however, it was still comparatively difficult to determine the start and end temperatures of the mass loss phases. Figure 5.10 and Figure 5.11 illustrate the methodology used within this investigation.

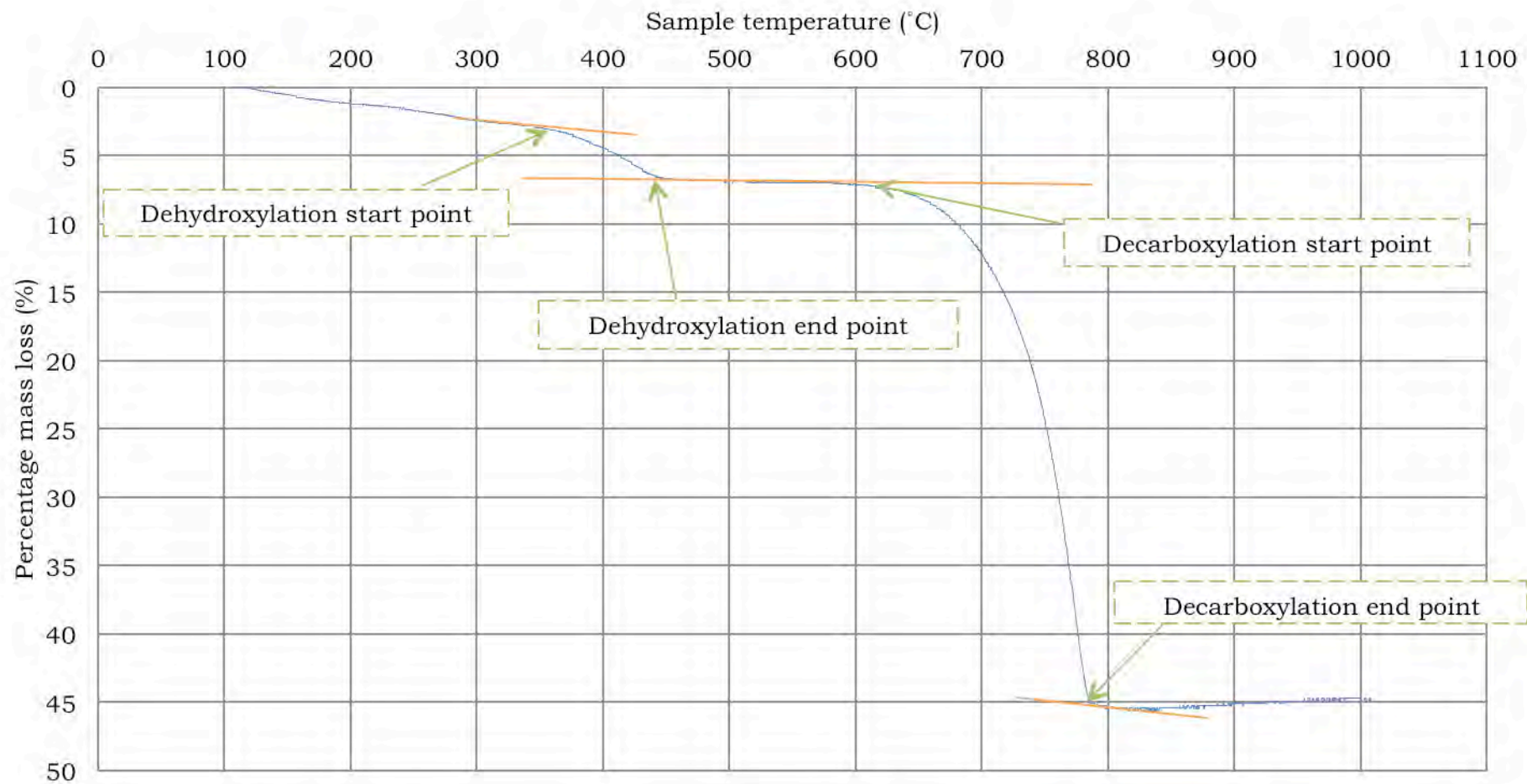


Figure 5.10 – Typical methodology for the determination of the start and end temperatures of dehydroxylation and decarboxylation mass loss phases in edge samples of hemp-lime specimens.

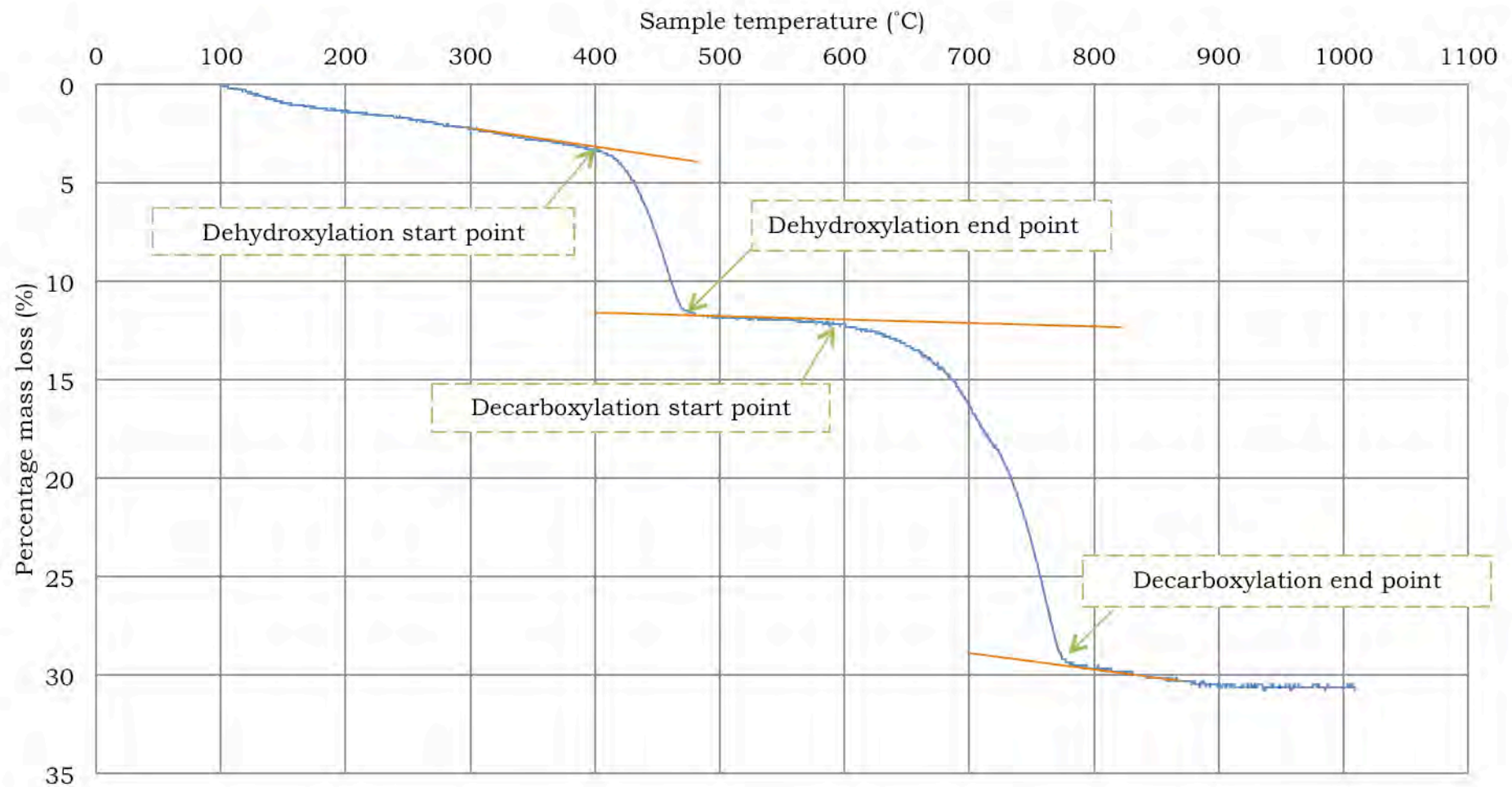


Figure 5.11 – Typical methodology for the determination of the start and end temperatures of dehydroxylation and decarboxylation mass loss phases in core samples of hemp-lime specimens.

This methodology involves overlaying lines on the mass loss curves obtained from the TG tests. In effect, the mass loss curve before and after each phase is tangentially extended. The point at which the mass loss curve and the extended line diverge was taken as the start temperature of the respective mass loss phase; the point where the mass loss curve and the extended line converge was taken as the end temperature of the respective mass loss phase. This allows consistent and comparable determination of the start and end temperatures between the different binders and/or curing ages. These temperatures and their corresponding masses then allowed determination of the percentages of calcium hydroxide and calcium carbonate that were present in the sample.

Any increase in the mass of CaCO_3 at the different curing ages compared to the mass present in the fresh, un-cured binder could only occur due to the carbonation of Ca(OH)_2 . This increase in mass can then be directly correlated to a mass of CO_2 which was used to cause that carbonation and hence provide interval and ultimate values for the carbon sequestration on hemp-lime at different curing ages. An additional method would have involved calculating the decrease in Ca(OH)_2 due to carbonation compared to the original mass present in the fresh binder, however the methodology used within this study bypasses any complications in determining any mass loss in Ca(OH)_2 from the synthesis of C_3S and Ca(OH)_2 which partially synthesises at a temperature of around 320°C , resulting in lower weight losses at the dehydroxylation temperature of Ca(OH)_2 [Valenti & Cioffi, 1985].

5.3.2 TG analysis of bio-aggregates

Before TGA testing of the binder from the composite specimens could proceed it was necessary to determine the thermal decomposition profiles for both hemp shiv and oil seed rape in the event that small particles and/or fibres made it through the sampling process. This was unlikely however as, during sample collection, only whole particles were removed from the composite specimens, lightly ground with a pestle and mortar and then

passed through a fine 64 μ m sieve. Visually there were no traces of particle or fibre in the resulting sample so this step was purely taken as a precautionary one. Approximately 15mg of each aggregate was used in two separate tests with a heating rate of 10°C/min between 20°C and 1000°C. The mass loss curves are presented in Figure 5.12.

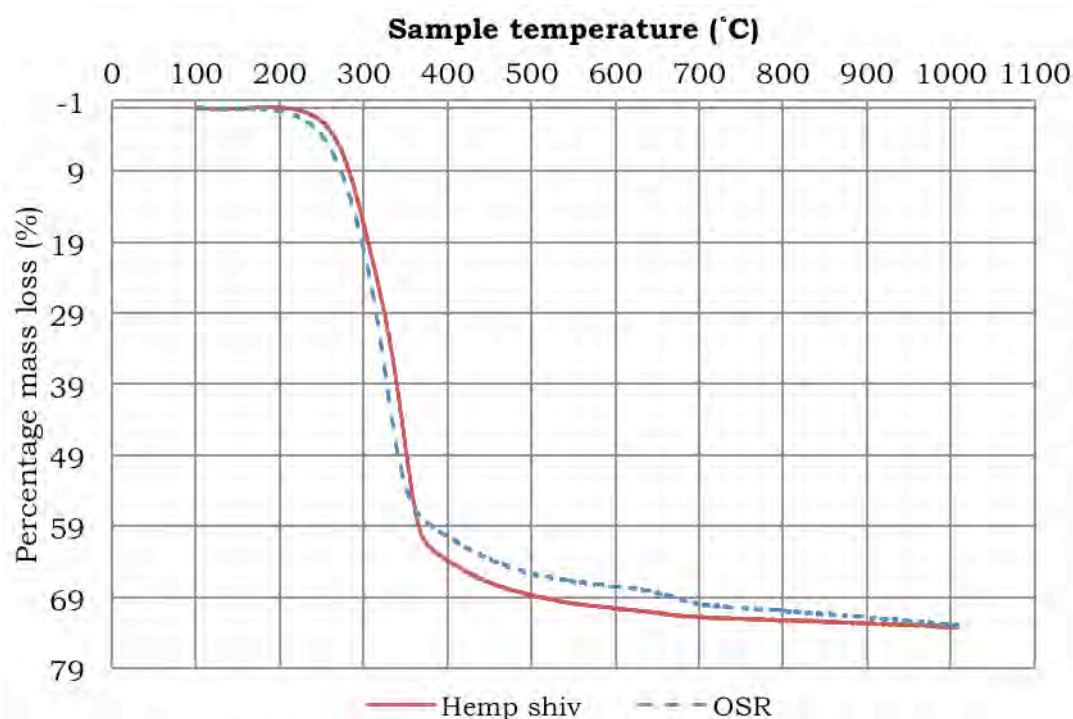


Figure 5.12 – TGA mass loss curve for hemp shiv and OSR particles.

Hemp shiv displayed a mass loss of 63% between 220°C and 380°C. Subsequently a further 10% mass loss was observed between 380°C and 1000°C. Oil seed rape displayed a mass loss of 58% between 200°C and 370°C and a further 15% mass loss between 370°C and 1000°C. These data was then used to determine if any shiv particles were in the binder samples when they were tested.

5.3.3 Carbon content of hemp shiv

As a result of the review of available literature in Chapter 2 it is possible to estimate a range of carbon sequestration values for hemp shiv. Hons [1996,

unpublished] and Ian Pritchett from Lime Technology Ltd. respectively estimated that 1.46 and 1.84 grams of carbon dioxide were necessary to produce 1 gram of dry hemp shiv material. Table 5.3 therefore presents the range of sequestered CO₂ possible based on these calculation for the three specimen densities used in this investigation.

Table 5.3 – CO₂ sequestration values for specimen densities and constituent ratios used within this investigation.

Specimen dry density (kg/m³)	Wet material mass at fabrication (kg/m³)	Constituent ratio of hemp shiv (%)	Mass of hemp shiv (kg)	Range of sequestered CO₂ (kg)
THB52.5R-220	2.080	24	0.499	0.73-0.92
THB52.5R-275	2.328	21	0.489	0.71-0.90
THB52.5R-330	3.036	16	0.486	0.71-0.89
THB42.4N-275	2.328	21	0.489	0.71-0.90
BC-275	2.328	21	0.489	0.71-0.90
FR-275	2.328	21	0.489	0.71-0.90
NHL5-275	2.328	21	0.489	0.71-0.90

Considering the comparatively large variations in densities between the three specimens there was almost no difference in the amount of CO₂ each one had sequestered in the hemp shiv.

5.3.4 TG analysis of fresh binder

To determine a baseline for the quantity of Ca(OH)₂ and CaCO₃ and CO₂ originally present in the binders, samples of fresh binder were subjected to TGA testing under the same testing methodology as all other samples. Figure 5.13 presents the mass loss curves against sample temperature

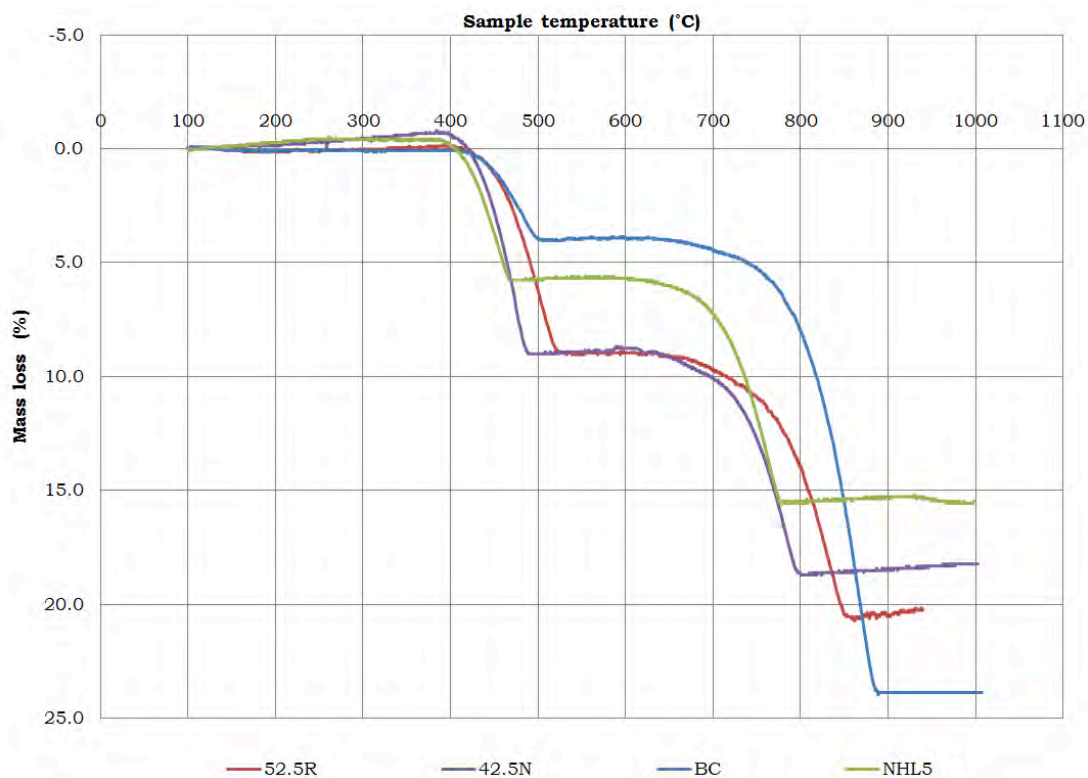


Figure 5.13 – TGA analysis of fresh binder

The results allowed for the calculation of embodied carbon dioxide content by determining the mass loss during the decarboxylation phase of the test i.e. the percentage mass of carbon dioxide already present in the binder before any carbonation has taken place. The values for embodied Ca(OH)_2 and CaCO_3 content were also determined. These values were subsequently used for comparison against the mineralogical values obtained during TGA testing of the composite specimens, principally for the determination of sequestered carbon dioxide. Table 5.4 presents the mineralogical mass ratios of Ca(OH)_2 , CaCO_3 and CO_2 .

Table 5.4 – Embodied mineralogical content of fresh binders.

Binder	Embodied Ca(OH)_2 (%)	Embodied CO_2 (%)	Embodied CaCO_3 (%)
THB52.5R	37.1	17.6	7.8
THB42.5N	43.1	11.0	4.9
BC	15.4	36.1	15.9
NHL5	23.3	18.5	8.1

In these instances, the mass loss during the decarboxylation phases were as a result of the calcium carbonate present in the hydration phases of the NHL5 binder and the cement content of the pre-formulation hemp-lime binders. Furthermore, part of the mass loss during this phase would have been caused by the calcite aggregate/filler which is added to the pre-formulated binders to strengthen the binder matrix [Mike Lawrence pers.comm. June 2011].

Results indicated that THB-52.5R contained 37.1% calcium hydroxide and 7.8% CaCO_3 which equated to 17.6% embodied CO_2 . The respective values for THB42.5N were 43.1, 4.9 and 11%. These results empirically confirmed the previously held assumption that THB52.5R contained a higher percentage mass of cement than THB42.5N. If 100% carbonation were to occur in the THB binders as the current Life Cycle Assessment estimates, the percentage of calcium hydroxide in the sample should reduce to 0%.

The BC binder contained 15.4% Ca(OH)_2 , 15.9% embodied CO_2 and 36.1% CaCO_3 . BC binders are marketed as an air lime based binder with the addition of cements and aggregates/fillers. This result empirically confirmed the assumption that BC binders contained significantly more cement than THB binders.

Evrard (2008) stated that Tradical PF70 binder contained 75% CL90 and 15% cement by mass. The TGA results do not support these numbers.

5.3.5 TG analysis of hydration products

The development of the hydration products over time of the binder was determined through TGA testing of binder pastes of varying water/binder(w/b) ratios cured at varying ages from six hours to 28 days. The main objective within this series of tests was to attempt to quantify the percentage mass increase (if any) of calcium hydroxide as a result of the hydration of the cement constituent.

Following sample collection and storage as detailed in Chapter 3, TGA testing was carried out following an identical heating regime as that set out for samples collected from the composite specimens. Figure 5.14 and Figure 5.15 presents the mass loss curves for 0.4w/b and 0.5w/b ratio pastes respectively at curing ages of 6, 24 hours 3, 7 and 28 days.

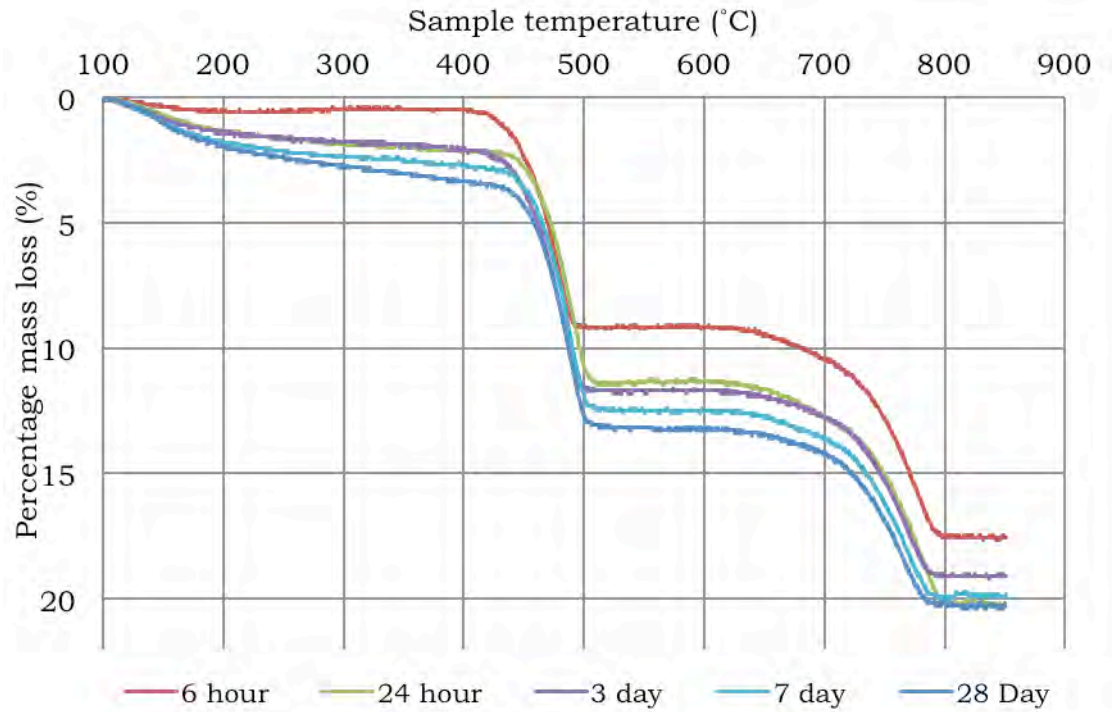


Figure 5.14 – TGA mass loss curves for 0.4w/b ratio THB52.5R pastes.

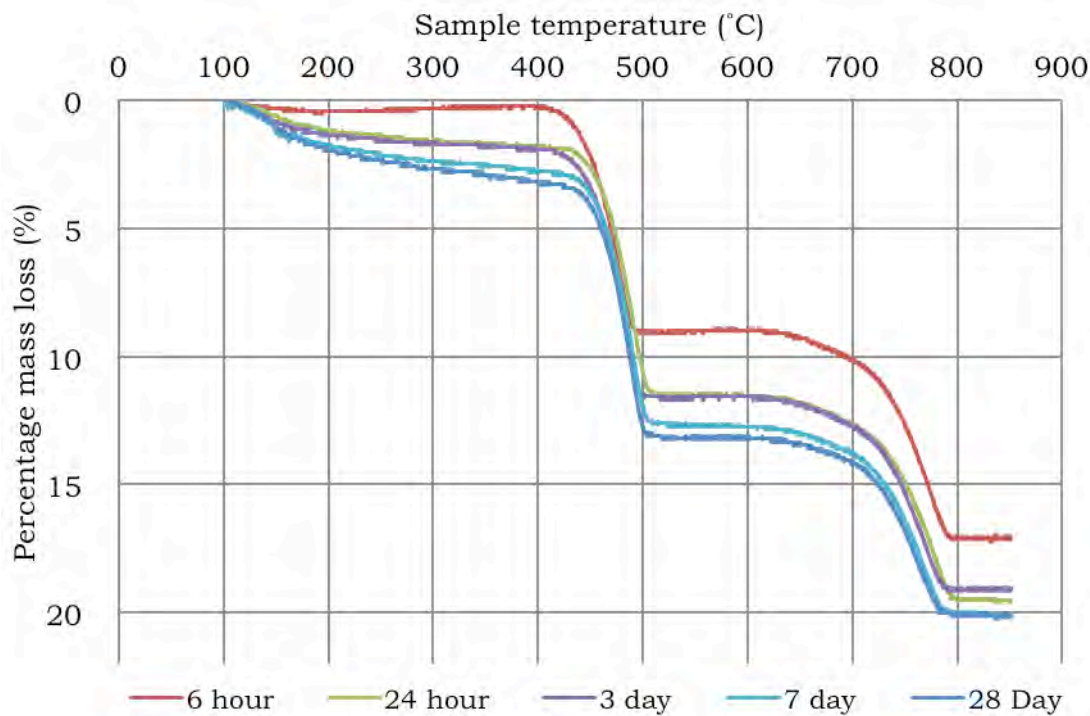


Figure 5.15 – TGA mass loss curves for 0.5w/b ratio THB52.5R pastes.

Overall the tests produced positive and negative results. Furthermore, in this case they must be assumed to be incomplete. Testing was only carried out up to 28 days of curing; as an increase in mass for hydration products was observed between seven and 28 days it is not clear whether or not the masses observed at 28 days were the ultimate mass increases or if they indeed carried on increasing past this curing period. Further testing, with longer curing periods, may or may not confirm this but due to logistical constraints these tests have not been possible within this investigation.

The slope increase over time between 100°C and approximately 400°C visually indicated an increase in hydration products (**Error! Reference source not found.**).

By applying the methodology described above the quantities of Ca(OH)_2 and CaCO_3 was determined as curing progressed and are presented in Table 5.5.

Table 5.5 – Ca(OH)₂ and CaCO₃ development of THB52.5R binder pastes over time

Testing age	Mass Ca(OH) ₂ (%)		Mass CaCO ₃ (%)	
	0.4 w/b	0.5 w/b	0.4 w/b	0.5 w/b
6 hours	35.3	35.0	18.5	18.2
24 hours	36.6	38.6	19.2	17.2
3 days	38.3	39.3	16.5	16.7
7 days	38.1	38.9	16.4	16.2
28 days	39.5	38.6	15.1	14.9

Over the 28 day period there was a 5% increase in calcium hydroxide. Over the same period there was a 3.5% decrease in the mass of calcium carbonate. Reassuringly, there was no increase in the mass of calcium carbonate which confirms that the methodology used to prevent carbonation during the curing process was successful.

When combined with the mass of calcium hydroxide already present in the binder prior to use it can be stated that the binder has the potential to use 43% of its mass in the carbonation process to sequester CO₂ from the atmosphere.

5.3.6 Thermogravimetric analysis of hemp-lime composite specimens

Via TGA testing of the edge and core samples collected from the composite specimens at each testing age the empirical determination of the degree of CO₂ sequestration undertaken by the binder was evaluated. Table 5.6 presents the edge and core CO₂ content results for all binders and/or curing regimes at all carbonation ages.

Table 5.6 – Edge and core CO₂ sequestration development over time for all binders.

Specimen ID	Edge					Core				
	7 day	21 day	84 day	173 day	353 day	7 day	21 day	84 day	173 day	353 day
	CO ₂ content (%)					CO ₂ content (%)				
THB52.5R-220	24.4	24.7	27.0	26.9	25.8	15.2	12.4	19.1	19.9	19.9
THB52.5R-275	25.4	26.2	26.9	26.8	26.5	11.6	12.1	18.2	19.5	20.8
THB52.5R-330	23.8	24.4	24.3	24.9	25.4	15.0	11.4	13.8	18.9	25.9
THB42.5N-275	-	24.1	25.1	25.8	26.7	-	17.9	18.2	18.2	21.2
BC-275	-	25.0	23.7	25.1	27.6	-	18.5	20.8	21.2	22.1
FR-275	-	26.7	27.8	28.1	20.8	-	12.6	15.4	12.6	13.3
NHL-275	-	19.0	21.7	-	-	-	10.5	12.4	-	-

Overall the results were successful in providing insight into the CO₂ sequestration potential of the binders investigated. Furthermore, clear differences were observed between the edge and the core samples. At 353 days of carbonation all edge samples were within 2.6% of the CO₂ obtained at 7 days of carbonation. Core samples were within 10.9% with THB52.5-330 specimens displaying the largest CO₂ content increase indicating that density may not necessarily have a great affect on the sequestration potential of the composite specimen. As expected, the edge of the specimens carbonated at a greater rate then the core, however, in almost all cases the core samples did not reach the same level of CO₂ content as the edge sample. Only THB52.5R-330 specimens displayed greater levels of CO₂ in core samples compared the edge samples.

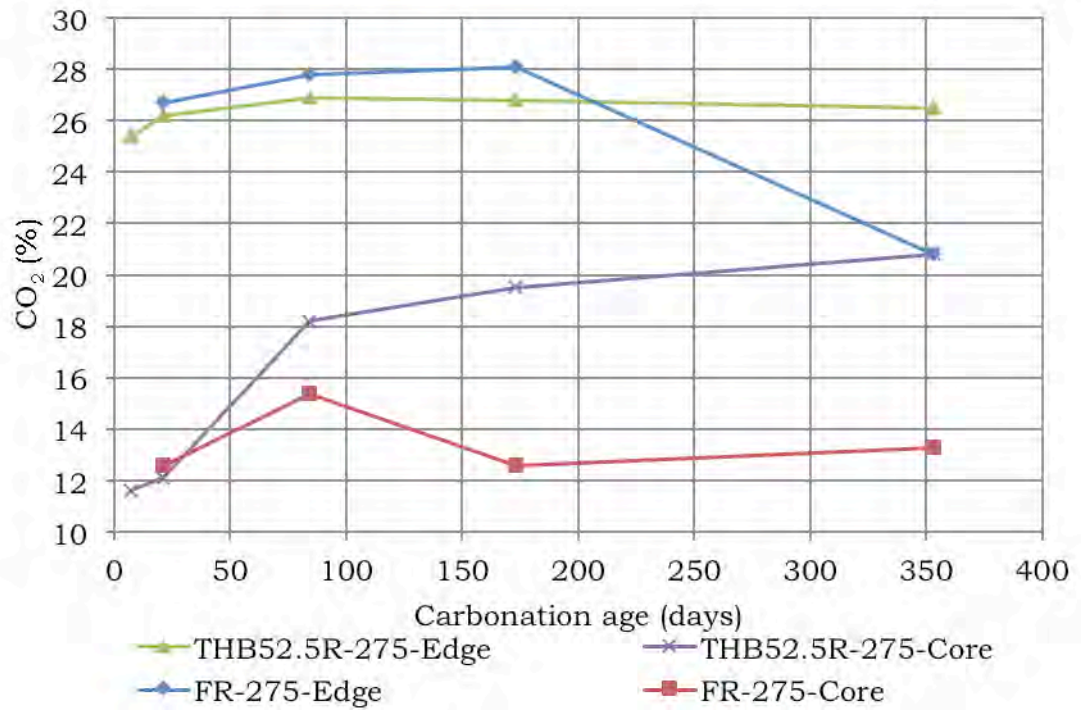


Figure 5.16 – CO₂ content development of the two curing regimes.

By comparing the results to the mineralogical content originally present in the binders it was possible to calculate the percentage of CO₂ that was sequestered from the atmosphere. Table 5.7 presents the average CO₂ content taken as the arithmetic mean between the edge and core samples along with the percentage mass increase due to the sequestration.

Table 5.7 – Average CO₂ content and sequestration values for all binders at all ages.

Specimen ID	Carbonation age				
	7 day	21 day	84 day	173 day	353 day
	Average CO ₂ content [CO ₂ sequestration] (%)				
THB52.5R-220	19.8 [12]	18.6 [10.8]	23.1 [15.3]	23.4 [15.6]	22.9 [15.1]
THB52.5R-275	18.5 [10.7]	19.2 [11.4]	22.3 [14.5]	23.2 [15.4]	23.7 [15.9]
THB52.5R-330	19.4 [11.6]	17.9 [10.1]	19.1 [11.4]	21.9 [14.1]	25.7 [17.9]
THB42.5N-275	-	21.0 [16.1]	22.6 [17.7]	22.0 [17.1]	24.0 [19.1]
BC-275	-	21.8 [5.9]	22.3 [6.4]	23.2 [7.3]	24.9 [9.0]
FR-275	-	19.7 [11.9]	21.6 [13.8]	20.4 [12.6]	17.1 [9.3]
NHL-275	-	14.8 [6.7]	17.1 [9.0]	-	-

THB42.5-275 specimens displayed the highest sequestration potential of 19.1% with BC-275 and NHL5-275 displaying the lowest potential of 9%.

The sequestration potential for THB52.5R specimens increased as the bulk density of the specimens increased. It is hypothesised that this may have been caused by the increased ratio of water in the fabrication mix as the density increased.

Table 5.8 present the calculations to determine the mass of sequestered CO₂, including the sequestration from the hemp shiv and the binders, for each specimen fabricated in this investigation using hemp shiv. Furthermore, these values are used to determine the sequestration values per m³ of material; direct comparison against current literature can then be made.

Table 5.8 – Total CO₂ sequestration values, including hemp shiv, for all binders and bulk densities of large specimens.

Specimen ID	THB52.5R-220	THB52.5R-275	THB52.5R-330	THB42.5N-275	BC-275	FR-275	NHL5-275
Specimen wet mass at fabrication (g)	2080	2328	3036	2328	2328	2328	2328
Binder proportion at fabrication (%)	27	36	36	36	36	36	36
Binder mass at fabrication (g)	562	838	1093	838	838	838	838
Embodied CO₂ mass in binder (g)	44	65	85	41	133	65	68
Final CO₂ mass in binder (g)	129	199	281	201	209	143	143
Sequestered CO₂ from binder (g)	85	134	196	160	76	78	75
Total sequestered CO₂ including hemp (g)	815-1005	844-1034	906-1086	870-1060	786-976	788-978	785-975
Average specimen dry mass at 360 days (g)	1183	1522	1876	1552	1462	1516	1423*
CO₂ per m³	152-187	153-187	159-191	154-192	148-184	143-179	152-188

Initial assumptions that there may be large variations in the quantity of CO₂ sequestration between the different specimen bulk densities do not seem to be correct. There was a 3-7kg/m³ sequestration difference between THB52.5R-220 and THB52.5R-330 specimens indicating that there may be no sequestration advantage in reducing the density of the material. However, other factors need to be taken into consideration. A lower density material should provide more favourable thermal characteristics when used within the fabric of a building, reducing heating/cooling costs and hence improving

the building's carbon footprint. Conversely, a lower bulk density would not provide the same thermal buffering effect between day and night temperature changes as the thermal mass of the material would be decreased. This material property has been concluded to reduce private/commercial running costs [Bevan & Wooley, 2008; Yates, 2002]. In all instances THB52.5R binders displayed higher sequestration values per m³ than was estimated by Ian Pritchett at Lime Technology Ltd. and by the French LCA report. It is hoped future investigations can use these values to better determine the real life sequestration potential of hemp-lime within a holistic LCA study. However, it must be borne in mind that the values presented in this thesis are purely the sequestration potential of the material itself. No addition for the amount of CO₂ given off during production and transportation of both the hemp shiv and the formulated binders, and indeed the water used in the mix, has been accounted for. Therefore a direct comparison against the LCA values is not possible.

Table 5.9 presents the average CO₂ content of all the binders used within this investigation against the carbon content of the fresh binders therefore providing an estimate for the degree of carbonation in the binder compared to its potential. The average CO₂ content at 353 days is calculated as the mean between the edge and the core sample.

Table 5.9 – Calcium hydroxide content comparison of 353 day cured binders against fresh binders.

Binder	Fresh Ca(OH)₂ (%)	Core Ca(OH)₂ (%)	Outer Ca(OH)₂ (%)	Mean Ca(OH)₂ (%)	Ca(OH)₂ decrease (%)	Carbonated (%)
THB42.5N-275	43.0	11.5	7.5	9.5	24.5	57.1
THB52.5R-220	37.1	16.5	8.6	12.6	24.5	66.0
THB52.5R-275	37.1	13.6	8.5	11.1	26.0	70.1
THB52.5R-330	37.1	9.6	7.6	8.6	28.5	76.8
BC-275	15.4	4.3	5.2	4.8	10.6	69.0
FR-275	37.1	26.7	14.7	20.7	16.4	44.2

It can be observed that even after a period of 360 days full carbonation had not taken place and residual amounts of Ca(OH)₂ were still present in the binder. This may confirm the ‘Malteser’ effect previously discussed. FR-275 specimens displayed the lowest degree of carbonation. This was expected purely due to the dynamics of the curing regime compared to the demoulded specimens

5.4 Summary of findings

As a result of the TGA testing of hemp-lime composite materials the following conclusions were observed:

- No significant differences in CO₂ sequestration were observed between specimens of different bulk densities.
- The hemp shiv component of the composite material is by far the largest CO₂ sink.
- Attempts to increase the CO₂ sequestration potential of the composite material in practice should be made by increasing the constituent ratio of hemp shiv.

- The CO₂ sequestration of the binder increased as the constituent ratio of water increased; in turn the carbonation potential also increased.

CHAPTER 6 - MECHANICAL CHARACTERISTICS OF HEMP-LIME

6.1 Introduction

Results from the physical and mechanical property testing of the experimental hemp-lime mixes are presented and discussed in this chapter. Data are presented from uni-axial compression testing, including stress-stress responses and specimen failure modes. Drying rates for the experimental hemp-lime specimens are also analysed and discussed. As novel experimental methodologies have been developed in this work, the effectiveness of these new approaches, including for example specimen manufacture to achieve target density, are critically appraised.

6.2 Consistency in composite specimen fabrication

To produce reliable and representative physical and mechanical characterisation results for the different hemp-lime mixes investigated, consistent control of the specimen bulk density was of utmost importance. A novel fabrication approach, based on mass batching of materials, was developed for this study. The approach relied on understanding initial wet and final dry moisture contents of the composite materials. As outlined earlier in Chapter 3, the objective was to manufacture specimens using THB52.5R binder to achieve final bulk densities of 220, 275 and 330kg/m³ at equilibrated moisture contents of 6-7% after 91 days. At each testing age three specimens for each binder type, bulk density and/or curing regime were randomly selected for mechanical testing. Average specimen diameters were determined from three measurements taken at the top, mid-height and the bottom of each cylinder using Vernier callipers. Specimen heights were also measured using the Vernier callipers.

Table 6.1 presents the mean bulk densities, range and moisture contents of the hemp-lime specimens at each testing age up to 360 days after fabrication. However, the most accurate indication of fabrication consistency was determined when the bulk densities were corrected for moisture content. With the moisture content subtracted Table 6.2 presents the dry density of the hemp-lime specimens at each testing age in conjunction with the average difference from the mean.

The results indicated that one of the main objectives of the investigation was successfully achieved with an overall average difference from the mean of 0.8% across 130 specimens. Furthermore, in the case of 28 day THB52.5R-275 specimens, a 0% variation of bulk density between the three specimens was achieved.

Table 6.1 – Mean bulk densities of specimens at all testing ages.
Symbols † and * indicate results obtained from one and two specimens respectively.

Specimen ID	Mean bulk density (kg/m ³) [Mean moisture content (%)] (Range)				
	14 days	28 days	91 days	180 days	360 days
THB52.5R-220	256 [24.3] (244-269)	221 [9.7] (221-222)	221 [6.3] (220-221)	220 [6.0] (219-221)	220 [6.2] (219-220)
THB52.5R-275	304 [19.3] (300-307)	273 [9.0] (273-273)	278 [6.3] (276-282)	279 [6.3] (276-281)	281 [6.7] (280-283)
THB52.5R-330	401 [26.3] (390-408)	345 [11.3] (344-348)	342 [6.0] (340-345)	356 [7.3] (354-359)	355 [6.9] (355-356)
THB42.5N-275	-	283 [10.0] (281-287)	282 [8.0] (280-284)	287 [6.7] (283-289)	287* [6.2] (287-288)
BC-275	-	273 [10.0] (272-274)	273 [8.0] (273-274)	272 [7.0] (269-274)	272 [6.6] (269-274)
NHL5-275	-	277 [7.2] (275-278)	264* [6.1] (264-265)	267 [6.3] (266-268)	-
FR-275	-	427 [18.3] (426-427)	293 [16.7] (290-296)	281 [14.0] (280-283)	283 [11.6] (281-286)
SH-275	-	277 [10.8] (274-281)	283 [6.5] (281-285)	282 [6.0] (280-283)	283* [6.3] (283-284)
0.3OSR-275	-	278 [9.1] (277-280)	278 [6.4] (277-280)	282 [6.4] (283-286)	285 [6.7] (284-287)
0.6OSR-275	-	277† [9.5]	282 [6.7] (281-283)	283 [6.7] (281-285)	285 [6.6] (284-286)
OSR-275	-	275 [9.4] (273-277)	275 [6.2] (273-277)	283 [6.3] (281-285)	282 [6.4] (281-282)

Table 6.2 – Mean dry bulk densities of specimens at all testing ages.
Symbols † and * indicate results obtained from one and two specimens respectively.

Specimen ID	Mean dry bulk density (kg/m ³) [Average difference from the mean (%)] (range {kg/m ³ })				
	14 days	28 days	91 days	180 days	360 days
THB52.5R-220	193 [2.1] (188-196)	200 [0.5] (199-201)	207 [0.5] (206-208)	207 [0.5] (206-208)	206 [0.5] (205-207)
THB52.5R-275	245 [0.6] (243-246)	248 [0] (248-248)	261 [1.2] (258-265)	261 [1.0] (259-264)	262 [0.6] (280-283)
THB52.5R-330	295 [1.0] (293-299)	306 [1.1] (303-310)	322 [0.6] (320-324)	330 [1.2] (326-334)	331 [0.2] (330-331)
THB42.5N-275	-	255 [2.0] (251-261)	259 [0.4] (258-260)	267 [1.9] (263-272)	270* [0.2] (269-270)
BC-275	-	246 [0.4] (245-247)	251 [1.0] (249-254)	253 [1.0] (250-255)	254 [0.6] (252-255)
NHL5-275	-	257 [0.8] (254-258)	248* [0.2] (248-249)	250 [1.0] (247-252)	-
FR-275	-	348 [0.7] (346-351)	244 [1.8] (240-249)	242 [0.8] (240-244)	251 [0.6] (249-252)
SH-275	-	247 [1.2] (245-251)	264 [0.8] (263-267)	265 [0.6] (263-266)	265* [0.4] (264-266)
0.3OSR-275	-	253 [0.4] (252-254)	260 [0.6] (259-262)	266 [0.9] (264-269)	266 [0.4] (265-267)
0.6OSR-275	-	251 [†]	263 [0.4] (262-264)	264 [0.8] (262-266)	266 [0.4] (265-267)
OSR-275	-	249 [0.4] (248-250)	258 [0.8] (256-260)	265 [0.9] (263-268)	264 [0.4] (263-265)

The 14 day old THB52.5R-220 specimens displayed the largest variation in bulk density with a spread of 25 kg/m³ and the largest percentage difference from the mean of 5% across the three specimens. This may have been the result of different specimen placement in the conditioning room for the following reason; specimens placed at the back of the shelves may not have had as readily available free flowing air as specimens at the front of the shelves, hence inhibiting free water evaporation. Future investigations may monitor this by rotating the placement of one sample of specimens against a control. Due to unfortunate loss of low strength specimens during handling throughout the study, no results were available for 360 day old NHL5 specimens.

Following 91 days of curing the THB52.5R-220 specimens achieved an average bulk density of 221kg/m³, just 0.5% above the target bulk densities. THB52.5R-275 specimens displayed an average bulk density of 278 kg/m³ with a range of 276–282 kg/m³. This indicates an increase of 1% above the target bulk density with an average difference of 1.2% from the mean. The average 91 day bulk density for THB52.5R-330 specimens was 342 kg/m³ with a range of 340–345 kg/m³. Although the average bulk density was 3.6% above the target, the average difference of 0.7% from the mean correlates well to the other two densities and indicates that the novel approach to the fabrication process has been successful in reliably producing specimens to the target bulk density and to within very tight ranges. The small variations in the overall results could be defined as the intrinsic variability in the material, variabilities which may no longer be possible to eliminate under empirical conditions.

The increase in the measured bulk densities from the target bulk densities may be a result of mass increase in the binder matrix due to carbonation. This factor was not included in the initial calculations into the wet mass required as the ultimate degree of carbonation was not known. It can be seen that in most cases the bulk density increases after 91 days as carbonation progresses through the specimens; this can potentially be linked to the chemical characteristics of the binder as discussed in Chapter 6.

Specimens fabricated with OSR (with or without additional hemp-shiv aggregate) behaved similarly to hemp shiv aggregate specimens in relation to changes in bulk density with age indicating that any differences in the pore structure between hemp shiv and OSR did not have a marked influence on the moisture loss of the composite material.

Figure 6.1 displays a typical THB52.5R-275 specimen prior to compressive testing.



Figure 6.1 – Typical THB52.5R-275 specimen prior to testing.

It can be seen that the fabrication methodology produced specimens with a very homogenous distribution of material with no visible variation (e.g. voidage) in surface material or layering between subsequent handfuls of material whilst casting and apparent random particle orientation. The visual homogeneity in density was consistent across all specimens including those of lower and higher densities.

To further verify the methodology used within this investigation the bulk densities of the small specimens were compared to those of the large specimens. Table 6.3 presents the comparison of bulk densities in conjunction with the moisture contents of the small specimens.

Table 6.3 – Mean bulk density of small specimens used for phenolphthalein testing compared to large specimens used for strength testing.

Specimen ID	Mean density (kg/m^3) (mean density of large specimen) [moisture content (%)]				
	14 days	28 days	91 days	180 days	360 days
THB52.5R-220	235 (256)[21.8]	223 (221) [6.5]	223 (221) [6.4]	221 (220) [6.2]	221 (220) [6.2]
THB52.5R-275	286 (304) [18.3]	278 (273) [9.2]	279 (278) [6.2]	281 (279) [6.7]	284 (281) [6.7]
THB52.5R-330	346 (401) [22.2]	338 (345) [10.5]	338 (342) [6.2]	335 (356) [6.2]	339 (355) [6.3]
THB42.5N-275	-	284 (283) [10.3]	284 (282) [7.7]	287 (287) [6.8]	289 (287) [6.7]
BC-275	-	274 (273) [9.8]	274 (273) [7.5]	274 (272) [7.1]	276 (272) [6.9]
FR-275	-	415 (427) [16.9]	279 (293) [15.9]	278 (281) [13.7]	280 (283) [11.0]

In this case it is not possible to use this comparison to determine the consistency of the fabrication method as only one small specimen for each testing age, density and binder was fabricated. However, it can be seen from these results that the bulk densities of the small specimens correlated well to those of the large specimens. Notably, the 14 day large THB52.5R specimens displayed higher densities than the smaller specimens. This could

be due to the higher moisture contents of the larger specimens as the moisture had a longer distance to travel to the surface of the specimens for evaporation. At testing ages of 91, 180 and 360 days the mean densities compared well to those of the large specimens used for strength testing. This may possibly mean that the size of the specimen does not have any effect on the target bulk density as long as the wet densities and constituent ratios at fabrication are identical.

Fabrication methods employed within previous investigations [Evrard, 2003; Cerezo, 2006] theorised that by applying an equal compressive force to subsequent layers specimens of equal bulk density would be produced, however, specimens fabricated by Cerezo averaged differences of 4.2% from the mean with some specimens over 7% off the target density. One particular series displayed a range variation of 110 kg/m³ between the specimens which were intended to be the same target bulk density.

6.3 Mechanical characterisation

6.3.1 Treatment of results

In order to provide comparable results between the different binder types, bulk densities and curing regimes, the following analysis regime was set out for the treatment of results obtained from the tests:

- The maximum stress was obtained from the maximum load recorded by the testing rig and the mean cross-sectional area of each individual specimen.
- The specimen strains were determined from platen displacements relative to original capped specimen lengths.

Specimen elastic modulus was determined from the average elastic moduli results measured between a strain of 0 and 0.002. This allowed determination of the materials immediate reaction to loading and reduced

the variation due to human calculation. Previous investigations [Cerezo, 2005] determined the elastic modulus by free-hand drawing a tangent line from the origin along the initial quasi-elastic line. This approach may be open to high degrees of variability.

6.3.2 Results and discussion

The mean ultimate compressive strength (f_{cm}), the strength range between the three specimens, strain at failure and mean initial tangent static modulus of elasticity (E_{cm}) for all specimens at all ages are given in Table 6.4.

Overall the composite material displayed low ultimate compressive strengths (0.021 – 0.21 N/mm²) and initial tangent moduli (3.3 – 27.5 N/mm²). These values of compressive strength are comparable with synthetic rigid foam insulation materials (compressive strengths around 0.10 – 0.12 N/mm²). In all instances the compressive strength and elastic modulus displayed a tendency to increase as curing progressed whilst the failure strain decreased. Except for SH - 275, all specimens achieved their highest elastic modulus after 360 days of curing.

The results of these indications may not be an indication of how the material is behaving within a wall as it would be confined by the material around it and the plaster and render on the faces. Compressive testing purely on the hemp-lime layer within a built wall may give some indication into the structural contribution hemp-lime implies on the built wall.

The initial tangent elastic modulus increased with specimen density. The peak strain of the specimens was comparatively high after 14 days. This may be attributed to the high moisture content of the specimens compared with that at 28, 91 and 180 days. As moisture content decreases, the binder matrix is likely to become more brittle, leading to a lower failure strain as the specimen age increases.

Table 6.4 – Mechanical characteristics of all specimens at all ages.
Symbols † and * indicate results obtained from one and two specimens respectively.

Specimen ID	Age (days)	f_{cm} (N/mm²) (Range)	Strain at failure (Range)	E_{cm} (N/mm²) (Range)
THB52.5R-220	14	0.021 (0.018-0.024)	0.094 (0.079-0.12)	4.8 (4.0-5.7)
	28	0.030 (0.028-0.033)	0.033 (0.025-0.042)	3.5 (3.2-4.2)
	91	0.029 (0.026-0.033)	0.043 (0.038-0.051)	3.4 (3.2-3.8)
	180	0.031 (0.028-0.033)	0.037 (0.032-0.04)	3.3 (2.4-4.2)
	360	0.030 (0.027-0.032)	0.035 (0.031-0.033)	5.6 (4.9-6.0)
THB52.5R-275	14	0.029 (0.022-0.033)	0.094 (0.066-0.13)	5.6 (4.2-7.0)
	28	0.049 (0.034-0.057)	0.10 (0.066-0.13)	3.6 (3.3-4.0)
	91	0.052 (0.044-0.063)	0.10 (0.083-0.13)	3.3 (2.2-4.3)
	180	0.057 (0.055-0.058)	0.070 (0.053-0.084)	2.8 (2.2-3.8)
	360	0.054 (0.045-0.061)	0.073 (0.062-0.089)	8.4 (7.6-9.8)
THB52.5R-330	14	0.13 (0.092-0.16)	0.12 (0.089-0.14)	22.4 (13.0-32.0)
	28	0.18 (0.17-0.19)	0.056 (0.051-0.060)	14.3 (12.1-16.0)
	91	0.20 (0.17-0.22)	0.053 (0.047-0.057)	15.0 (10.7-18.8)
	180	0.21 (0.20-0.22)	0.048 (0.042-0.058)	16.7 (15.9-17.8)
	360	0.21 (0.18-0.23)	0.046 (0.042-0.049)	27.4 (23.6-29.3)
THB42.5N-275	28	0.092 (0.081-0.11)	0.10 (0.092-0.12)	4.3 (3.4-5.3)
	91	0.093 (0.091-0.098)	0.091 (0.077-0.11)	4.1 (3.9-4.2)
	180	0.11 (0.095-0.12)	0.090 (0.068-0.10)	4.7 (4.0-5.1)
	360	0.13 (0.12-0.13)	0.087 (0.79-0.94)	7.1 (3.5-10.7)

Specimen ID	Age (days)	f_{cm} (N/mm ²) (Range)	Strain at failure (Range)	E_{cm} (N/mm ²) (Range)
BC-275	28	0.055 (0.051-0.059)	0.054 (0.050-0.056)	6.3 (5.4-7.3)
	91	0.057 (0.053-0.061)	0.040 (0.029-0.047)	5.2 (4.2-6.3)
	180	0.058 (0.056-0.060)	0.031 (0.025-0.039)	5.0 (4.6-5.2)
	360	0.056 (0.050-0.060)	0.027 (0.025-0.032)	7.8 (4.1-11.3)
FR - 275	28	0.087 (0.076-0.093)	0.22 (0.19-0.26)	10.2 (8.6-11.1)
	91	0.094 (0.089-0.10)	0.17 (0.11-0.24)	14.2 (12.3-15.6)
	180	0.089 (0.086-0.091)	0.084 (0.059-0.098)	11.9 (11.8-12.0)
	360	0.086 (0.066-0.11)	0.086 (0.065-0.11)	5.2 (3.8-6.0)
NHL5 - 275	28	0.014 (0.011-0.017)	0.040 (0.029-0.052)	3.6 (3.2-4.0)
	91	0.020* (0.019-0.021)	0.020 (0.019-0.021)	3.3 (3.7-4.0)
	180	0.020 (0.020-0.020)	0.029 (0.021-0.041)	3.9 (3.5-4.4)
	360	-	-	-
SH - 275	28	0.051 (0.051-0.052)	0.038 (0.028-0.047)	7.8 (7.2-8.7)
	91	0.045 (0.032-0.053)	0.035 (0.032-0.038)	3.8 (3.3-4.3)
	180	0.043 (0.035-0.053)	0.033 (0.031-0.037)	9.4 (8.3-10.6)
	360	0.057 (0.051-0.062)	0.035 (0.029-0.040)	5.4 (7.9-8.2)
0.3OSR - 275	28	0.11 (0.090-0.13)	0.15 (0.11-0.21)	4.9 (4.4-5.2)
	91	0.11 (0.088-0.12)	0.14 (0.085-0.18)	6.0 (5.6-6.5)
	180	0.10 (0.09-0.12)	0.11 (0.089-0.12)	5.5 (5.0-6.0)
	360	-	-	-

Specimen ID	Age (days)	f_{cm} (N/mm ²) (Range)	Strain at failure (Range)	E_{cm} (N/mm ²) (Range)
0.6OSR - 275	28	0.11[†]	0.16[†]	5.3[†]
	91	0.13 (0.11-0.14)	0.18 (0.14-0.24)	4.2 (3.3-4.5)
	180	0.15 (0.14-0.15)	0.17 (0.16-0.17)	6.7 (5.5-8.6)
	360	-	-	-
OSR-275	28	0.14 (0.12-0.15)	0.25 (0.22-0.27)	3.5 (2.7-4.0)
	91	0.19 (0.14-0.22)	0.17 (0.13-0.21)	5.3 (4.1-6.5)
	180	0.16 (0.15-0.17)	0.24 (0.24-0.24)	5.0 (4.4-5.4)
	360	-	-	-

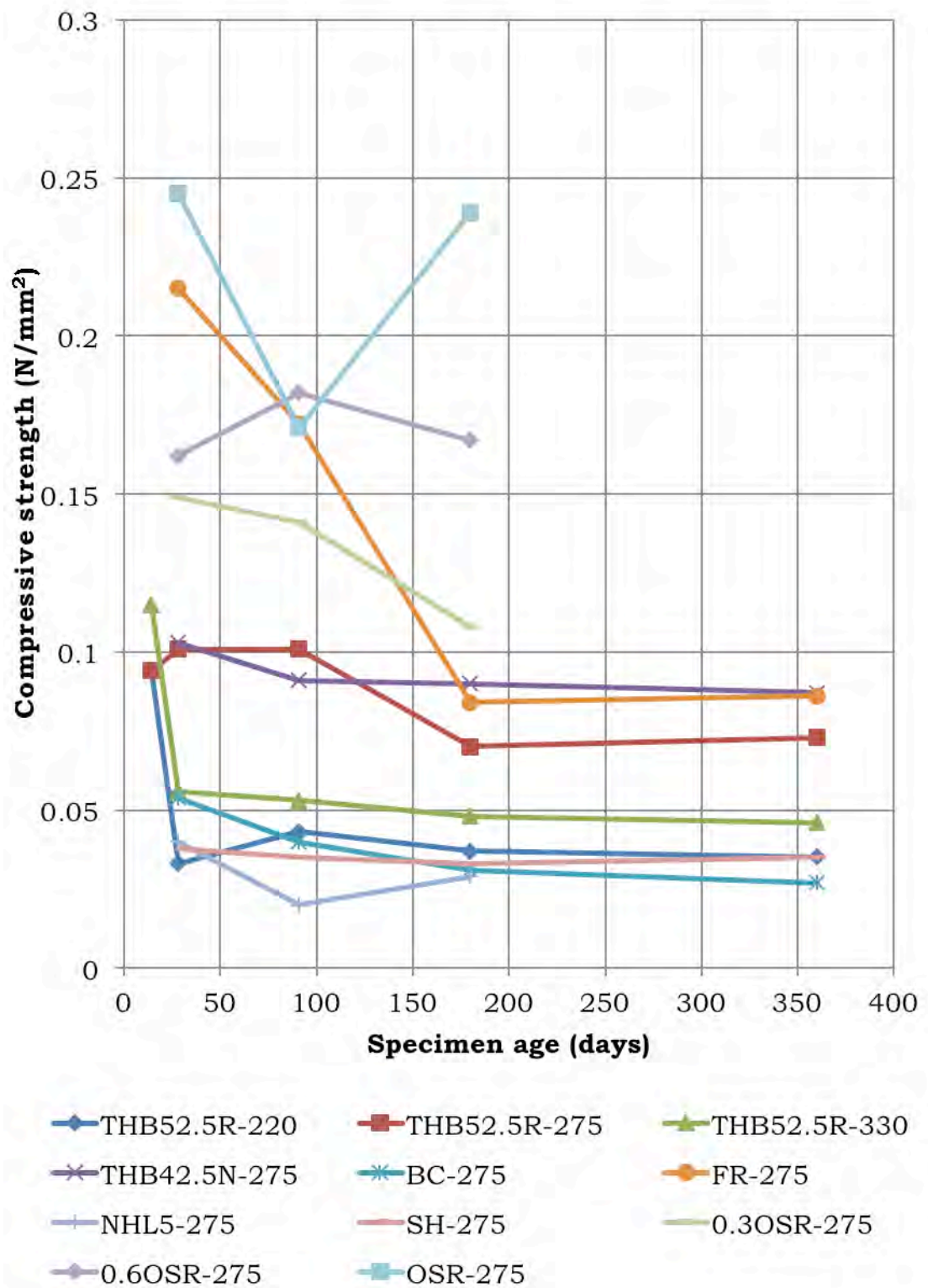


Figure 6.2 – Compression strength against age for all composite specimens at all ages.

The highest values of compressive strength were displayed by THB52.5R-330 specimens with a range of 0.13 - 0.21N/mm². The lowest values were displayed by NHL5 specimens with a range of 0.014 - 0.020N/mm² between 28 and 180 days. Due to loss of specimens during handling throughout the study, no results were obtained for 360 day old NHL5 specimens.

Although compressive strengths of the hemp-lime composites were low, a degree of inter-particle integrity is required within the material in order to allow plasters and renders to be applied. The mix proportions used for specimens at a density of 275 kg/m³ do not initially show a significant increase in strength or stiffness compared with specimens of density 220 kg/m³, although by 180 days they had developed twice the ultimate compressive strength. In addition, there was a noticeable improvement in specimen integrity during handling and specimen preparation; for example, a number of 220 kg/m³ specimens collapsed during careful handling in the laboratory.

The observed increase in strength up to 14 days can be attributed to the development of hydrate minerals within the hydraulic phase of the binder. By this stage the hydration phase of setting and hardening within the binder has most likely completed. Therefore, any further gain in strength beyond 14 days can be largely attributed to further drying out of the material and carbonation of the calcium hydroxide content within the binder. In the case of THB52.5R-220 and 275 specimens there were respective strength increases of 47 and 97% between 14 and 180 days. Following this, their average respective strengths decreased by 3 and 5%. This may indicate that 220 and 275kg/m³ hemp-lime specimens of these particular formulations, size and densities reach their ultimate compressive strengths after 180 days of curing and any subsequent variation in strength may be down to the inherent variabilities in the material. THB52.5-330 specimens displayed an increase in strength of 62% between 14 and 360 day specimens and were between 519-600% and 267-350% greater than THB52.5R-220 and 275 specimens respectively.

The THB42.5N-275 specimens were, on average, 37% stronger than THB52.5R-275 specimens and 33% stronger than BC-275 specimens. This result may indicate that the compressive strength of hemp-lime composites may not necessarily be directly related to the strength of the binder as BC mortars displayed the highest values of flexural and compressive strength when tested as standard sand prisms.

The ultimate compressive strength of specimens mixed with OSR increased as the proportion of OSR used in the mix increased. 0.3OSR - 275, 0.6OSR - 275 and OSR - 275 specimens displayed compressive strengths between 0.10-0.11, 0.11-0.16 and 0.14-0.17N/mm² respectively. Furthermore, the strain at failure increased as the proportion of OSR increased with 360 day old 0.3OSR - 275 specimens displaying a failure strain of 0.092 compared to 0.20 for OSR - 275 specimens of the same age, an increase of 117%. By comparing the stress vs. strain plots of the two specimens, clear differences in the behaviour under loading can be observed. Figure 6.1 displays two typical stress vs. strain plots for 360 day old 0.3OSR and OSR-275 specimens.

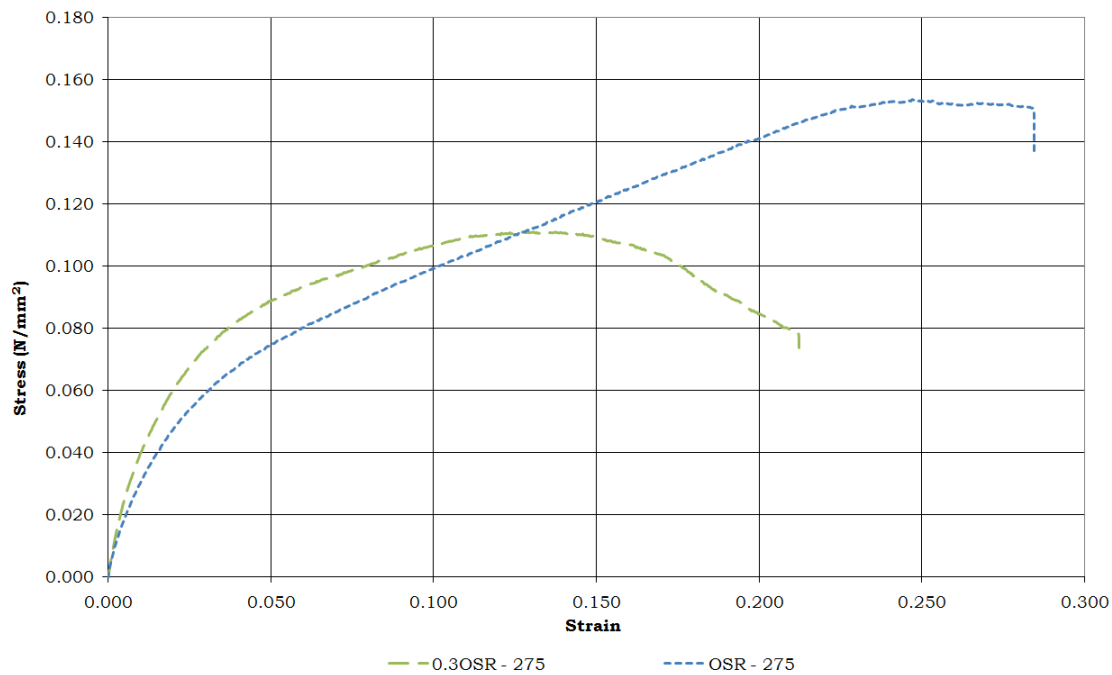


Figure 6.1 - Stress vs. strain comparison of 360 day old 0.3OSR-275 and OSR-275 specimens.

The initial response to loading between the two specimens is very similar with tangent moduli of 7.9 and 6.9N/mm² for 0.3OSR and OSR-275 respectively. As loading progressed 360 day old 0.3OSR - 275 specimens failed at an average stress of 0.11N/mm² and at an average failure strain of 0.092.

Although performance confirms that hemp-lime is probably best suited to non-load-bearing applications, it should be noted that materials of even lower strength and stiffness (e.g. straw bales) are often used in load-bearing wall construction. It is also worth noting that prefabricated hemp-lime blocks of higher density have been successfully used in load-bearing applications.

6.3.3 Specimen failure

As testing progressed, it became apparent that the majority of cylinders displayed failure planes within the top two thirds of the specimen height; in total 93% of specimens displayed this behaviour (all available photos of specimens at failure are provided in Appendix II). When taking into consideration that the specimens were tested in the same orientation as they were fabricated, it was hypothesised that the orientation of testing compared to the orientation of fabrication had an effect on the position of the failure plane. To determine the validity of the hypothesis, a series of compressive tests were carried out on specimens in the reverse orientation to when they were fabricated. A total of six specimens were tested in the reverse orientation, two of each density using the THB52.5R binder. All specimens displayed failure points within the lower two thirds of the specimen height indicating that the orientation of testing compared to the orientation of fabrication does have a bearing on the location of the failure point on hemp-lime specimens. Figure 6.3 presents the failure of two specimens of identical density. The specimen on the left was tested in the same orientation as when fabricated; the specimen on the right was tested in the reverse orientation. Both specimens display typical failure modes considering the fabrication/testing orientation combination.



Figure 6.3 – THB52.5R-220 specimen failure tested in the same orientation as fabrication (left). THB52.5R-220 specimen failure tested in the reverse orientation as when fabricated (right).

A further hypothesis was made suggesting that the lower half of the specimen had a greater bulk density than the top half of the specimen. This may have been due to material slumping during fabrication, specimen transportation to the conditioning room and handling of the specimens whilst they were still moulded. To ascertain whether or not this was the case two 360 day old specimens, one THB52.5R-275 and one THB52.5R-330, were sawn in half using a band saw and the bulk densities measured. The bulk densities of the bottom halves of the 275 and 330kg/m³ specimens were 6 and 9% greater than the top halves respectively indicating that measurable amounts of material slumping took place during fabrication which in turn may have affected the positions of the failure planes in compression. Although only taken from two specimens (due to low numbers of spare specimens) further investigations may provide a more detailed insight into slumping values for different density specimens when using the

fabrication technique detailed in this investigation. This, however, falls outside the remit of this thesis.

CHAPTER 7 - CONCLUSIONS

7.1 Introduction

The success of any empirical investigation is never immediately apparent. Only after repeat tests by other users following the same guidelines (round robin testing for example) can the results of an investigation be validated and built upon. This chapter presents the conclusions for this investigation, both those in relation to the aims and objectives originally set out and those which have been developed as a result of the fabrication and testing procedures. Furthermore, as a result of this work, a number of recommendations for future investigations are also presented which may supplement the practical and empirical knowledge of hemp-lime

- To review, improve, verify and document fabrication, curing and testing techniques for the empirical investigation of hemp-lime and its constituents.

- To further characterise the material as it currently stands in the UK construction industry paying particular attention to mix proportions, density and compressive strength.
- To document the progression of the carbonation front across the material cross-section under laboratory conditions both within the composite and the standard sand mortar prisms.
- To empirically determine the amount of CO₂ the binder within the composite could sequester over the whole life of a building.

7.1.1 Specimen fabrication

The novel methodology developed and applied during this investigation allowed for the fabrication of specimens of different bulk densities to within a maximum of 2.6% from the average. Overall, an average percentage difference from the mean of 0.8% empirically confirmed that target bulk densities can be achieved reliably, confidently and with a high level of repeatability. However, the methodology can only be confirmed through continual use of the same procedures within different investigations. It may be assumed that this value of low variability may be the intrinsic empirical variability when manually fabricating hemp-lime specimens.

The calculation methodology for determining the mass of wet material at fabrication in order to achieve desired densities may be of particular importance. The methodology can be used with different material ratios and/or desired density values. In essence this allows researchers to confidently fabricate specimens to any desired final density.

The following conclusions were also made:

- The use of wax-lined cardboard moulds did not affect the moisture content of the specimens during curing.
- An average moisture content between 11-12% was consistent with previous investigations.
- Differences between the top half and the bottom half of fabricated specimens was identified as a possible cause for the failure locations under compression loading.

7.1.2 Material characterisation

The new processing plant at Hemp Technology Ltd. is reliably and consistently producing very well graded hemp shiv. Results from this investigation have confirmed that grading hemp shiv via the sieving method is a viable and reliable way of empirically determining the length particle distribution curve of hemp shiv.

The following conclusions were also made:

- The repeatability of the mortar fabrication process was confirmed through the low variability of bulk densities at each testing age.
- A total water absorption value of 396% was observed for UK harvested hemp shiv with four distinct phases of absorption over a 14 day period.
- THB52.5R formulated binders displayed faster setting times than previous formulations as a result of the increased ratio of cement.
- BC binders displayed the largest values of flexural and compressive strengths over the testing period

7.1.3 Carbonation

The carbonation depth, in conjunction with rates of carbonation, are able to be accurately distinguished through the use of phenolphthalein indicator staining on standard sand mortar specimens.

NHL5 mortar specimens displayed the highest rate of carbonation; possibly due to the comparatively small ratio of hydraulic constituents in the binder.

BC mortar specimens displayed the lowest rate of carbonation; possibly due to the comparatively large ratio of hydraulic constituents in the binder creating a tighter pore structure on the outer layer of the specimens during early phases on carbonation hence inhibiting the ingress of CO₂.

7.1.4 Carbon dioxide sequestration

The methodology and analysis used in this investigation was successful in determining the carbon dioxide increase in the binder due to carbonation

and hydration. There was minimal difference with regards to ultimate CO₂ sequestration values for THB52.5R-220, 275 and 330 specimens. The largest sink in the composite material was the hemp shiv, therefore, varying the binder mix proportion with a focus on increasing the hemp-shiv ratio will increase the carbon sequestration potential of the material when used within the fabric of a building.

The binders did not reach 100% of their carbonation potential. This was assumed to be a result of an impervious outer layer of calcium carbonate being formed within the binder matrix which inhibited the ingress of CO₂ for further carbonation within.

7.2

Recommendations for further work

During the course of this investigation a number of areas where empirical knowledge seemed to be lacking were identified. The following list details these areas in no particular order of priority.

- What is the optimum density/constituent ratio balance to get the best CO₂ sequestration when taking into consideration the transport and production of the material?
- Determine carbonation constants for a much larger range of densities and different binder/water ratios.
- Determine the rate of carbonation on hemp-lime wall sections with render and plaster, render and permanent shuttering on the interior, different render and plaster thicknesses, different types of render and plaster (NHL, air lime, lime and hemp etc.)
- Carry out an LCA for UK hemp. The French LCA was not carried out in accordance with international standards (BS EN 14040) so was not validated by Ecobilan.
- Creep of hemp-lime under self weight and its influence on air-tightness.
- Adhesion strength of render to hemp-lime composite for calculation into structural shear contribution.
- Detailed study into the biological, physical and chemical differences between hemp shiv from different origins. Germany, France, Belgium, UK, Spain etc.
- Empirically investigate the CO₂ sequestration of hemp shiv from different origins. Hemp shiv is the largest carbon sink in the material so the variability may be large.
- No tests on the degradation of hemp concretes has so far been carried out
 - What can be done with used hemp lime after use in a wall?

- The emission and nutrients it can give to soil
 - Can it be used as roof infill in another projects?
- Structural connection between a hydrated layer of hemp-lime and a new layer; cold-joint and its shear strength development over age.
- The relationship between binder matrix and fire resistance
- CL90 lime mixed with high strength pozzolans
 - Setting characteristics
 - LCA implications

REFERENCES

- AAFC**, 2013. *Canada's Industrial Hemp Industry*. Agriculture and Agri-Food Department – Government of Canada. www.agr.gc.ca. Retrieved 2013-12-10.
- ALLIN, S.**, 2005. *Building with hemp*. Kenmare: SEED Press.
- ARANDIGOYEN, M., LANAS, J., ALVAREZ, J.I.**, 2004. Carbonation of lime-cement mortars: a description of this process through the fractal dimension. In: D. KWIATKOWSKI AND R. LIFVENDAHL, eds. *Proceedings of the 10th international congress on deterioration and conservation of stone*, 27 June - 2 July 2004, Stockholm: ICOMOS, pp.1057-1064.
- ARDENNE, F. C.**, 2007. *Agrobat: Caractérisation du béton de chanvre*.
- ARNAUD, L.**, 2000. Mechanical and thermal properties of hemp mortars and wools: experimental and theoretical approaches. *Proceedings of the 3rd international symposium on bioresource, hemp and other fibre crops*. Wolfsburg, Germany. 2005.
- ARNAUD, L.**, 2009. Comparative study of hygro-thermal performances of building materials. *Proceedings of the 11th International Conference on Non-*

Conventional Materials and Technologies (NOCMAT 2009), 6-9 September 2009 University of Bath, UK.

ARNAUD, L., and CEREZO, V., 2001. *Qualification physique des matériaux de construction à base de chanvre. Rapport final de recherche pour le compte de l'Ademe.* France: La chanverrière de l'Aube. CNRS 0711462.

ASTM C31/C31M-12. *Standard practice for making and curing concrete test specimens in the field.* ASTM International.

BARKER, M., 2008 [viewed 2011-07-16]. Time to bin industry's lavish habits. *Construction News* [online]. Available from: <http://www.cnplus.co.uk/news/time-to-bin-industrys-lavish-habits/953199.article>

BC, 2013. Batichanvre datasheet. www.c-e-s-a.fr. Retrieved 2013-12-10.

BERUTO, D.T., BARBERIS, F., BOTTER, R., 2005. Calcium carbonate binding mechanisms in the setting of calcium and calcium-magnesium putty-limes. *Journal of Cultural Heritage*, 6, pp.253-260.

BEVAN, R. and WOOLLEY, T., 2008. *Hemp lime construction - a guide to building with hemp lime composites.* Bracknell: BRE press.

BLASTING, T.J., 2013. *Recent Greenhouse Gas Concentrations.* Carbon Dioxide Information Analysis Center [online]. DOI: 10.3334/CDIAC/atg.032.

BOUTIN, M.-P., FLAMIN, C., QUINTON, S., GOSSE, G., INRA, L., 2005. *Etude des caractéristiques environnementales du chanvre par l'analyse de son cycle de vie.* France: Ministère de l'Agriculture et de la Pêche: (MAP 04 B1 05 01).

BOUYER, T., 2008. *De la qualité de matériau béton-chanvre: Rapport de stage.* ENGREF:

BRADSHAW, R.H.W., COXON, P., GREIG, J.R.A, HALL, A.R., 1981. *New fossil evidence for the past cultivation and processing of hemp (Cannabis sativa L.) in eastern England.* Vol. 89(3), pp.503-510.

BRUIJN, P. D., 2008. *Hemp concretes - mechanical properties using both shives and fibres.* Dissertation: Swedish university of agricultural sciences.

- BUTSCHI, P.Y., DESCHENAUX, C., MIAO, B., SRIVASTAVA, N.K., 2003.** Utilisation du chanvre pour la prefabrication d'elements de construction. *Proceedings for the 31st Canadian Society for Civil Engineering*. Montreal: Canadian Society for Civil Engineers.
- BS EN 196-1:2005.** *Methods of testing cement - Part 1: Determination of strength*. BSI.
- BS EN 196-3:2005.** *Methods of testing cement. Determination of setting time and soundness*. BSI.
- BS EN 197-1:2011.** *Composition, specifications and conformity criteria for common cements*. BSI.
- BS EN 459-1:2010.** *Building lime. Definitions, specifications and conformity criteria*. BSI.
- BS EN 459-2:2010.** *Bulding lime. Test methods*. BSI.
- BS EN 993-1:1995.** *Methods of test for dense shaped refractory products. Determination of bulk dentisy, apparent porosity and true porosity*. BSI.
- BS EN 1015-10:1999.** *Methods of test for mortar for masonry. Determination of dry bulk density of hardened mortar*. BSI.
- BS EN 1015-11:1999.** *Methods of test for mortar for masonry. Determination of flexural and compressive strength of hardened mortar*. BSI.
- BS EN 12390-1:2012.** *Testing hardened concrete. Shape, dimensions and other requirements for specimens and moulds*.BSI.
- BS EN ISO 14040:2006.** *Environmental management - life cycle assessment - principles and framework*. BSI.
- BOSCA, I. and KARUS, M., 1998.** *The Cultivation of Hemp: Botany, Varieties, Cultivation and Harvesting*. Sebastopol, CA: Hemptech.
- CEREZO, V., 2005.** *Propriétés mécaniques, thermiques et acoustiques d'un matériau á base de particules végétales: Approche expérimentale et modélisation théorique*. PhD thesis: L'Ecole national des sciences appliquees de Lyon.

CEYTE, I., 2008a. *Béton de chanvre, définition des caractéristiques mécaniques de la chénavotte*. TFE de l'ENTPE:

CEYTE, I., 2008 (in French). *Etat, acteurs privés et innovation dans le domaine des matériaux de construction écologiques : Le développement du béton de chanvre depuis 1986* (MASTER - Politiques publiques et gouvernements comparés thesis). 'Institut d'Etudes Politiques de Lyon.

CHANVRE, C. E., 2007. Règles professionnelles d'exécution. [*professional rules for manufacture*].

COLLET, F., 2004. *Comparaison hydrique et thermique de matériaux naturels à des matériaux de construction usuels*. PhD thesis: INSA de Rennes,

COLLET, F., BART, M., SERRES, L. and MIRIEL, J., 2008. Porous structure and water vapour sorption of hemp-based materials. *Construction and building materials*, 22 (6), pp.1271-1280.

CONSTRUCTING EXCELLENCE, 2008. *Construction and sustainable development in Plain English*. Construction Excellence in the Built Environment [online]. Section 3, page 2.

CORDIER, C., 1999. Caractérisation thermique et mécanique des bétons de chanvre.

COURGEY, S., 2003. Béton de chanvre. *La maison écologique*, 13

COURGEY, S., 1993. La construction de murs à base de fibres de chanvre.

CSH (DEPARTMENT FOR COMMUNITIES AND LOCAL GOVERNMENT), 2013. *Code for sustainable homes*. England: Parliament of the United Kingdom.

CSTB, 2007. *Analyse des caractéristiques des systèmes constructifs non industrialisés*. Centre Scientifique et Technique du Bâtiment: (France).

DEFRA (DEPARTMENT FOR ENVIRONMENT, FOOD AND RURAL AFFAIRS), 2013. *Industrial fibre crops: business opportunities for farmers*. London: Parliament of the United Kingdom.

DESHENAU, C., MACHERET, C., 2000. *Agglomérés de chanvre: Rapport technique*. Ecole d'Ingénieur et d'Architecte de Fribourg (EIAF). Switzerland.:

DEWEY, L.H., MERRILL, J.L., 1916. *Hemp hurds as paper making material*. United States Department of Agriculture, Bulletin No. 404. EBook #17855.

ELFORDY, S., LUCAS, F., TANCRET, F., SCUDELLER, Y. and GOUDET, L., 2008. Mechanical and thermal properties of lime and hemp concrete ("hempcrete") manufactured by a projection process. *Construction and Building Materials*, 22 (10), pp.2116-2123.

EUROPEAN COMMISSION, 2009. *Flax and Hemp - AGRI C5*. European Commission Agriculture and Rural Affairs (online). EU: Available from: http://www.eiha.org/attach/553/09-02_C1_Flax_hemp_presentation_26_February_2009_circa.pdf.

EVARD, A., 2003. *Béton de chanvre: Synthèse de propriétés physiques*. Saint Valerien: Association Construire en Chanvre.

EVARD, A., DE HERDE, A., 2006. Dynamic interactions between heat and mass flow in Lime-Hemp Concrete. *Research in Building Physics and Building Engineering*. London: Taylor & Francis Group. ISBN 0-415-41675-2.

EVARD, A., 2008. *Transient hygrothermal behaviour of lime-hemp materials*. PhD thesis: Université Catholique de Louvain.

GARCIA-JALDON, C., 1992. *Caractérisation morphologique et chimique du chanvre (cannabis sativa) pré-traitement à la vapeur et valorisation*. PhD thesis: Université de Grenoble,

GARNIER, P., 2000. *Le séchage des matériaux poreux. Approche expérimentale et approche théorique par homogénéisation des structures périodiques: Rapport de dea*. PhD thesis: Department of Civil Engineering, ENTPE.

GIBBS, C. P., 2006. *Strength optimisation of hemp-lime*. MEng undergraduate dissertation: Architecture & Civil Engineering, University of Bath.

GOURLAY, E., 2008. Report: Caractérisation de la chènvote et influence des caractéristiques de la chènvote sur celles des bétons de chanvre-chaux.

GOYER, S., 2007. *Caractérisation des propriétés microstructurales et hydriques de bétons légers. Application à la modélisation des transferts hydriques*.

HELMICH, R., 2008. *The structural contribution of hemp-lime*. MEng undergraduate dissertation: Architecture & Civil Engineering, University of Bath.

HEWLETT, P.C., 1998. *Lea's chemistry of cement and concrete*, London: Edward Arnold.

HM GOVERNMENT, 2008. *Climate Change Act*. London: Parliament of the United Kingdom.

HMRC, 2013. Her Majesty's Revenue & Customs. *A general guide to landfill tax*. www.hmrc.co.uk. Retrieved 2013-12-10.

HMRC, 2013a. Her Majesty's Revenue & Customs. *Aggregates Levy - introduction*. www.hmrc.co.uk. Retrieved 2013-12-10.

HOUST, Y.F., 1996. The role of moisture in the carbonation of cementitious materials. *International Journal for Restoration of Buildings and Monuments*, 2, pp.49-66.

HUSTACHE, Y., ARNAUD, L., 2008. *Overview of the state of knowledge of hemp concretes and mortars*. c. e. chanvre,

HUSTACHE, Y., ARNAUD, L., 2008a. *Programme d'essais complémentaires concernant la mise en œuvres des bétons de chanvre sur chantier. Validation des règles professionnelles: Rapport final*. Association Construire en Chanvre:

JEFFERSON, W., 2005. *Energy systems and sustainability metrics. Sustainable energy: Choosing among options*. Cambridge, MA: MIT.

JOHANNESSEN, B., UTGENANT, P., 2001. Microstructural changes caused by carbonation of cement mortar. *Cement and Concrete Research*, 31, pp.925-931.

KHESTL, F., 2010. Fast growing renewable materials in building industry. *Second international conference on sustainable construction materials and technologies*, Ancona, Italy.

KIOY, S. M., 2005. *Lime-hemp composites: Compressive strength and resistance to fungal attacks*. MEng undergraduate dissertation: Department of Architecture & Civil Engineering, University of Bath.

KYMÄLÄINEN, H.-R., SJÖBERG, A.-M., 2008. Flax and hemp fibres as raw materials for thermal insulations. *Building and Environment*, 43 pp.1261-1269.

KOZŁOWSKI, R., PRZEMYSŁAW, B. and MACKIEWICZ T.M., 2004 IENICA Interactive European Network for Industrial Crops and their Applications: Report from Poland. Available from: <http://www.ienica.net/reports/poland.pdf>, accessed May 12th 2011.

LANDSBERG, D. V., 1992. The history of lime production and use from early times to the industrial revolution. *Zement-Kalk-Gips*, 45 pp.199-203.

LAWRENCE, R. M. H., 2006. *A study of carbonation in non-hydraulic lime mortars*. PhD thesis: Architecture & Civil Engineering, University of Bath.

NGUYEN, T. T., PICANDET, V., AMZIANE, S. and BALEY, C., 2008. Optimisation de l'usage du béton de chanvre dans la conception d'un écomatériau pour le génie civil. *Revue des Composites et des Matériaux Avancés*, 18 (2), pp.227-232.

NIKTER, M., 2006. *Microbial quality of hemp (cannabis sativa l.) and flax (linum usitatissimum l.) from plants to thermal insulation*. Undergraduate dissertation: Department of Agrotechnology, University of Helsinki.

OATES, J.A.H., 1998. *Lime and limestone: chemistry and technology, production and uses*, Weinheim: Wiley-VCH.

O'DOWD, J., QUINN, D., 2005. *An investigation of hemp-lime as a building material*. MEng undergraduate dissertation: University College Dublin.

PIOTROWSKI, S., AND CARUS, M., 2011. *Ecological benefits of hemp and flax cultivation and products*. Nova Institut (online). Available from: http://eiha.org/attach/643/11-05-13_Ecological_benefits_of_hemp_and_flax.pdf.

RADONJIC, M., HALLAM, K.R., ALLEN, G.C., HAYWARD, R., 2001. Mechanism of carbonation in lime-based materials. *Journal of the Building Limes Forum*, 8, pp.50-64.

RIZZA, M., 2003. *Hemp concrete mixtures and mortars, preparations method and uses*. US 6913644 B2

- SAMRI, D.**, 2008. *Analyse physique et caractérisation hygrothermique des matériaux de construction: Approche expérimentale et modélisation numérique [physical analysis and hygrothermal characterisation of construction materials: Experimental approach and numerical modelling]*. PhD thesis: ENTPE, France.
- SEDAN, D., PAGNOUX, C., SMITH, A. and CHOTARD, T.**, 2008. Mechanical properties of hemp fibre reinforced cement: Influence of the fibre/matrix interaction. *Journal of the European ceramic society*, 28 (1), pp.183-192.
- SEDAN, D., PAGNOUX, C., CHOTARD, T., SMITH, A., LEJOLLY, D., GLOAGUEN, V., KRAUSZ, P.**, 2007. Effect of calcium rich and alkaline solutions on the chemical behaviour of hemp fibres. *Journal of Materials Science*, 10.1007/s10853-007-1903-4.
- SSBA**, 2004. UK Legislation. *Sustainable and Secure Buildings Act*. www.legislation.gov.uk. Retrieved 2013-12-10.
- STAFFORD, P.**, 1992. *Psychedelics encyclopedia*. California: Ronin Publishing.
- STERN, N., P. S., BAKHSHI, V., BOWEN, A.** , 2006. *Stern review: The economics of climate change*. London:
- TAYLOR, H.F.W.**, 1964. *The Chemistry of Cements*. 2nd Edition. London: Thomas Telford.
- VAN BALEN, K., VAN GEMERT, D.**, 1994. Modelling lime mortar carbonation, *Materials and Structures*, 27 (171), pp.393-398.
- VAN BALEN, K.**, 2005. Carbonation reaction of lime, kinetics at ambient temperature, *Cement and Concrete Research*, 35 (4), pp.647-657.
- VAN DER WERF, H.**, 1994. *Crop physiology of fibre hemp*. PhD Thesis: Wageningen, Denmark.
- VON LANDSBERG, D.**, 1992. The history of lime production and use from early times to the Industrial Revolution. *Zement-Kalk-Gips*, 45, pp.199-203.

WILD, S., KHATIB, J.M., 1997. Portlandite consumption in metakaolin cement pastes and mortars. *Cement and Concrete Research*, 27 (1), pp.137-146.

WOOD, A., 2009. *The feasibility of using oilseed rape by-products in sustainable construction*. MEng undergraduate dissertation: Architecture & Civil Engineering, University of Bath.

YATES, T., 2002. *Client report: Final report on the construction of the hemp houses at Haverhill, Suffolk*. UK: Building Research Establishment (report number – 209-717 Rev. 1).

APPENDIX I – CALCULATION OF WET MASS OF MATERIAL DURING FABRICATION

The table below provides the methodology by which the wet mass of material at fabrication was calculated. Three cylinders (Cylinders 1, 2 and 3) of increasing density were fabricated for each material ratio. The nine specimens were then cured for a period of 14 days (to allow a significant amount of hydration to take place) and then dried in an oven at 90°C until no further changes in mass were observed. The dry densities were then recorded and a 7% moisture content was added to the value. In all three cases the desired dry densities (220, 275 and 330kg/m³) fell below the dry density of the middle specimen. It was therefore safe to assume that the required values of wet mass of material at fabrication lay between the wet masses of cylinders 1 and 2.

By calculating the difference in wet mass between the two cylinders and then the difference in dry mass between the two cylinders a ratio between these two values was calculated. This ratio essentially indicated how many

units of wet material were required to produce 1 unit of dry material. As the final desired densities of our cylinders were known along with the volume of the moulds, the mass of composite material in the moulds at those desired densities was then calculated. The difference between this mass and the dry mass of cylinder 1 was then multiplied by the ratio value to give the required wet mass of material at fabrication to achieve the desired densities of specimens with 7% moisture content.

	Material ratio		
	1:1	1.5:1	2:1
Cylinder 1 wet mass (g)	2003	2144	2762
Cylinder 2 wet mass (g)	2346	2503	3434
Wet mass difference (g) - □	343	359	672
Cylinder 1 dry mass (g) - (including 7%MC)	1118	1343	1597
Cylinder 2 dry mass(g) - (including 7%MC)	1332	1566	1970
Dry mass difference (g) - □	214	222	373
Ratio □/□	1.60	1.61	1.80
Aimed dry density (kg/m³)	220	275	330
Volume of cylinder (m³)	0.0053	0.0053	0.0053
Dry mass required (g) - □	1166	1458	1749
Difference between dry mass required and cylinder 1 dry mass (□-□) = □	48	114	152
□*ratio (g)	77	184	274
Cylinder 1 wet mass + (□*ratio)	2080	2328	3036
Wet density (kg/m³)	393	439	573

APPENDIX II – COMPOSITE SPECIMEN
COMPRESSION TESTING PHOTOGRAPHS

THB52.5R-220 compression specimens



14 days



28 days



91 days



180 days

Not available

360 days

THB52.5R-275 compression specimens



14 days



28 days



91 days



180 days

Not available

360 days

THB52.5R-330 compression specimens



14 days



28 days



91 days

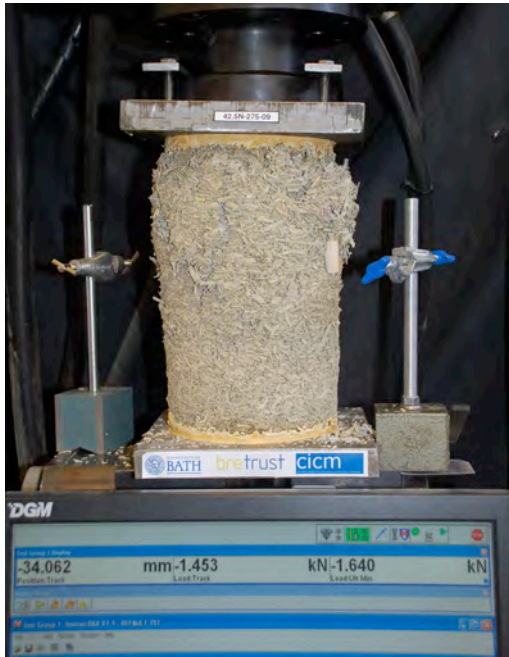


180 days

Not available

360 days

THB42.5N-275 compression specimens



28 days



91 days

Not available

180 days

Not available

360 days

BC-275 compression specimens



28 days



91 days

Not available

180 days



360 days

FR-275 compression specimens



28 days



91 days

Not available

180 days

Not available

360 days

SH-275 compression specimens



28 days



91 days



180 days

Not available

360 days

NHL5-275 compression specimens



28 days



91 days



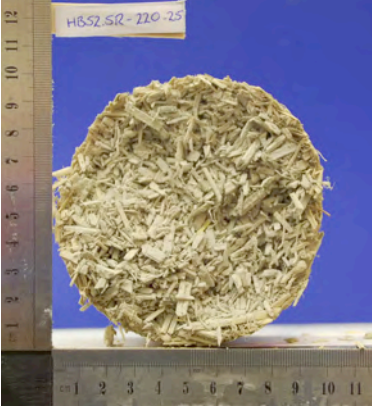
Not available

180 days

Not available

360 days

APPENDIX III – COMPOSITE SPECIMEN
CARBONATION TESTING PHOTOGRAPHS

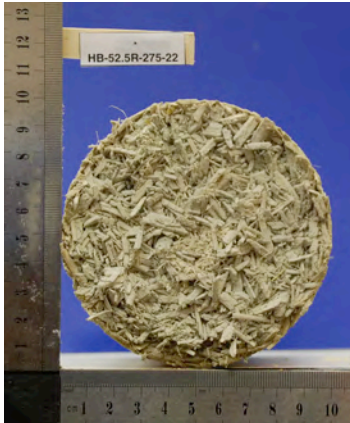
THB52.5R-220 composite carbonation specimens	
 <p>A circular composite specimen, 52.5R-220-22, after 14 days of carbonation. The specimen is roughly circular with a diameter of about 10 cm. It has a yellowish outer layer and a bright pink inner core. A ruler is visible at the bottom for scale.</p>	 <p>A circular composite specimen, 52.5R-220-23, after 28 days of carbonation. The specimen is roughly circular with a diameter of about 10 cm. It has a yellowish outer layer and a pink inner core. A ruler is visible on the left and bottom for scale.</p>
14 days	28 days
 <p>A circular composite specimen, 45.5R-220-25, after 91 days of carbonation. The specimen is roughly circular with a diameter of about 10 cm. It has a yellowish outer layer and a pink inner core. A ruler is visible on the left and bottom for scale.</p>	Not available
91 days	180 days
Not available	
360 days	

THB52.5R-275 composite carbonation specimens



14 days

28 days




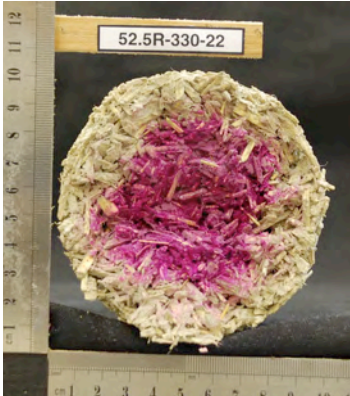


Not Available

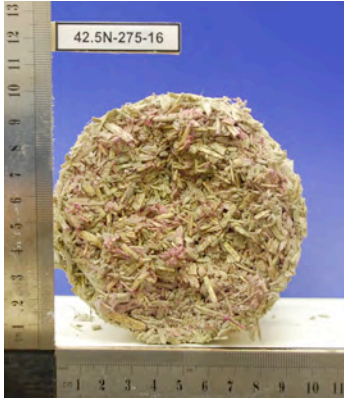
91 days


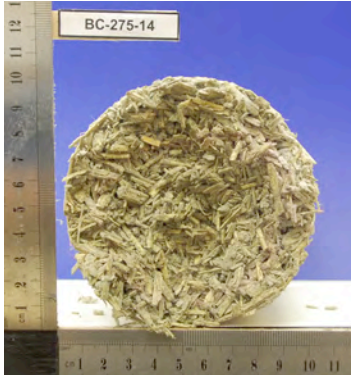
180 days

Not available

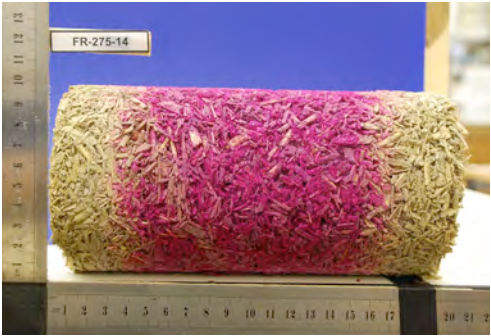
360 days

THB52.5R-330 composite carbonation specimens	
 <p>52.5R-330-20</p>	 <p>52.5R-330-22</p>
14 days	28 days
 <p>HB-52.5R-330-23</p>	 <p>HB-52.5R-330-25</p>
91 days	180 days
Not available	
360 days	

THB42.5N-275 composite carbonation specimens	
	
28 days	91 days
Not available	Not available
180 days	360 days

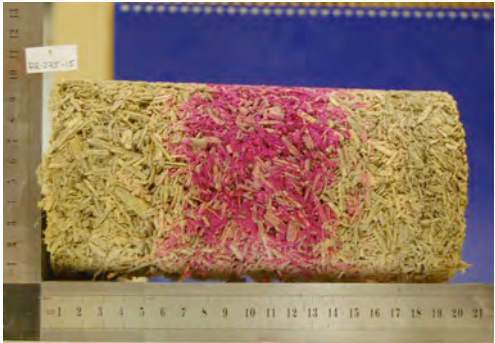
BC-275 composite carbonation specimens	
 <p>A circular composite specimen, BC-275-16, is shown next to a vertical ruler. The specimen is light green and fibrous, with a small pinkish-red mark in the center. The ruler shows a scale from 1 to 12 cm.</p>	 <p>A circular composite specimen, BC-275-14, is shown next to a vertical ruler. The specimen is light green and fibrous. The ruler shows a scale from 1 to 12 cm.</p>
28 days	91 days
Not available	Not available
180 days	360 days

FR-275 composite carbonation specimens



28 days

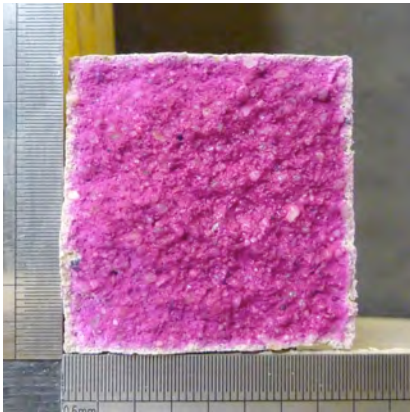
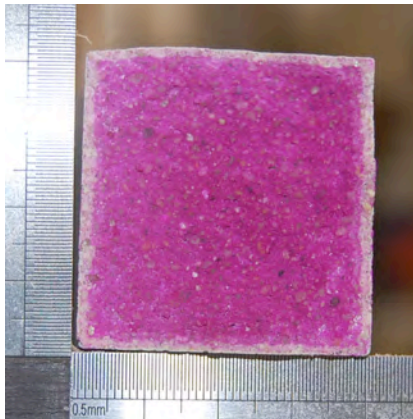
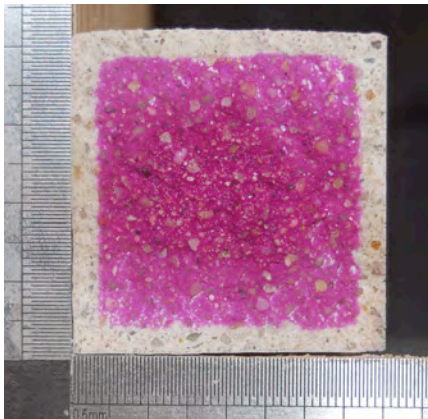
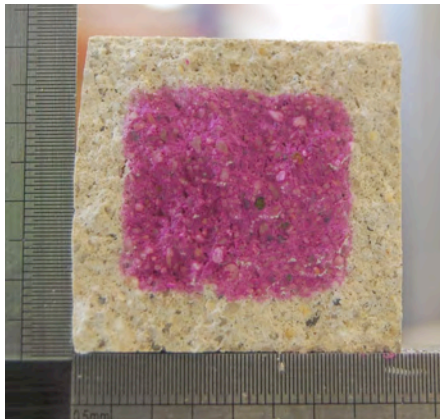
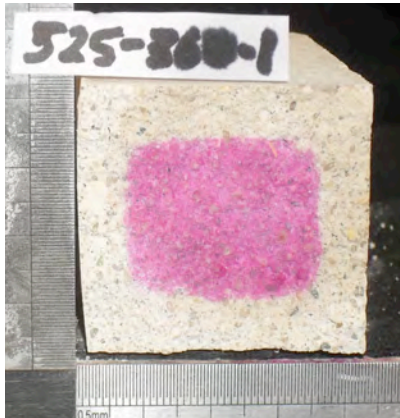
91 days



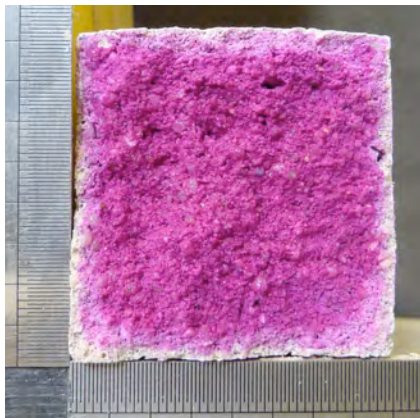
180 days

360 days

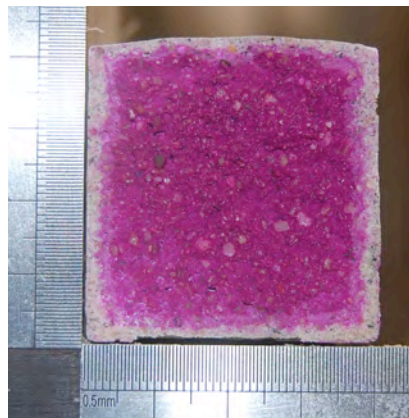
APPENDIX IV – MORTAR SPECIMEN CARBONATION TESTING PHOTOGRAPHS

THB52.5R mortar carbonation specimens	
	
14 days	28 days
	
91 days	180 days
	
360 days	

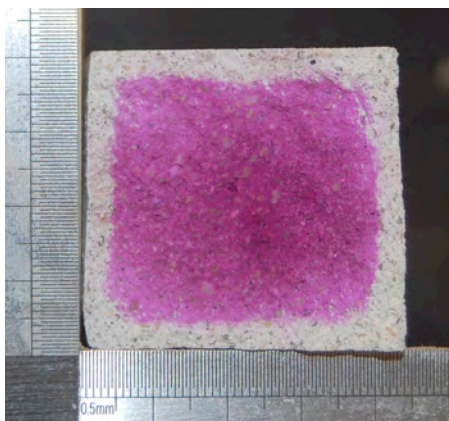
THB42.5N mortar carbonation specimens



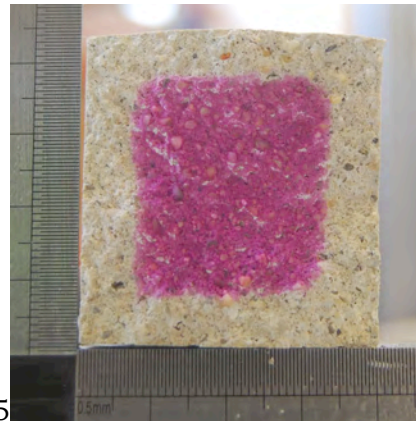
14 days



28 days



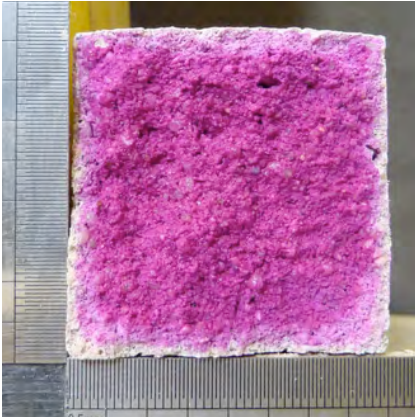
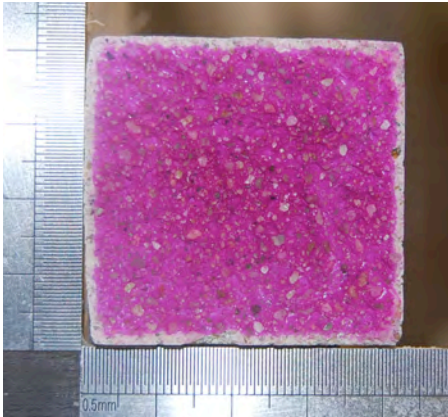
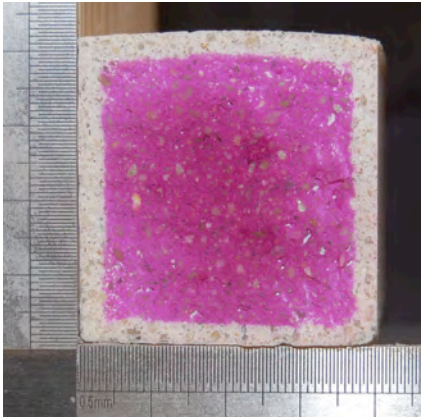
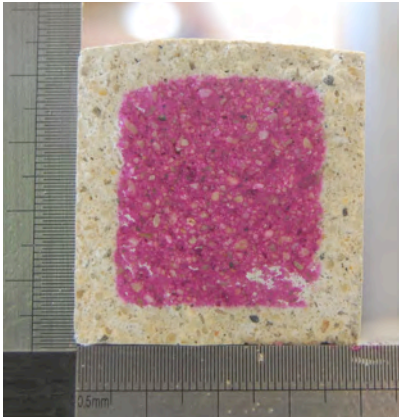
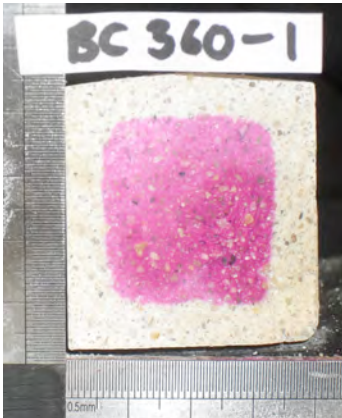
91 days

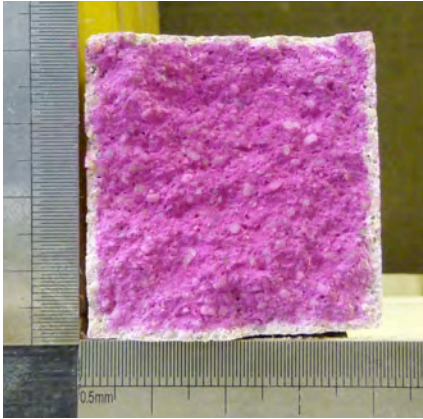
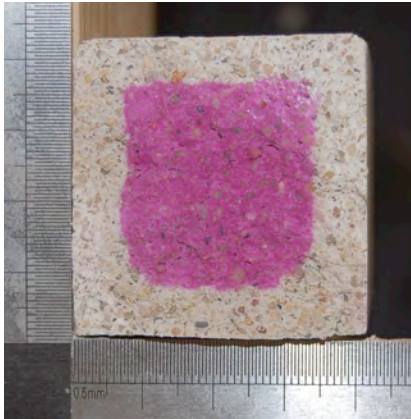
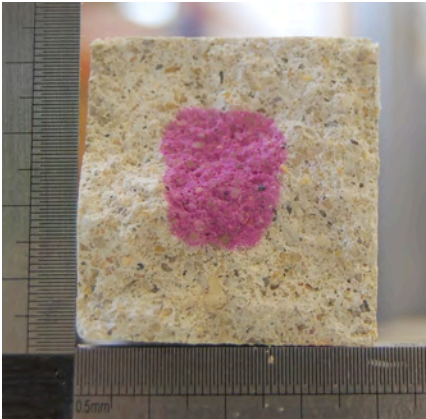
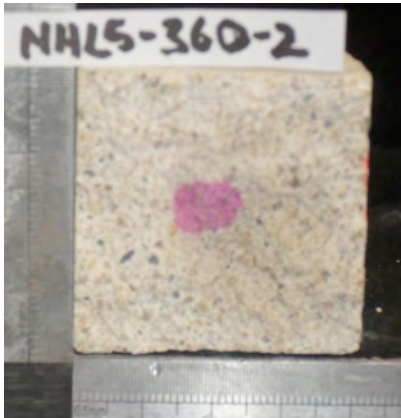


180 days



360 days

BC mortar carbonation specimens	
	
14 days	28 days
	
91 days	180 days
	
360 days	

NHL5 mortar carbonation specimens	
	Not available
14 days	28 days
	
91 days	180 days
	
360 days	

APPENDIX V – PEER REVIEWED PUBLICATIONS